UNIVERSITÉ DE LIÈGE
FACULTÉ DES SCIENCES
DÉPARTEMENT DE BIOLOGIE, ÉCOLOGIE ET ÉVOLUTION

HAVFORSKNINGSINSTITUTET
BENTHIC RESOURCES AND PROCESSES RESEARCH GROUP

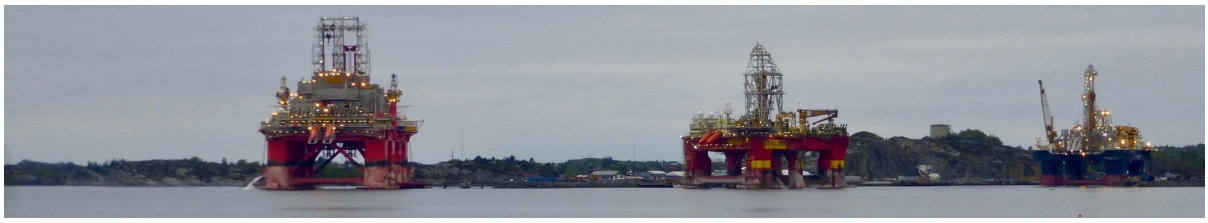

The response of a boreal deep-sea sponge holobiont to an acute crude oil exposure: a mesocosm experiment

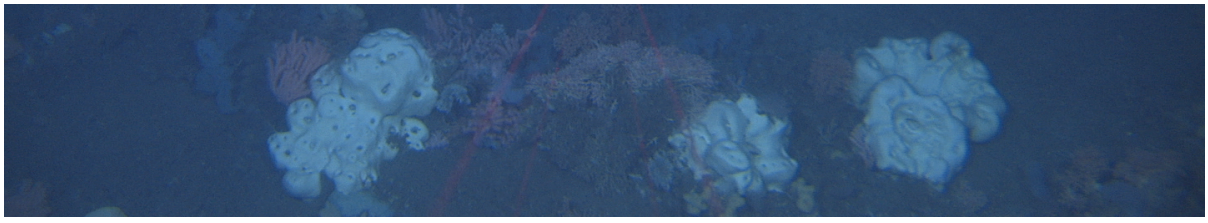

Mémoire de fin d'études présenté par Chloé STÉVENNE
en vue de l'obtention du grade de Master en biologie des organismes et écologie,
à finalité approfondie

Promoteurs :

Dr. R. BANNISTER
Prof. J.-C. PLUMIER
Année académique 2017-2018

Front page images:

Top: Personal picture, oil platforms under maintenance near Bergen, Norway
Bottom: MAREANO, Havforskningsinstitutet, sponge aggregation on the Norwegian Continental Shelf with *Geodia barretti*

Université de Liège
Faculté des Sciences
Département de Biologie, Écologie et Évolution

Havforskningsinstitutet
Benthic Resources and Processes Research Group

The response of a boreal deep-sea sponge holobiont to an acute crude oil exposure: a mesocosm experiment

Réponse d'une éponge holobionte boréale des milieux benthiques profonds à une exposition aiguë à du pétrole brut : une expérience en mésocosme

Membres du jury:

Docteur Raymond BANNISTER, Promoteur
Professeur Jean-Christophe PLUMIER, Promoteur
Docteur Stéphane ROBERTY
Professeur Mathieu POULICEK
Professeur Patrick DAUBY

Année académique 2017-2018

Acknowledgements

I would like to thank Dr Raymond Bannister for giving me the opportunity to integrate the Institute of Marine Research of Norway and gain valuable experience within the Benthic Resources and Processes research group. Thank you so much for your trust, your contagious enthusiasm and positivity, your encouragements and your valuable feedbacks.

I wish to thank Professor Jean-Christophe Plumier for supervising my thesis, always available for advice, answering my questions and helping me.

Thank you to Dr Bryan Wilson for his priceless help with the bioinformatics, his advice, his positive outlooks and “joie de vivre” which motivated me in my work.

Thank you to Dr Sonnich Meier for co-supervising this project, for his spontaneous help and rapid answers to my questions. Thank you to Elise Otnes, for the time we spent working together at Austevoll research station, for her company and her help with the chemistry data.

A special tusen takk to all who helped me during lab work. Tusen takk to Cathinka Krogness for her help at Austevoll research station and her continuous kindness. Tusen takk to Annhild Engevik for her previous help with the mesocosms and in the lab. Tusen hjertelig takk to Stig Maehle who would always come forward to help me with all aspects of my work at the microbial lab. Tusen takk to Anders Thorsen for his help with the microscope work. Danke schön to Dr Oliver Müller from the University of Bergen who spontaneously offered his help with the bioinformatics. Tusen takk to Laila Unneland and to all the people from the Institute of Marine Research who have, closely or remotely, helped me and allowed me to complete this thesis.

Lastly, I would like to thank my parents, France and Jean-Marc, for their trust and for always supporting me through all my projects. You have always been present when I needed you most but you have also allowed me to leave and learn from international experiences. I would like to thank my sister, Manon, for her honest feedbacks, her advice, her kindness and her craziness that will always bring a smile to my face. Finally, I would like to thank Gilles for his continuous support, for all the experiences we shared around the realisation of our theses in Norway and for his reassuring words when I most needed them.

Table of Contents

Abstract i

Résumé ii

List of abbreviations iii

1. Introduction ..... - 1 -
1.1. Oil spills and pollution in the marine environment ..... - 1 -
1.1.1. The petroleum industry and offshore oil production ..... *- 1 -*
1.1.2. Oil in Norway ..... *- 1 -*
1.1.3. Composition and types of oil ..... *- 3 -*
1.1.4. Inputs of oil in the ocean and oil spills ..... *- 3 -*
1.2. Benthic deep-sea environments ..... - 4 -
1.2.1. Ecology of deep-sea benthic ecosystems ..... *- 4 -*
1.2.2. Roles of deep-sea benthic communities ..... *- 5 -*
1.2.3. Vulnerability of the deep-sea ..... *- 6 -*
1.3. Sponges (Porifera) ..... - 7 -
1.3.1. Biology of sponges ..... *- 7 -*
1.3.2. Roles of sponges in the environment ..... *- 8 -*
1.3.3. Sponges seen as holobionts ..... *- 8 -*
1.3.4. Sponges grounds in the deep sea ..... *- 9 -*
1.4. Geodia barretti ..... - 10 -
1.4.1. Biology, ecological importance and economical value of Geodia barretti ..... *- 10 -*
1.4.2. Microbiome of Geodia barretti ..... *- 11 -*
1.4.3. Geodia barretti as a model organism ..... *- 11 -*
1.5. Hypotheses ..... - 12 -
1.6. Objectives ..... - 12 -

2. Materials and methods ..... - 13 -
2.1. Collection of sponge specimens ..... - 13 -
2.2. Experimental design and oil exposure setup ..... - 13 -
2.3. Respiration rates ..... - 15 -
2.4. Bacterial count ..... - 16 -
Water sampling ..... *- 16 -*
Bacterial count ..... *- 16 -*
2.5. Water filtration and tissue sampling for further analysis ..... - 19 -
2.6. Lysosomal membrane stability ..... - 19 -
2.7. DNA extraction, sequencing and processing ..... - 21 -
DNA extraction ..... *- 21 -*
1st PCR: amplification of the 16S V4 region ..... *- 22 -*
2nd PCR: addition of unique barcodes through a nested PCR ..... *- 22 -*
Clean-up & pooling ..... *- 23 -*
High-throughput sequencing (HTS) ..... *- 24 -*
Bioinformatics on raw data (performed by Dr. B. Wilson) ..... *- 24 -*
Bioinformatics on OTU table ..... *- 24 -*
Search for oil degraders ..... *- 25 -*
2.8. Data analysis and statistics ..... - 25 -

3. Results ..... - 26 -
3.1. Respiration rates ..... - 26 -

3.2. Bacterial count ..... - 28 -
3.3. Lysosomal membrane stability ..... - 28 -
3.4. Microbiome ..... - 29 -
Comparison of sponge and seawater microbial communities ..... *- 30 -*
Sponge microbial communities ..... *- 31 -*
Oil degraders in sponges ..... *- 35 -*

4. Discussion ..... - 37 -
4.1. Physiological effects on the sponge host ..... - 37 -
Respiration ..... *- 37 -*
Cellular stress ..... *- 39 -*
Sponge pumping rates and bacterial densities ..... *- 40 -*
4.2. Effects on the associated microbiome ..... - 41 -
4.3. Implications and future prospects ..... - 44 -

5. Conclusion ..... - 47 -

References ..... - 48 -

Supplementary Material ..... - 54 -
A. **Summary of experimental and recovery periods** ..... - 54 -
B. **Chemistry of the water during exposure period** ..... - 55 -
C. **Weight of sponge explants & volume of water in incubation chamber** ..... - 55 -
D. **Respiration data & summary** ..... - 56 -
E. **Lysosome data & summary** ..... - 58 -
F. **Sponge respiration – LME model checking plots** ..... - 60 -
G. **Background respiration – ANOVA model checking plots** ..... - 61 -
H. **LMS – ANOVA model checking plots** ..... - 62 -
I. **Table of barcoded F- and R-primers for 2nd PCR (nested)** ..... - 63 -
J. **Taxonomic profile of sponge and seawater samples at the class level** ..... - 64 -
K. **Alpha diversity of sponge and water microbial communities** ..... - 64 -

Abstract

The response of a boreal deep-sea sponge holobiont to an acute crude oil exposure: a mesocosm experiment

Chloé STÉVENNE

Supervisors: Dr. R. BANNISTER & Prof. J-C. PLUMIER
UNIVERSITY OF LIÈGE – Département de Biologie, Ecologie et Evolution
HAVFORSKNINGSINSTITUTET – Benthic Resources and Processes Research Group
Academic school year 2017-2018

Exploration and extraction of petroleum reserves in deep-sea marine ecosystems are ongoing activities world-wide and are continuously expanding with the identification of new reservoirs. Whilst a wealth of knowledge is known on the effects of oil spills on fish and other organisms in shallow water environments, there is a dearth of studies on the effects of subsurface oil spills (blowout events like the Deepwater Horizon) on deep-sea ecosystems. With exploration activities in deep-sea ecosystems predicted to increase, there are concerns regarding the accidental release of hydrocarbons into deep-sea ecosystems and the subsequent cascading effects on associated fauna. Sponges are abundant and ecologically valuable, known to be highly efficient filter feeders, contributing significantly to benthic pelagic coupling and providing habitat for a suite of organisms. However, sponges, which are sessile in nature, accumulate contaminants present in their ambient environment, potentially making them vulnerable to oil spills. Surprisingly, the impacts of oil on deep-sea sponges remain unexplored, despite sponges being particularly dominant around oil and gas exploration locations in the Northern Atlantic. Here are presented the findings from a mesocosm study, where the locally abundant deep-sea sponge *Geodia barretti* was exposed to three ecologically relevant oil concentrations for a duration of 8 days, followed by a recovery period of 30 days. A holistic approach elucidating the effects of oil on *G. barretti* focused on measuring changes in physiology (respiration rates), cellular stress (lysosomal membrane stability), and the structure of the sponge-associated microbiome using high-throughput sequencing of 16s rRNA gene amplicons.

G. barretti did not demonstrate strong sub-lethal stress effects in response to an acute crude oil exposure. Respiration showed varying patterns of increased and decreased rates with no significant effect from the treatments while lysosomes were significantly impacted by oil, displaying destabilisation of lysosomal membranes. A 30 day recovery period allowed the sponges to recover to control levels. *G. barretti*'s microbiome was stable at the phylum and class level across all treatments and days of exposure. Some evidence suggest that this high microbial abundance sponge could naturally host microorganisms which play a role in oil degradation / detoxification. Further research should investigate the effects of a long-term oil exposure on *G. barretti*'s physiology, cellular stress, metabolism and associated microbial community. Of particular interest is the uncovering of the functions of the sponge microbiome in relation to oil contamination.

Such studies enhance our understanding of the vulnerability and / or resilience of deep-sea sponges to hydrocarbon exposure, providing useful data for managing risks associated with oil and gas exploration in the Northern Atlantic.

Résumé

Réponse d'une éponge holobionte boréale des milieux benthiques profonds à une exposition aiguë au pétrole brut : une expérience en mésocosme

Chloé STÉVENNE

Promoteurs : Dr. R. BANNISTER & Prof. J-C. PLUMIER
UNIVERSITÉ DE LIÈGE – Département de Biologie, Ecologie et Evolution
HAVFORSKNINGSINSTITUTET – Benthic Resources and Processes Research Group
Année académique 2017-2018

L'exploration et l'extraction de réserves pétrolières dans les écosystèmes marins profonds sont des activités qui se diversifient dans les océans autour du globe grâce à l'identification de nouveaux réservoirs. Alors qu'il existe une richesse de connaissances sur les effets de pertes accidentelles d'hydrocarbures en mer sur les poissons et sur d'autres organismes des eaux peu profondes, les effets de pertes accidentelles de pétrole dans les fonds marins profonds (telle la catastrophe du Deepwater Horizon) ne sont que peu étudiés. L'attrait croissant de l'exploitation pétrolière en milieux marins profonds génère des inquiétudes par rapport aux impacts qu'une pollution aux hydrocarbures aurait sur les milieux benthiques et sur la faune associée. Les éponges, abondantes en milieu marin, possèdent une valeur écologique importante : elles sont connues pour leur haute capacité de filtration (microphagie suspensivore) qui leur permet de contribuer de manière significative au couplage benthique-pélagique et elles constituent un habitat pour une variété d'organismes. Cependant, les éponges, de par leur nature sessile, accumulent les contaminants présents dans l'environnement les rendant potentiellement vulnérables à une exposition au pétrole. Étonnement, les impacts du pétrole sur les éponges des fonds benthiques profonds sont non élucidés malgré la dominance des éponges aux alentours de sites d'exploration pétrolière dans l'Atlantique Nord. Ici nous présentons les résultats d'une étude en mésocosme pendant laquelle une éponge abondante de l'Atlantique Nord, *Geodia barretti*, était exposée à trois concentrations de pétrole brut pendant 8 jours suivis par une période de récupération de 30 jours. L'approche holistique s'est concentrée sur la mesure des changements physiologiques (taux de respiration), de stress cellulaire (stabilité des membranes lysosomales) et de structure de la communauté microbienne associée à l'éponge en utilisant le séquençage haut débit du gène ARNr 16S.

G. barretti n'a pas démontré d'effets de stress sub-létaux marqués en réponse à l'exposition aiguë au pétrole brut. La respiration a montré des variations avec des taux réduits ou élevés mais sans effet significatif induit par les traitements tandis que les lysosomes étaient significativement impactés par le pétrole avec une déstabilisation des membranes lysosomales. Une période de récupération de 30 jours a permis aux éponges de retourner à des valeurs contrôles. Le microbiome de *G. barretti* était stable au niveau du phylum et de la classe pour les différents traitements et au cours des différents jours d'exposition. Quelques indices suggèrent que cette éponge à haute densité microbienne pourrait naturellement abriter des microorganismes qui jouent un rôle dans la dégradation / détoxification du pétrole. Etudier les effets d'une exposition à long-terme sur la physiologie, le stress cellulaire, le métabolisme et la communauté microbienne de *G. barretti* constituent des prospectives de recherches futures. La découverte des fonctions du microbiome de l'éponge en relation avec une contamination au pétrole est d'un intérêt certain.

De telles études améliorent notre compréhension de la vulnérabilité et / ou de la résilience des éponges des fonds marins profonds à une exposition aux hydrocarbures. Elles fournissent ainsi des données utiles pour la gestion des risques associés à l'exploration pétrolière dans l'Atlantique Nord.

List of abbreviations

ANOVA – Analysis Of Variance
APPEA – Australian Petroleum Production & Exploration Association
Bp – Barometric pressure
bp – base pairs
BSA – Bovine Serum Albumin
CCA – Constrained Correspondence Analysis
CMFS – Ca^{2+} Mg^{2+} Free Saline
DAPI – 4',6-diamidino-2-phenylindole
DI H_2O – Deionized water
DMSO – Dimethyl Sulfoxide
DNA – Deoxyribonucleic Acid
DO – Dissolved Oxygen
DOC – Dissolved Organic Carbon
DW – Dry Weight
DWH – Deepwater Horizon
EDTA – Ethylenediaminetetraacetic acid
EEZ – Exclusive Economic Zone
EIA – U.S. Energy Information Administration
HEPES – 4-(2-hydroxyethyl)-1-piperazineethanesulfonic acid
HMA – High Microbial Abundance
HPLC – High Performance Liquid Chromatography
HTS – High-Throughput Sequencing
IRT – Inhibitor Removal Technology®
ITOPF – International Tanker Owners Pollution Federation
LMA – Low Microbial Abundance
lme – linear mixed effect model
LMS – Lysosomal Membrane Stability
MAPK – Mitogen-Activated Protein Kinase
NAS – U.S. National Academy of Sciences
NCS – Norwegian Continental Shelf
NINA – Norwegian Institute for Nature Research
NOAA – National Oceanic and Atmospheric Administration
NSC – Norwegian Sequencing Center
OSPAR – Oslo-Paris Convention for the Protection of the Marine Environment of the North-East Atlantic
OTU – Operational Taxonomic Unit
PAH – Polycyclic Aromatic Hydrocarbon
PERMANOVA – Permutational Multivariate Analysis of Variance
PCR – Polymerase Chain Reaction
POC – Particulate Organic Carbon
POP – Persistent Organic Pollutants
QIIME – Quantitative Insights into Microbial Ecology
RH – Relative Humidity
RNA – Ribonucleic Acid
ROS – Reactive Oxygen Species
rpm – rounds per minute
rRNA – ribosomial Ribonucleic Acid
SIMPER – Similarity Percentage
SRB – Sulphate Reducing Bacteria
TSS – Total Suspended Solids
VOC – Volatile Organic Compound
WW – Wet Weight

1. Introduction

1.1. Oil spills and pollution in the marine environment

1.1.1. The petroleum industry and offshore oil production

According to the Australian Petroleum Production & Exploration Association (APPEA), "oil is the world's most important fuel and underpins our high standard of living" (APPEA 2017). Oil and its associated by-products are essential for transportation systems but also for the production of plastics, lubricants, waxes, asphalts, pesticides, fertilisers and many other chemicals (APPEA 2017) making their production one of the most lucrative industry in the world. Globally, in 2016, it was estimated that 96.5 million barrels of oil were consumed each day, while approximately 92 million barrels were produced daily (BP 2017). Total world consumption of liquid fuels is predicted to rise from 95 million barrels per day (b/d) in 2015 to 113 million b/d by 2040, representing a 18% increase (EIA 2017a). As the demand for oil steadily increases, exploration for new sites is taking place. Due to a decline in easily accessible resources, oil drilling is increasingly carried out in deeper offshore areas. The offshore oil and gas industry has followed a rapid growth in the recent decades and it now represents over 30% of the global oil production (Bennear 2018). Improved technologies allow drilling in deeper waters, with "ultra-deep-water" oil and gas extraction taking place at Shell's deepest oil project, the Stones field located in the Gulf of Mexico, which extracts oil and gas from around 2900 meters (SHELL 2018).

1.1.2. Oil in Norway

Norway is Europe's first and the world's 14th most important producer of petroleum extracting more than 2% of the global reserves (EIA 2017b). Norwegian petroleum activities take place in the North Sea, the Norwegian Sea and the Barents Sea, with about 85 active fields of production and 8800 km of pipeline networks (Norwegian Petroleum Directorate and Norwegian Ministry of Petroleum and Energy 2018). The Norwegian Exclusive Economic Zone (EEZ) spreads over those 3 large marine ecosystems (**Figure 1**) which are considered of great ecological and economical value as they host a vast variety of marine species, are key fishing areas and contain significant petroleum reservoirs (Blanchard et al. 2014).

The Lofoten area, located between the Norwegian Sea and the Barents Sea, is unexploited but contains promising oil and gas reservoirs which fuel ongoing debate. This region has a high ecological value with a rich bird life, important spawning and nursery areas for abundant fish stocks, and important benthic communities such as sponge aggregations and the world's largest deep-sea cold-water coral reef, the Røst Reef (Freiwald et al. 2004; Blanchard et al. 2014). The Norwegian Institute for Nature Research (NINA) investigated the vulnerability of the Lofoten and Barents Sea areas to oil spills and concluded that these ecosystems were more fragile in the face of an accidental spill (Forsgren et al. 2009). Indeed, cold water temperature, darkness and ice slow down the oil degrading process and impede clean-up activities; moreover, fewer species confer less resilience to the ecosystem and some keystone species such as fish and important benthos are thought to be particularly vulnerable to oil exposure (Forsgren et al. 2009). However, few studies have actually studied the effects of oil exposure on deep-water benthic fauna along the Norwegian Continental Shelf (NCS).

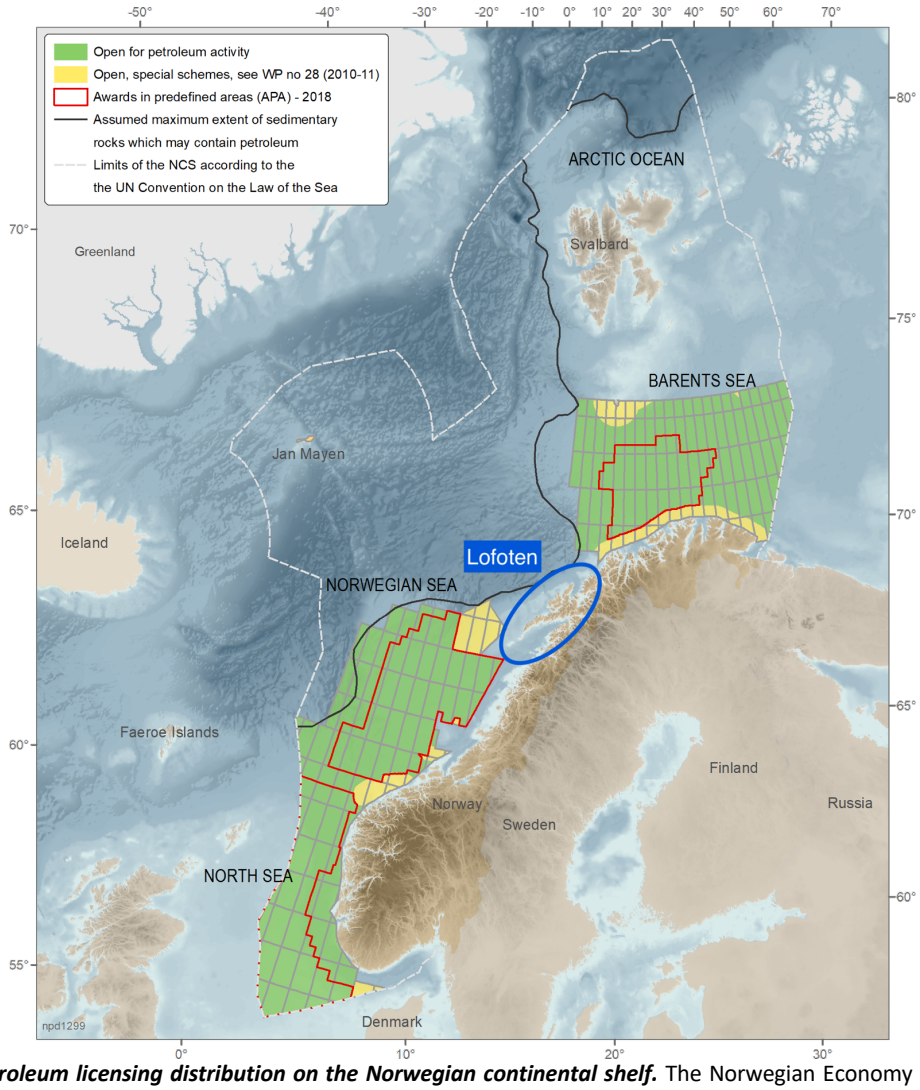

Figure 1 - Petroleum licensing distribution on the Norwegian continental shelf. The Norwegian Economy Exclusive Zone (EEZ) encompasses the North Sea, the Norwegian Sea and the Barents Sea. The Lofoten area is currently closed for petroleum activities but is at the centre of on-going debates. NCS = Norwegian Continental Shelf. Modified from (Norwegian Petroleum Directorate 2018).

Due to global warming, the sea ice cover in the Arctic is retreating opening new commercial routes in the north and creating new possibilities for the petroleum industry. It was predicted that by mid-century, new trans-arctic shipping routes will be navigable during the warmer months (Smith and Stephenson 2013). The US Geological Survey estimated that "about 30% of the world's undiscovered gas and 13% of the world's undiscovered oil" may be found in the area north of the Arctic circle (Gautier et al. 2009) and another study stated that exploitation of oil and gas in the Arctic is "technologically possible in the future" (Petrick et al. 2017). To this day, five of the eight countries bordering the arctic region (Norway, Canada, Greenland, Russia and the United States) are pursuing the exploration of oil and gas reserves and / or development of their extraction in the Arctic (Word 2014). High stakes surround oil exploration in the North and on the NCS but very few studies evaluating the impacts of accidental spills in northern ecosystems exist.

1.1.3. Composition and types of oil

Oil and natural gas constitute what we commonly call petroleum. They originate from the decomposition and pressurization of organic material which occurred over millions of years and are trapped in geological basins such as black clay layers under the seabed, layers of sandstones, shales or coals (APPEA 2017; Norwegian Petroleum Directorate 2017). Oils are composed of various chemicals whose proportions in each type of oil varies greatly meaning that their toxicity is often difficult to assess (NOAA 2017a). Oils are classified in four main types: very light (e.g. gasoline), light (e.g. diesel), medium (most crude oils) and heavy (heavy crude oils) (NOAA 2017b).

If released in the marine environment, lighter and medium oils mostly endanger the water column and intertidal resources whereas heavy oil not only severely impact intertidal areas but also contaminate sediments on the long term as their weathering rate is slow and their evaporation or dissolution low (NOAA 2017b). Crude oils release volatile organic compounds (VOCs), toxic when inhaled but not persistent in the ocean, as well as polycyclic aromatic hydrocarbons (PAHs) which present a high resilience in the environment (NOAA 2017c). PAHs are a class of organic compounds containing only hydrogen and carbon and they consist of two or more aromatic rings (Boehm 1964). The weathering of petrogenic compounds is a complex mechanism involving different processes such as evaporation / volatilization, solubilization and biodegradation by microorganisms. Most PAHs are non-volatile and solubilization may only be significant for the 2- and 3-ringed PAHs meaning that biodegradation is the main process through which PAHs may be weathered (Boehm 1964). The resilience of PAHs in the environment has raised many concerns and PAHs are considered the main class of compounds responsible for toxic effects in marine organisms (Sørensen et al. 2017). PAHs were found to be efficiently incorporated in lipid-rich tissues of filter feeding animals as their low water solubility and hydrophobicity enhances their aggregation potential with particulate matter (Batista et al. 2013).

1.1.4. Inputs of oil in the ocean and oil spills

As global oil production is increasingly carried out offshore concerns about loss of hydrocarbons in the marine environment are valid. On average, 1 300 000 metric tons of petroleum were released in the sea each year between 1990 and 1999 (NAS 2002). Understanding the significance of this massive loss of petroleum substances in the environment each year presents challenges. Indeed, diverse inputs of oil exist: they have different sizes, different rates of discharge and release different types of petroleum substances. Depending on all those factors and on the location of the spill, impacts on the natural environment vary greatly (NAS 2002). The NAS (2002) distinguishes between four main types of oil inputs: natural seeps, petroleum consumption, petroleum extraction and transportation. Natural seeps contribute to around 45% of the input of oil in the ocean but, as the rate of release is low, the surrounding biota can adapt and survive. Petroleum consumption leads to the release of hydrocarbons which contributes to about 40% of the inputs in the marine environment. Those are slow chronic releases, they are frequent and widespread and mostly endanger estuaries and bays where anthropogenic activities are present. The most hazardous releases are related to petroleum extraction and petroleum transportation via tankers or pipelines. They respectively account for 3% and 12% of yearly

oil inputs in the ocean but their potential for large accidental spills makes them a real threat to the surrounding environment especially if they occur close to coastal areas (NAS 2002).

Oil spills are the accidental loss of important quantities of oil in the marine environment; they can originate from incidents at extraction platforms (ex: blowouts, leakages, …), from tanker incidents or leakages from transport pipelines. Over 10 000 spills due to tanker incidents were recorded between 1970 and 2016 with an estimated 5.73 million tons of oil lost in the marine environment (ITOPF 2014). Accidental releases of hydrocarbons can originate from various routine activities during each phase of the development of an oil field (appraisal, development, production and decommissioning) (Vad et al. 2018) and the likelihood of an accidental blowout or spill is increasing with the depth of the operations (Muehlenbachs et al. 2013). Such incidents, depending on their size, can have unprecedented consequences on various marine organisms and, consequently, on ecosystem functioning.

One of the most dramatic incident in the history of oil production is the Deepwater Horizon (DWH) blowout that occurred in the Gulf of Mexico in April 2010. In spite of all the efforts to contain the spill, an estimated 3.7 million barrels of oil remained in the environment out of the 4.9 million barrels originally released (Murawski et al. 2016). Contamination spread to an area of 144 192 km^2 on the northern coastal and continental shelf of the Gulf of Mexico (Murawski et al. 2016) and extended to the deep-sea ecosystems with effects on the benthic communities found as far as 14 km away from the spilling site (Fisher et al. 2016). A shift in species composition of phytoplankton could be observed along with an increase in bacterial densities, fish larvae presented cardiac malfunction and abnormalities (Murawski et al. 2016). Bacteria and phytoplankton exposed to oil and dispersant secrete sticky exopolymeric substances which contribute to trapping hydrocarbons in marine snow and transporting them to the deep-sea benthic environment (Murawski et al. 2016). Notable changes in meiofauna and macrofauna abundance and diversity which persisted for at least four years were observed (Baguley et al. 2015; Fisher et al. 2016). Following the DWH, an increase in oxygen consumption and in denitrification indicated that there was a possibility the nature of the microbial communities was altered (Fisher et al. 2016). Tissue necrosis was observed in deep-sea corals whose skeletons were sometimes secondarily colonized by hydrozoans (Fisher et al. 2016).

In a world where oil consumption is high and where environmental pollutions are increasingly regarded as important issues to solve, it seems that acquiring a more comprehensive and in-depth knowledge of the impacts of oil pollution is essential. Marine environments are particularly important to study as there is an increased focus on seabed mining (Bell et al. 2015) and as offshore oil production and transportation are not negligible. Moreover, it seems that major oil spill events have recently stimulated research interests on the effects of hydrocarbon spills (Negri et al. 2016).

1.2. Benthic deep-sea environments

1.2.1. Ecology of deep-sea benthic ecosystems

The deep-sea is the largest ecosystem on Earth but remains one of the least explored and least understood region of the globe. The pelagic deep-sea below 200 m represents approximately 95% of the total volume of the ocean (Thurber et al. 2014). The zone comprised between 200 m and 1000 m is called the dysphotic zone (also referred as the twilight zone) and is characterized by a rapid dissipation of light as depth increases which means that

photosynthesis is impossible (NOAA 2018). The physical environment of the deep-sea floor is considered as extreme: pressure is high, light is (mostly) absent and temperature and food inputs are low (Thistle 2003). For a long time, the deep sea was considered a dark barren and lifeless environment that could be remorselessly exploited for biological and sea-floor resources, but, by the end of the 20th Century, the deep-sea was recognized as a rich diversified habitat with unique ecosystems that can support high biodiversity (Ramirez-llodra et al. 2011).

The species found in the deep sea are diverse and, at high taxonomic levels, they are similar to the species found in shallow water environments (Thistle 2003). As depth progresses from shelf to slope, diversity of the in-fauna (burrowing animals living in the bottom deposit of the ocean) and epibenthic fauna increases significantly at depths between 100 and 300 m (Canganella and Kato 2014). Deposit feeders (animals ingesting and retrieving nutrients from the sediment), necrophages and suspension feeders (animals filtering or intercepting epibenthinc plankton or organic particles in the water column) are dominant in the deep-sea (Thistle 2003).

1.2.2. Roles of deep-sea benthic communities

Deep-sea benthic communities often form what we call “biogenic habitats”. Biogenic habitats, as defined by Thurber et al. (2014), are “areas of extensive three-dimensional structure created by organisms themselves” which “can cover tens of square kilometres of the deep seafloor”. They provide enhanced dietary resources, diversified substratum on which benthic organisms can settle, they constitute a refuge from predators or from physical disturbances and they act as nurseries for several deep-sea species (Thurber et al. 2014).

Deep-sea benthic fauna carry out vital functional roles in the environment. They are a critical part of the base of the food web through their biomass production, they participate in sediment bioturbation and stabilization, they comprise active organic decomposers which regenerate nutrients and they are home to complex microbial communities which notably have important roles in waste detoxification (Fisher et al. 2016). The abundance of bacteria and archaea associated with benthic fauna and surface sediments increases significantly at higher latitudes where they play vital key roles in biogeochemical cycling (Danovaro et al. 2016). They are involved in carbon and nutrient cycling and energy transfer to the higher trophic levels (Danovaro et al. 2016).

The food web interactions in benthic deep-sea ecosystems remains challenging to model and to understand due to the fact that it is not an easily accessible environment for sampling and measurements. The main processes occurring in the deep-sea are known but most environmental studies only bring forward isolated parts of the ecosystem which means that we do not yet comprehend the extent of their contribution to global food chains and biogeochemical cycles (Soetaert and van Oevelen 2009). The deep-sea constitutes a carbon sink and is believed to absorb ~ 25 % of anthropogenic carbon emissions (Fisher et al. 2016). Deep-sea benthic ecosystems depend on organic waste derived from primary production in the euphotic zone (0 to 200 m depth where photosynthesis occurs) which are primarily consumed by suspension and epibenthic feeders, such as sponges, which, in this way, actively participate to benthic-pelagic coupling (**Figure 2**) (Soetaert and van Oevelen 2009). Nutrient cycling and the function of biological pump of the deep-sea provide supporting services (e.g. biomass production and nutrient provisioning) and regulating services (natural carbon sequestration, buffer action on anthropogenic releases of carbon in the atmosphere, waste

absorption and detoxification) that directly or indirectly benefit the marine ecosystem and humans (Thurber et al. 2014).

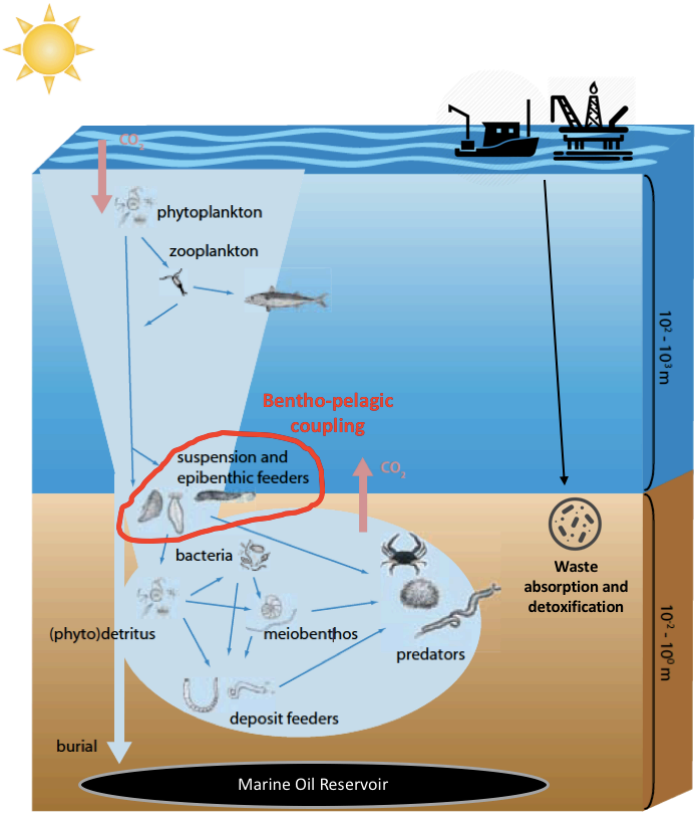

Figure 2 – Simplified view of the deep-sea food web and ecosystem function *(modified from (Soetaert & van Oevelen, 2009))*

Plankton in the euphotic zone participate to primary production. Detritus in the form of organic matter sink to the deep-sea where there are primarily consumed by suspension and epibenthic feeders through their active filtering of the water mass overlying the bottom. They constitute a crucial link in benthic-pelagic coupling. The remainder of particulate organic matter is ingested by bacteria, deposit feeders and meiobenthos which inhabit the sediment. The detritivores are in turn consumed by predators (secondary production). An important part of the organic matter is buried in the sediment constituting a major carbon sink. The deep-sea provides an environment where waste and pollutants are stored and / or detoxified through biotic and abiotic processes.

1.2.3. Vulnerability of the deep-sea

It is important that we enhance our understanding of the deep ocean and its resilience in the face of increased human activities. Indeed, because our knowledge is poor, it is very likely that effects on deep-sea ecosystems will go undetected and that changes will occur before its natural state is fully understood (Glover and Smith 2003).

The National Oceanic and Atmospheric Administration (NOAA), in its Strategic Plan for Deep-Sea Coral and Sponge Ecosystems, identifies the main anthropogenic threats to deep-sea ecosystems, all of which have not yet been adequately investigated. Human activities that represent a danger to deep-sea coral and sponges assemblages are bottom trawling, coral harvesting, mineral exploration and extraction, marine debris, submarine cable and pipeline deployment as well as oil and gas exploration (NOAA and Coral Reef Conservation Program 2010). Moreover, these ecosystems are likely to be impacted by processes such as global warming, ocean acidification and invasive species (NOAA and Coral Reef Conservation Program 2010). Conditions of low temperature, low organic carbon and low nutrient inputs in the deep-sea could make it particularly vulnerable to environmental changes. For example, hydrocarbons that accumulate in sediments following an oil spill will probably degrade more slowly in deep-sea benthic ecosystems than in shallow portions of the water column or at the surface (Fisher et al. 2016).

Benthic environments are particularly threatened by persistent organic pollutants (POP) such as PAHs which remain in sediments for long periods of time. Various studies emphasize that sessile benthic organisms are especially at risk as they live in close association with the sediment and are unable to actively avoid exposure due to their mostly sedentary lifestyles

(Egres et al. 2012; Lee and Lin 2013; Negri et al. 2016). Sponges, in particular, could be greatly impacted by oil particles and their ecological function may deteriorate as they are filter feeding sedentary organisms. Sub-lethal stress responses to total suspended solids (TSS) originating from water-based drilling muds were observed in the deep-sea sponge *Geodia barretti*, indicating a compromised health (Edge et al. 2016). It has been shown that sponges can accumulate anthropogenic contaminants such as PAHs (Batista et al. 2013). Because sponges are habitat-forming organisms, their contamination could further impact associated organisms and epifauna by having effects on the habitat use, feeding behaviors and survival (Roberts et al. 2008). Batista et al. (2013) found that marine sponges could be used as bioindicators as their levels of PAH contamination accurately reflected pollution in the surrounding environment. Understanding and characterizing responses of benthic organisms such as sponges and using them as bioindicators for oil pollution would help improve impact assessments models as well as provide information for petroleum industries and governments in view of the mitigation of environmental impacts (Negri et al. 2016).

The NOAA's Strategic Plan emphasize that exploration and research are imperative to locate and characterize deep-sea coral and sponge ecosystems, to understand their biology and ecology and to evaluate the extend and degree of impact caused by human activities (NOAA and Coral Reef Conservation Program 2010). As both J.J. Bell (2015) and A.P. Negri (2016) pointed out, very few studies on the impact of oil spills or hydrocarbon contamination on sponges have been carried out and are therefore greatly needed (Bell et al. 2015; Negri et al. 2016). Moreover, sponges are dominant in areas where oil and gas exploration are taking place (Bell et al. 2015) and, as they constitute vital components of marine ecosystems, it is essential we investigate the impacts of petroleum activities on their health (Edge et al. 2016).

1.3. Sponges (Porifera)

1.3.1. Biology of sponges

Sponges (phylum *Porifera*) are multicellular non-bilaterians organisms that evolved from the Precambrian (Carballo and Bell 2017). Considered the "phylogenetically-oldest extant Metazoans" (Brümmer et al. 2008), they are grouped into four distinct classes based on the nature of their skeleton. Demospongiae, Hexactinellida and Homoscleromorpha harbour siliceous spicules whereas Calcarea have biomineral-spicules of calcium-carbonate (van Soest et al. 2012). Sponges present a simple morphology: the outer layer is constituted of flattened cells called the pinacocytes whereas the inner chambers and canals are lined with flagella-bearing cells, the choanocytes, which create water currents for the filtering activity of the sponge. Those two cell types delimit the mesophyl, a collagenous matrix containing individual cells, supporting fibers such as spongin and spicules which constitute the skeleton (van Soest et al. 2012). Sponges possess many mobile cells and totipotent cells (Hogg et al. 2010), meaning that they are capable of tissue regeneration (Wulff 2010) and cellular rearrangement (Bond 1992). The simplicity and the adaptability of their body plan are undoubtedly linked to their evolutionary success over the last 700 million years (Carballo and Bell 2017). Sponges are strictly aquatic organisms but are found in a wide range of marine and freshwater environments ranging from tropical and temperate regions to polar seas (Bell and Carballo 2008). They successfully colonize coastal and deep-sea areas and settle in various habitats, from hard- to soft-bottoms environments (Thakur and Singh 2016).

1.3.2. Roles of sponges in the environment

Despite their simple body-plan and their sessile lifestyle, sponges are particularly efficient at capturing food through their filter-feeding activity (Pallela and Ehrlich 2016) with the capacity to pump up to 900 times their body volume of water per hour (Ludeman et al. 2017). The ingested suspended particles and dissolved nutrients are released as by-products which can be used by other organisms. In this way, sponges contribute greatly to the recycling of nutrients between benthic and pelagic communities known as benthic-pelagic coupling (Ludeman et al. 2017).

Sponges are important members of benthic communities across different ecosystems in marine and freshwater environments (Bell et al. 2015). Bell (2008) highlights the diversity of sponges' contributions to the ecosystem's functioning: they bioerode or consolidate sediments which shape the benthic substrate, they are vital to the nutrient cycling and energy flow as part of the benthic-pelagic coupling, they facilitate primary production through their association with microorganisms, they serve as food for higher trophic levels, they provide habitats or shelter and their interactions or associations with other organisms have potentially unique impacts which still need to be investigated (Bell 2008). Additionally, sponges, in association with the microorganisms they host, have shown detoxifying abilities (e.g. detoxification of cadmium, mercury, okadaic acid) which suggest that they might participate in bioremediation of certain contaminants (Santos-Gandelman et al. 2014; Konoki et al. 2015; Mori et al. 2016).

Sponges, as a side-effect of their sessile nature, have evolved the capacity to produce a wide array of secondary metabolites which they use to support their symbiotic fauna, for predator defence and for spatial competition (Hogg et al. 2010). The compounds sponges metabolize are highly bioactive and, in addition to their ecological value (Thakur and Singh 2016), they have an economical value. More than 5300 different metabolites from marine sponges have been characterized with more being discovered each year and many present biomedical applications due to their properties such as anticancer, anti-inflammatory or antifungal (Sunil Kumar 2016).

1.3.3. Sponges seen as holobionts

The evolutionary success of sponges is undoubtedly linked to the intricate relationship they maintain with their microbial symbionts. Microorganisms can represent between 40% and 60% of the sponge total biomass and are found in the mesophyl either intercellularly or intracellularly (Carballo and Bell 2017). Although little is known about the nature of the symbiotic relationships between sponges and their associated microbiome, microorganisms are certainly indispensable to the sponge's health. The association between sponges and microbes appeared over 600 million years ago in the Precambrian and is believed to be one of the most ancient symbiosis between prokaryotes and a metazoan (Wilkinson 1984). Sponge-microbe co-speciation is supported by different studies and sponges display specific microbial communities which often differ greatly from the surrounding seawater and sediment (Schöttner et al. 2013). Sponges also developed a resistance against pathogenic microbes via the production of antimicrobial compounds which are highly specific in effect (Thakur and Singh 2016). Some evidence showed that sponges benefit from the metabolites produced by a consortium of organisms such as ammonium-oxidizing archaea, nitrite-oxidizing and sulphate-reducing bacteria as well as anaerobic phototrophs or cyanobacteria

for shallow water species (Webster and Blackall 2009). Because the sponge metabolism is so intricately linked to the activities of its microbial partners, the term “holobiont” is more accurate to define the ecological unit formed by the sponge and all its associated symbiotic microorganisms, particularly in its responses to environmental factors (Webster and Taylor 2012).

1.3.4. Sponges grounds in the deep sea

The most representative sponges inhabiting the deep ocean are the hexactinellids (Hyalospongiae) with six-rayed silica spicules, and the Desmospongiae with either different-shaped silica spicules or the protein spongin (Canganella and Kato 2014). Sponges represent the most diverse faunal group in cold-water reefs ecosystems which are considered “biodiversity hotspots” in the deep sea (Schöttner et al. 2013). Deep-sea sponge aggregations (**Figure 3**), as defined by the OSPAR commission, are sponge aggregations principally composed of Hexactinellida and Demospongiae, occurring between water depths of 250-1300 m on soft or hard substrata where the water temperature ranges from 4 to 10 ºC and where the current is of moderate velocity (OSPAR commission 2010). The desmosponge aggregations of NCS are dominated by the species *Geodia barretti*, *Geodia macandrewii*, *Geodia atlantica*, *Geodia phlegraei* and *Sryphnus spp.* whose combined abundance and biomass reached those of sponge populations in tropical barrier reefs (Kutti et al. 2013a). Sponge grounds in the deep sea are particularly important: because of the sparsity of complex structural habitats, sponge aggregations represent the main benthic habitat and refuge for fish and other benthic fauna (Hogg et al. 2010). In this way, sponge grounds constitute a patchy network of habitats which greatly enhance the benthic biodiversity as well as the microbial richness in the deep sea (Hogg et al. 2010). Additionally, cold-water coral reef systems and neighbouring sponge grounds are believed to play a vital role in marine biogeochemical cycling as they represent hotspots of carbon processing in a nutrient-limited deep-sea ecosystem (Cathalot et al. 2015).

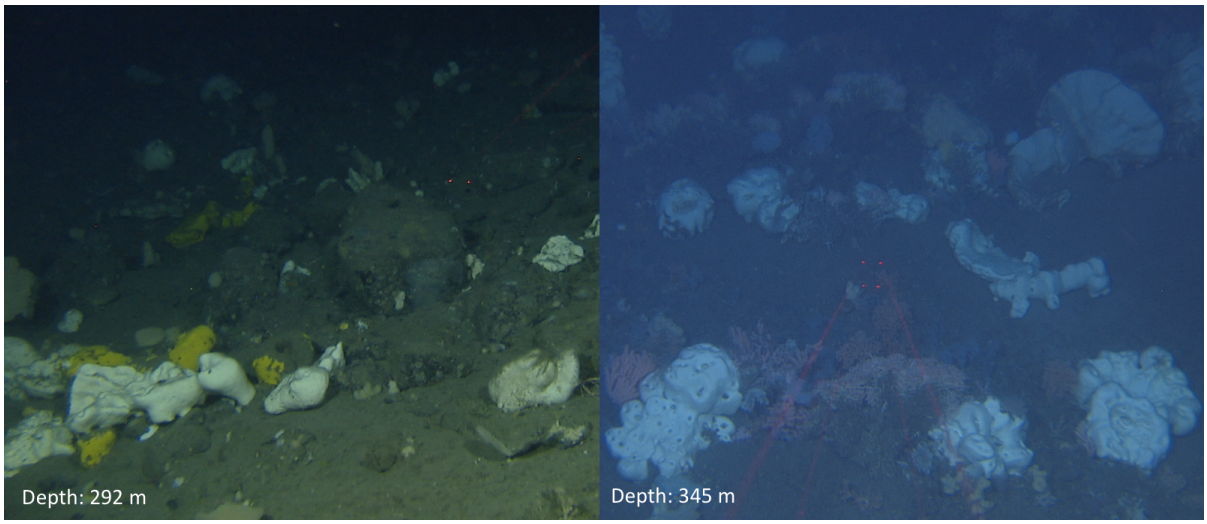

Figure 3 – Sponge aggregations on the Norwegian Continental Shelf. Sponge aggregations on the NCS are dominated by *Geodia spp*. (white sponges) and *Stryphnus spp.* (yellow sponges). They constitute complex habitats which enhance the local benthic biodiversity and microbial richness in the deep-sea. Images obtained during analysis of video footage from MAREANO (P. Mortensen, Institute of Marine Research & MAREANO project, www.mareano.no).

1.4. Geodia barretti

1.4.1. Biology, ecological importance and economical value of *Geodia barretti*

Geodia barretti (Bowerbank 1858) is a boreal desmosponge of the family Geodiidae. It is a leucon type sponge, usually white, light yellow or light brown in colour, it is spherical or of an irregular shape and can grow to up to at least 80 cm in diameter and 38 kg of wet weight (WW) (Cárdenas et al. 2013). The sponge possesses one to many openings named preoscules which are depressions up to several centimetres protecting the true oscules; the mesophyl is rich in silica spicules and is protected by an outer layer, the cortex (**Figure 4**) (Cárdenas et al. 2013). *G. barretti* dominate boreal "osturs" which are deep-sea desmosponge aggregations occurring around Norway, Sweden, the Faeroe Islands, parts of the western Barents Sea and the South of Iceland (OSPAR commission 2010). *G. barretti* thrives at depths from 30 to 2000 m and in temperatures ranging from 3 to 9ºC (Cárdenas et al. 2013). Some specimens have been found as far south as the Mediterranean and as far north as the Arctic ocean north of Svalbard (Cárdenas et al. 2013). Around Norway, *G. barretti* is abundant in fjords and on the continental shelf, from shallow to deep habitats (OSPAR commission 2010).

G. barretti is a dioecious and oviparous sponge with oocytes or spermatic cysts clustered within the mesophyl (Spetland et al. 2007). The sponge releases gametes early summer and in October, coinciding with the sedimentation of organic matter following the spring and autumn phytoplankton blooms (Spetland et al. 2007). This suggests that, like most deep-water sponges, *G. barretti*'s reproduction is highly dependent on seasonality of food supplies (Hogg et al. 2010). In the wild, the sponge showed rates of 1.5 µmol O_2 g^{-1} DW h^{-1} and water pumping rates of 3000 L kg^{-1} DW day^{-1} respiration (DW = dry weight) which is lower than shallow water desmosponge but is believed to increase contact time of seawater with the sponge and its associated microbial community (Kutti et al. 2013a). The sponge, although it shows slow metabolic rates, hosts vital functions in carbon and nutrient cycling. They filter up to 99% of bacteria in the water, efficiently feed on dissolved organic carbon (DOC) and detritus (POC, particulate organic carbon) and produce a net release of nitrogen as NO_3^- (Leys et al. 2017). A study on the Traenadypet coral MPA (Marine Protected Area) showed that, within a 300 km^2 area, the population of *G. barretti* could consume 60 tons of carbon and filter up to 250 million m^3 of water each day (Kutti et al. 2013a), meaning that this sponge species carries a significant ecological role in deep-sea benthic ecosystems.

G. barretti produces secondary metabolites which have potential for biotechnological applications. The sponge synthesizes the indole alkaloid barettin which was first isolated in 1986 and showed the ability to inhibit electrically induced muscular contractions (Lidgren et al. 1986). Barettin compounds possess an efficient antifouling activity against barnacles (Sjögren et al. 2004). Additionally, barettin showed antioxidant and anti-inflammatory functions which could have biomedical uses (Lind et al. 2013). In addition to its ecological importance, *G. barretti* has an economical value due to the secondary metabolites it produces and the possibility for biotechnology applications.

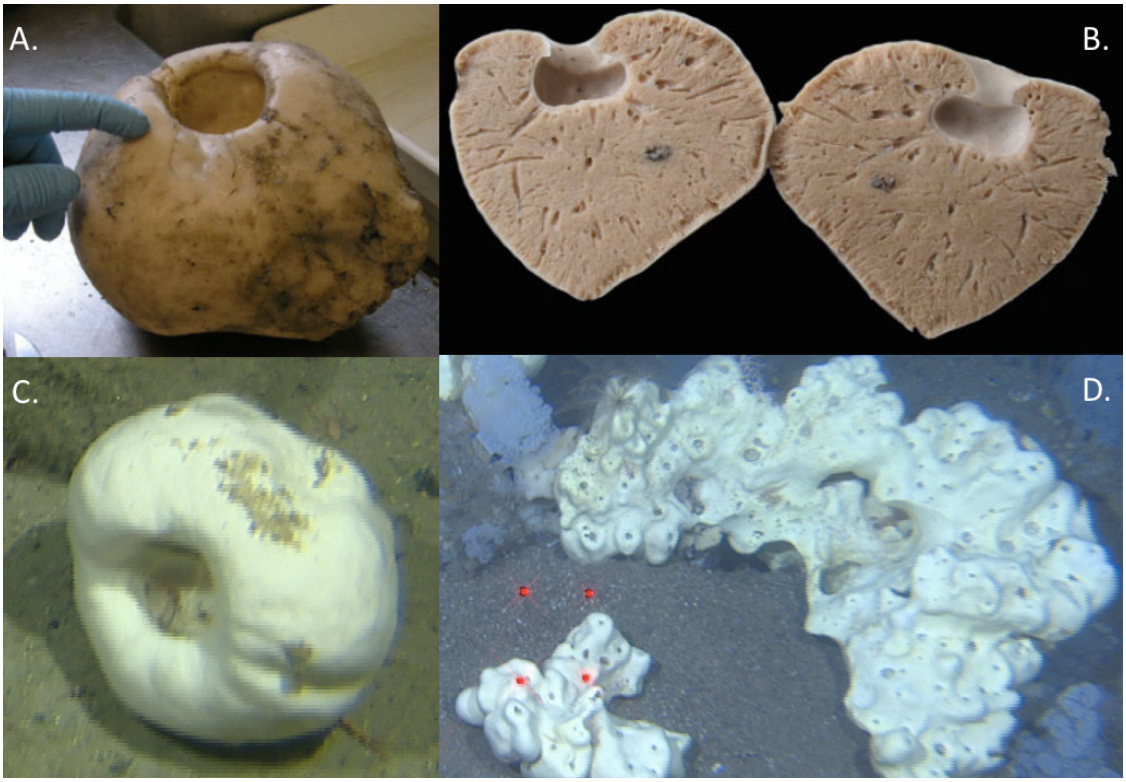

Figure 4 –Geodia barretti,* Bowerbank, 1858. *A. – External morphology of 10 cm wide specimen fixed in ethanol. The sponge present a round shape with a round opening: the preoscule. ***B.*** – Internal morphology of a 14 cm wide specimen cut in half. The sponge presents an opening on a cavity (the preoscule), an internal matrix of spicules-rich sponge tissue and canals (the mesophyl) and a thin external cortex. ***C. & D.*** – *In situ* specimens: small sponges usually present a round shape and a singular preoscule (C.) while larger specimens grow to complex irregular shapes and harbour many preoscules (D.). Images A. & B. modified from (Cárdenas et al. 2013). Images C. & D. obtained during analysis of video footage from MAREANO (P. Mortensen, Institute of Marine Research & MAREANO project, www.mareano.no).

1.4.2. Microbiome of *Geodia barretti*

G.barretti is a bacteriosponge, also called a high microbial abundance (HMA) sponge with an estimation of 2.9 x 10^{11} microbes per cm^3 of tissue which drive the sponge's metabolism (Hoffmann et al. 2009; Leys et al. 2017). HMA sponges are defined as sponges that have "compact, spherical growth forms, dense tissue with few canals, low pumping rates and a high density of diverse microbial cells" (Schöttner et al. 2013). The structure and the function of *G. barretti*'s microbiome have not yet been extensively studied. However, they are known to host complex nitrogen cycling with both aerobic (nitrification) and anaerobic (denitrification and anammox) microbial processes being fuelled by the sponge host's metabolic waste (Hoffmann et al. 2009). Additionally, *G. barretti* host favourable conditions (anoxic zones and high amounts of nutrients) for sulphate reducing bacteria (SRB) such as sulphate reducers from the *Desulfoarculus /Desulfomonile/ Syntrophus* cluster (Hoffmann et al. 2006). Therefore, *G. barretti*'s microbiome undoubtedly plays a major role in the sponge's ecological functions.

1.4.3. *Geodia barretti* as a model organism

In the past decade, *G. barretti*, a key species in benthic ecosystems of the Northern Atlantic, has been an organism of choice for several experiments which developed standardized methodologies to study the sponge. The species has been established as a good

model organism for studies looking to investigate physiological and cellular stress responses in the face of environmental and anthropogenic perturbations. The sponge survives well as cultivated explants in mesocosms (Hoffmann et al. 2003) which facilitates *ex situ* experimentation. The sponge's carbon and nitrogen budget have been described (Hoffmann et al. 2009; Leys et al. 2017) and signs of compromised health, necrotic tissues and disease-like syndromes have been characterised (Luter et al. 2017). *G. barretti* explants have been exposed to suspended sediments (Tjensvoll et al. 2013; Kutti et al. 2015), mine tailings and drill cuttings (Kutti et al. 2015), drilling muds (Edge et al. 2016), thermal stress (Strand et al. 2017) and oil drilling waste (Fang et al. 2018). Sub-lethal stress responses such as decreased or increased respiration rates, lysosome membrane destabilisation or changes in nutrients utilization have been observed during those experiments.

1.5. Hypotheses

Geodia barretti, an abundant and ecologically important deep-sea sponge, could be negatively impacted by an acute exposure to crude oil in terms of physiology, cellular integrity and associated microbial community.

Alternatively, as sponges are known to sometimes act as detoxifiers through their filter feeding activity and microbial symbionts, *Geodia barretti* and its microbiota could resist a simulated oil exposure without showing signs of sub-lethal stress.

1.6. Objectives

The main objective of this master's project is to elucidate the effects of an acute oil exposure on the abundant and ecologically important deep-sea sponge, *Geodia barretti*. In addition, this thesis will provide valuable data that will enhance our understanding of the vulnerability of deep-sea benthic ecosystems to hydrocarbon exposure. Such data is useful for risk assessments and ecosystem forecasting following oil spills in Northern Atlantic seas where oil and gas exploration are prevalent.

More specifically, we aim to decipher the responses of *Geodia barretti* during an acute exposure to oil of 8 days at 3 different oil concentrations and after a recovery period of 30 days at a whole organism (i.e. physiology), cellular and microbiome level:

- Sponge physiological responses will be characterised by measuring respiration rates, and bacterial consumption which will be used to determine the filtration rate.
- Cellular responses will be quantified by assessing lysosomal membrane stability (LMS).
- The structure of the sponge associated microbiome and of the water microbial communities will be uncovered using high-throughput sequencing of 16S rRNA gene amplicons. In this way, we will monitor, compare and identify potential shifts in prokaryote diversity of the sponge tissues and of the water following an acute oil exposure.

2. Materials and methods

2.1. Collection of sponge specimens

Explants of *G. barretti* were cultivated (see Kutti et al. 2015) at a depth of 170 m in commercial mussel lanterns for 12 months before they were harvested and transported to the deep-sea ecology laboratory of the Institute of Marine Research in Austevoll, Norway. Explants (n=80) of similar sizes (wet weight averaging 32 g) were transferred to 16 experimental 50L mesocosms (5 explants per tank) that were supplied with sand filtered seawater pumped directly from a depth of 160 m. Additional feeding of the sponges during the experimentation period was not necessary as the seawater naturally contains particles the sponges use as a source of food (Strand et al. 2017).

2.2. Experimental design and oil exposure setup

Following the DWH oil spill in the Gulf of Mexico, the properties and behaviour of the released oil in seawater were characterized. While larger droplets tend to rise to the sea surface (lower density than seawater), oil microdroplets with diameters <70 µm are neutrally buoyant and remain in the water column (Beyer et al. 2016). Total hydrocarbon doses in the water column in the months following the DWH oil spill ranged from 7.5 µg L^{-1} to 100 µg L^{-1} (Murawski et al. 2016) but hydrocarbon concentrations can potentially reach much higher concentration in certain locations (Beyer et al. 2016). The experimental setup aimed at reproducing conditions similar to those experienced by deep-water communities in the aftermath of an oil spill.

The oil used in the experiment was a weathered blend crude oil from the Heidrun oil field of the Norwegian Sea, a mix that is representative of oil types commonly found in the Lofoten area (Sørhus et al. 2015). As fast evaporation usually occurs after an oil spill at sea, the crude blend was artificially weathered through a one-step distillation at a vapour temperature of 200ºC resulting in the evaporation of the lighter components of the fresh oil, leaving residues corresponding to those remaining after a few days of weathering at 10ºC on the sea surface (Sørensen et al. 2017). The oil was pumped in a dispersion system by a HPLC pump (Shimadzu, LC-20AD Liquid Chromatograph Pump) with a flow of 5 µL min^{-1} together with a flow of seawater of 180 mL min^{-1} (Sørhus et al. 2017). The system described by Nordtug et al., (2011) was used to generate an oil dispersion with oil droplets of defined sizes ranging in the low µm (range 12-16 µm) (Nordtug et al. 2011) with an oil load of 26 mg L^{-1} (stock solution). This system includes 3-way magnetic valves which are mixing units allowing a precise dilution of the oil from the stock solution in clean seawater. The different dilutions were obtained by timing the relative sampling from the oil stock solution and clean water, this was performed by a computer-controlled relay (Sørhus et al. 2015). The Nordtug system was designed to maintain stable and reproducible concentrations of oil along with a continuous production of dispersed oil droplets of a defined size (Nordtug et al. 2011).

Sponge explants were exposed to different oil concentrations in the experimental mesocosms over a period of 8 days in order to simulate the conditions that benthic organisms may experience in the aftermath of an oil-spill event and to observe the sponges' responses

over time. The experimental oil exposure setup consisted of three treatments and one control, each with 4 replicates mesocosms:

- Low oil exposure (replicates L1, L2, L3 and L4): 33 µg oil L^{-1}
- Medium oil exposure (replicates P1, P2, P3 and P4): 100 µg oil L^{-1}
- High oil exposure (replicates H1, H2, H3 and H4): 300 µg oil L^{-1}
- Controls (replicates C1, C2, C3 and C4): no oil added to the tanks

The oil doses were determined by opening the magnetic valves for 1.1 seconds every minute for the low treatment, 3.4 sec min^{-1} for the medium treatment and 10.1 sec min^{-1} for the high treatment. During the experimental period, the oil pump stopped working twice. It was noticed on the morning of the 09/02 (day 4 of treatment for replicates 2 and 4) that the pump had stopped during the night, it was restarted in the morning after an estimation of 7.5 hours of stopped activity. The same occurred on the morning of the 12/02 (day 8 for replicates 1 and 3) and the pump was restarted.

Five replicate sponge explants (n=5) were placed into each of the 16 mesocosms (4 per treatment), and were exposed to the different experiment treatments for a period of 8 days. Respiration rates were measured and samples were taken after 24h, 48h, 4 days and 8 days of exposure to oil (**Figure 5**). On the ninth day, the remaining sponges (n=1/mesocosm) were moved to recovery mesocosms which were free of oil contamination for a period of 30 days. Transferring the remaining sponges from oil contaminated mesocosms required dilution of the water in which the sponges were kept. Each sponge was retrieved from its tank in an open plastic container (the sponges had to stay immersed in water at all time), the container with the sponge was then consecutively plunged into three 1 litre beakers containing clean seawater. In this way, the water in which the sponge was immersed was sequentially diluted. Finally, each sponge was transferred to 50L recovery mesocosms (identical to the treatment mesocosms). After 30 days spent in the recovery tanks (day 38 of the experiment), respiration rates were measured and samples were taken.

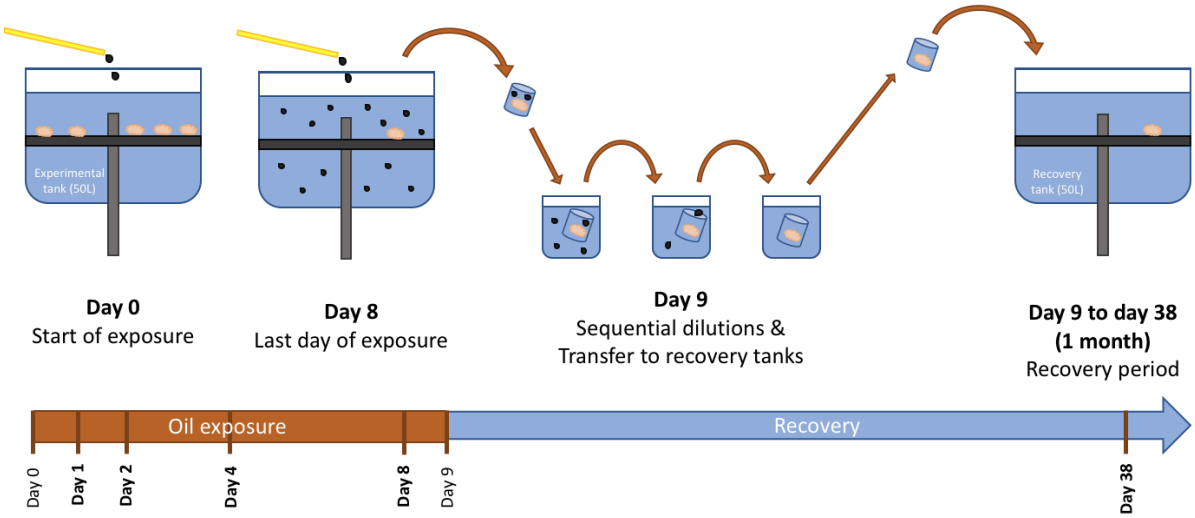

Figure 5 – Timeline and setup of the experiment. Day 0 - Representation of one experimental tank on the first day of exposure to oil: 5 sponge explants are set on a PVC false bottom in 50 L of seawater and micro-droplets of oil are dispensed to the tank. ***Day 8*** – Representation of one experimental tank on the last day of exposure to oil: one explant remains in the water (the other 4 have been sampled during time points day 1, 2, 4 and 8), oil is present in suspension in the water. ***Day 9*** – Representation of the sequential dilutions during the transfer of the remaining sponge explant from the exposure mesocosm to the recovery mesocosm: the sponge is placed in a small open plastic container and is sequentially immersed in 3 beakers containing oil-free seawater. ***Day 9 to day 38*** – After the sequential dilutions, the explant is transferred to a new tank for recovery over a period of 30 days. The last sampling point occurs on day 38. ***Timeline*** – The days marked in bold (day 1, 2, 4, 8 and 38) are the time points during which respiration measurements and sampling were performed.

During the experimental period, respiration rates (see **section 2.3**) were measured and water samples for bacterial counts (see **section 2.4**) were taken repeatedly on the same explant in each tank at each time point (24h, 48h, 4 days, 8 days and on day 38 after a 30 days recovery). Additionally, one explant per tank was sacrificed at each time point in order to take tissue samples for LMS assessment and sponge-associated microbiome analysis (see **sections 2.5**, **2.6** and **2.7**).

2.3. Respiration rates

Respiration rates of the sponges were repeatedly measured using the same 16 explants at each time point (day 1, 2, 4, 8 and 38) as a proxy for metabolic rate. This was performed by incubating the sponge in a sealed chamber equipped with a calibrated oxygen optode (PreSens, optic sensor) which recorded the oxygen air saturation for a duration of 3 hours at a rate of one measure every 15 seconds using the OXY-10 software (v3-33FB, PreSens). Each incubation chamber was composed of an acrylic cylinder and of an acrylic airtight lid holding approximatively 0.730 L of seawater. The incubation chamber was secured carefully with clips to the PVC false bottom minimizing disturbances to the experimental sponge explants. The lid was equipped with a stirring bar which rotated at a rate of 500 rpm, ensuring non-static conditions, and two holes sealed with plugs through which the oxygen sensor could be placed and water samples could be taken (**Figure 6**). Four different incubation chambers were used, one for the controls (C) and one for each treatment (L, P and H). In addition to sponge incubations, oxygen saturation was also measured in empty incubation chambers for a duration of 1.5 hours in order to control for background oxygen consumption by microorganisms present in the seawater.

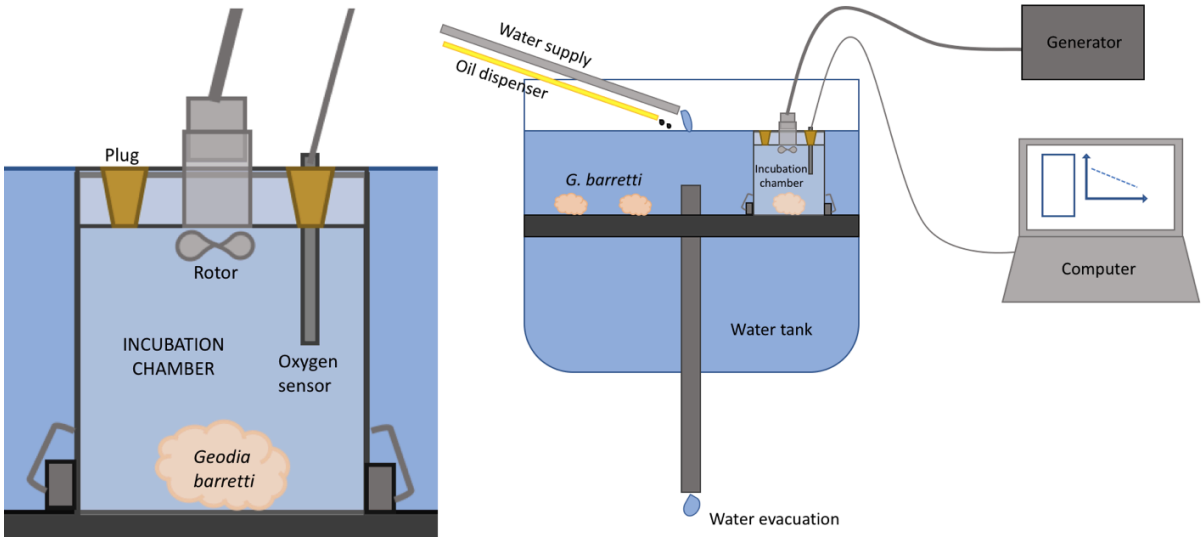

Figure 6 – Experimental setup during measurement of oxygen saturation. Left – Detailed representation of an incubation chamber: the sponge explant lay at the centre of the chamber, the chamber was secured to the PVC false bottom by clips, the oxygen sensor (optode) was placed through one of the holes in the lid and the holes were sealed with rubber plugs. During the incubation, the rotor operated at a rate of 500 rpm and created a water flow in the chamber. ***Right*** – Global view of the experimental setup for one tank: sponge explants lay on a PVC false bottom in a 50 L experimental tank filled with seawater. Sand filtered seawater was supplied to the tank and oil was dispensed at a fixed rate according to the concentration needed for each treatment (33 µg L^{-1}, 100 µg L^{-1} or 300 µg L^{-1}). A generator enabled rotation of the stirring bar in the incubation chamber and the measurements made by the oxygen sensors were recorded on a computer in real time.

Along with each incubation, temperature of the water, barometric pressure (Bp) and relative humidity (RH) were recorded at a rate of one measurement every 15 seconds using Logger Lite (v1.7, Vernier Software & Technology). Subsequently, the wet weight of each explant used for the incubations was determined by placing the sponge in a beaker filled with water on a scale. The wet weight was then converted to dry weight using a conversion ratio of 0.2 (dry weight = wet weight * 0.2), a ratio that was determined by Strand et al. (2017) by weighting the wet weight of whole *G. barretti* sponges and by drying them in an oven at 60ºC to constant weight (Strand et al. 2017). Subsequently, the oxygen saturation data (oxygen/% air saturation) was adjusted for changes in water temperature, Bp and RH and was transformed to a measure of dissolved oxygen (DO) in micromoles of oxygen per litre of water (µmol O_2 L^{-1}). The rate of oxygen consumption was calculated by subtracting the average DO value of the 10 last measures to the average DO value of the 10 first measures, multiplying it by the volume of the incubation chamber (in litres) and dividing it by the time of incubation (in hours) (See **Equation 1**). Oxygen consumption (µmol O_2 h^{-1}) was corrected by subtracting background respiration of seawater microorganisms to respiration measured in the incubation chambers with sponges (See **Equation 2**). Finally, the oxygen consumption value obtained was divided by the dry weight of the sponge in order to obtain a respiration value per gram of sponge tissue dry weight (µmol O_2 h^{-1} g (tissue DW)$^{-1}$) (See **Equation 3**). Overall, the respiration rate was calculated as follow:

Equation 1*.* Calculation of oxygen consumption rate*:*

$$Rate\ (\mu mol\ O^2\ h^{-1}) = \frac{(Average\ DO\ initial - Average\ DO\ final) * Volume\ of\ incubation\ chamber}{Time\ of\ incubation}$$

Equation 2*.* Correction for background respiration*:*

$$Rate_{sponge}(\mu mol\ O^2\ h^{-1}) = Rate_{incubation\ with\ sponge} - Rate_{incubation\ without\ sponge}$$

Equation 3. Rate of oxygen consumption per grams of dry sponge tissue:

$$RATE\ (\mu mol\ O^2\ h^{-1} g(tissue\ DW)^{-1}) = \frac{Rate_{sponge}}{Dry\ weight}$$

2.4. Bacterial count

Water sampling

Water samples were collected using sterile syringes before and after each incubation (including the incubations without a sponge which served as controls). For each treatment and each replicate, 13 mL of water were collected into centrifuge tubes and 100 µL of 25% v/v glutaraldehyde were subsequently added to the bacterial samples before they were stored in the fridge at 4ºC.

Bacterial count

The filtration efficiency of the sponge was evaluated by measuring the density of bacteria present in the water at the start and at the end of the incubation period (3h) and was corrected for the density of bacteria before and after a control incubation without a sponge (1.5h). Bacteria were counted using epifluorescence microscopy with SYBR Green I (Thermo

Fisher scientific). Although this method was previously carried out using a DAPI (4',6-diamidino-2-phenylindole) stain, this could not be used in this case as DAPI and oil absorb and emit fluorescence in similar wavelength (DAPI: max emission at 461 nm). As an alternative, SYBR Green I (absorbs blue light at 497 nm and emits green light at 520 nm) was used to stain the sample and the method was adapted until bacteria were visible by fluorescence microscopy. Fluoresbrite® YG Microspheres 1.00 µm (Polysciences Inc.) were used as a control for the method; they are fluorescent microspheres with an excitation and emission spectra similar to FITC (441/485 nm). The microspheres solution (4.55 x 10^{10} particles mL^{-1}) was diluted 10^6 times to a concentration of 4.55 x 10^{10} particles mL^{-1} to mimic natural seawater bacterial abundances. The diluted microsphere solution was analysed in the same way as the seawater and, in this way, served as a reference and control for the method.

The water samples were preserved in a fridge at 4ºC and were placed on ice when they were taken out for analysis. The samples were vortexed briefly before 4 mL were aliquoted out and 20 µL of SYBR Green I 100x (10 000x stock solution diluted 100 times) were added to it. The stained samples were incubated in the dark at room temperature for a duration of 15 to 20 min. After incubation, using a vacuum pump (Vacuum Pump V-700, Buchi), the 4mL stained samples were filtered onto a polycarbonate black membrane (cyclopore track-etched membrane, Whatman) which retained particle size > 0.2 µm (**Figure 7**). Immediately after the 4 mL of samples were filtered through, 1 mL of DI H_2O was added and filtered through in order to remove any excess SYBR Green stain. Using forceps, the membrane was carefully removed from the filtering surface and laid onto a glass slide, a droplet of 25 µL of phosphate-buffered saline (PBS) was added with a glass cover slip. The glass slide was immediately wrapped in foil to protect from light and it was placed onto ice in order to avoid evaporation until it was observed under the microscope.

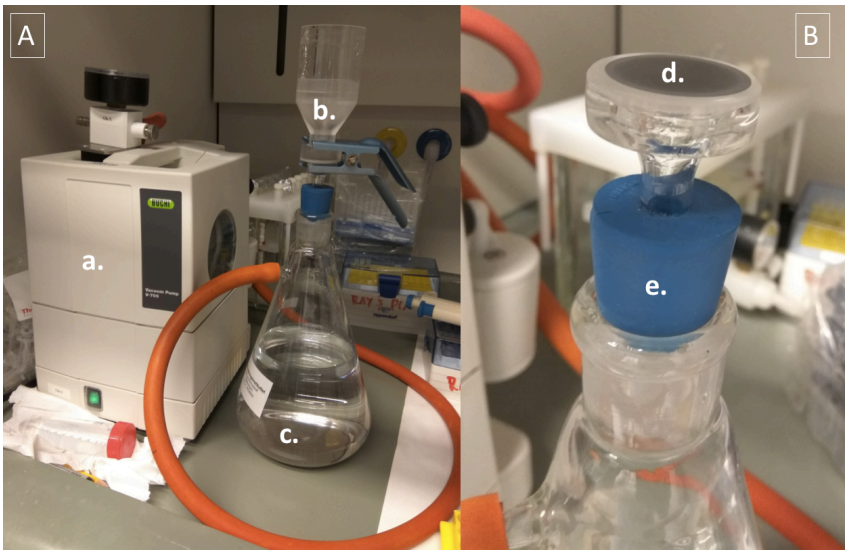

Figure 7 – Experimental setup for filtration of the stained samples. A (left) – Global view of the setup. The vacuum pump (a.) was connected to a suction flask (c.) in which the sample water was collected after it had been filtered from the funnel (b.) placed on top of the filter. ***B (right)*** – Close-up of the filter surface covered by a black polycarbonate membrane (d.) on which particles > 0.2 µm were retained during filtration. A plug (e.) sealed the suction flask allowing the suction to only go through the filter surface.

The membrane was observed by fluorescent microscopy using a 40x objective and a FITC filter (blue light, emission 513-556 nm, excitation 467-468 nm) in a dark room. The images were visualized using a digital camera (SPOT Flex 15.2 64 Mp, Diagnostic Instruments Inc.) and SPOT imaging software (v5.4, www.spotimaging.com). At least 15 pictures were taken

following a transect along the diameter of the membrane. Each picture for each sample was taken using the same camera setup which was: no binding, 600 msec exposure and a gain of 32. The images were processed using the plugin ObjectJ (v1.04h, https://sils.fnwi.uva.nl /bcb/objectj) of ImageJ (v1.52a, http://imagej.nih.gov/ij) which allowed to automatically count the particles visible on each picture. The luminescence threshold was set to 20 (on a scale of 1 to 225, lowering the threshold increases resolution and noise on the image) and the size threshold was set for size from 0.1 to 500. These parameters were chosen after several trials and errors until the count seemed most accurate for a subsample of 10 pictures.

Using the automatic count on ObjectJ, bacterial cells were marked and counted on each individual picture (see example on **Figure 8**). The counts on the pictures were manually reviewed in order to avoid any major miscount (for example, a contamination of excess stain or other fragmented particles on a picture could generate a large quantity of unspecific particles), errors were manually corrected or, if the error was judged too large, the picture was removed from the analysis. The number of cells per image was averaged over the 15 first pictures. Knowing the surface area of the image (0.1429 mm^2) and of the polycarbonate membrane (490.8739 mm^2), an estimation of the number of bacterial cells filtered from the 4 mL of samples onto the filter membrane could be calculated for each sample (**Equation 4**).

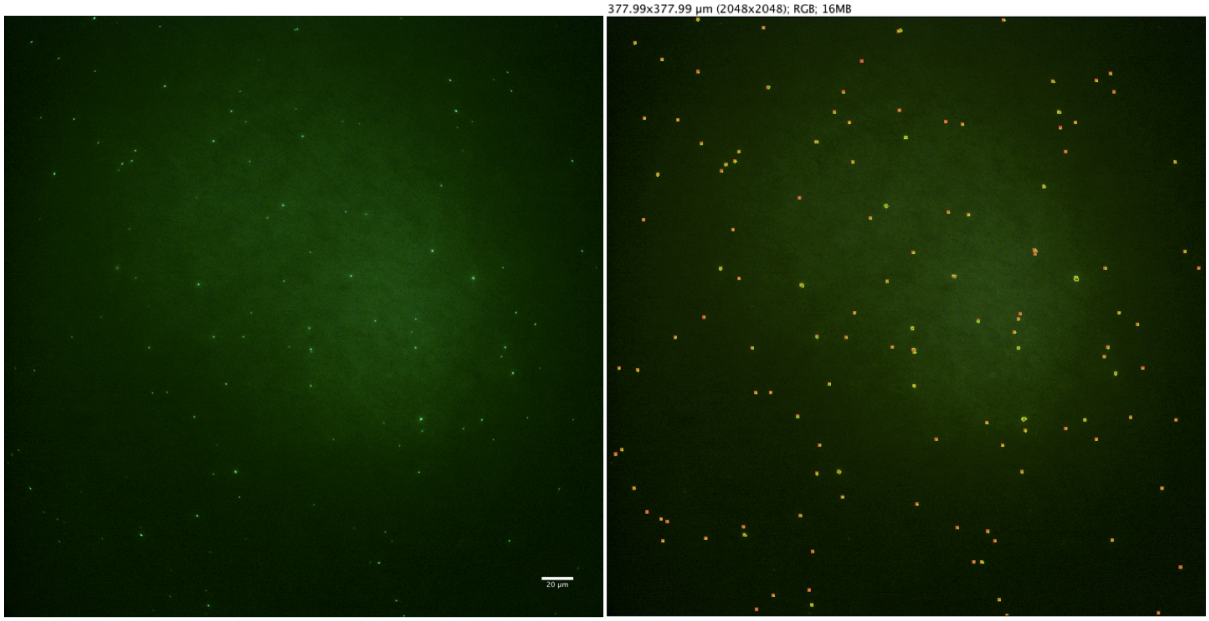

Figure 8 - Microscopy imagery and automatic cell count on ObjectJ. Left – Microscopy image (sample: D8L2 before control) of bacterial cells on the black polycarbonate membrane observed by fluorescent microscopy using a 40X objective and a FITC filter. The surface area of the image was 0.1429 mm^2 and the bacterial cells appeared as green fluorescent dots. ***Right*** – Same microscopy image analysed on ObjectJ for automatic cell count. The program marked each dot recognized as a bacterial cell and outputted the total count of cells on the image (not displayed here).

The aim was to determine the rate at which sponges were filtering. This would correspond in a retention of bacteria over time. Therefore, the abundance of bacteria after incubation was subtracted from the abundance of bacteria before incubation (**Equation 5**). The difference was then adjusted for the total volume of the incubation chamber and was divided by the exact time of incubation in order to obtain a rate of bacteria retention (positive value) or release (negative value) by minute in the chamber (**Equation 6**) Finally, the rate was corrected for the background rates measured in empty incubation chambers (**Equation 7**), this allowed to determine the sponge specific rate of release / retention of bacteria. Overall, the filtration rate was calculated as follow:

Equation 4. Total number (N) of bacterial cells filtered onto the membrane from the 4 mL of sample (with n the average number of cell on one picture for a certain sample)

$$N = n \times \frac{Surface\ of\ filter}{Surface\ of\ picture}$$

Equation 5. Difference (D) in bacterial abundance between start and end of the incubation period (calculated for the 4 mL of filtered sample water)

$$D = N_{before} - N_{after}$$

Equation 6. Rate of appearance / disappearance of bacterial cells in the incubation chamber (calculated for the volume of the whole incubation chamber)

$$Rate\ (nbr\ of\ bact/min) = \frac{\frac{D}{4} \times Volume\ of\ chamber}{Time\ of\ incubation}$$

Equation 7. Rate of retention / release of bacterial cells by the sponge (corrected for the rate of appearance / disappearance in control chamber without sponge)

$$Corrected\ RATE\ (nbr\ of\ bact/min) = Rate_{Incubation\ with\ sponge} - Rate_{Control\ incubation}$$

In addition to determining the rate of retention / release of bacteria over the incubation period, the global abundances of bacteria were compared between time points and treatments in order to assess whether time and / or treatment had an effect on bacterial densities in the water. Abundances were plotted as the average number of cells counted per field of view (surface area of field of view = 0.1429 mm^2).

2.5. Water filtration and tissue sampling for further analysis

In order to assess the composition of the microbes present in the water over the experimental period, 1 L of water per tank was filtered on a Sterivex filter (Millipore). The filters were preserved at -80ºC until further analysis. Water was filtered from all the tanks except tanks C3, L3, P3 and H3 on day 1, day 4 and day 8 (12 filters per day). For the recovery time point, water was filtered from all the tanks on day 38 (16 filters for the day).

One sponge explant per experimental tank was collected at each time point. It was transported in a small plastic container filled with seawater from the tank to the laboratory where tissues samples were prepared. Using a sterile scalpel, the outer cortex of the explant was excised from the choanosome to reduce the risk of surface contaminants associated with it. The choanosome was chopped into small pieces which were placed in 2 mL cryovials and were snap-frozen in liquid nitrogen prior to storage at -80ºC. Fresh tissue samples (approximately 3 mm^3) were collected for the lysosomal membrane stability assay which was performed directly after sponge dissection.

2.6. Lysosomal membrane stability

Lysosomal membrane stability (LMS) is used as a biomarker for cellular stress, this assay was first applied in bivalves (Ringwood et al. 1998, 2005, Edge et al. 2012, 2015) and then was

adapted to sponges by Edge et al. (2016) from which the following protocol is based on (Edge et al. 2016).

Prior to analysis, CMFS (Ca^{2+} / Mg^{2+} free saline) and neutral red ($C_{15}H_{17}ClN_4$) stock solutions were prepared. CMFS was obtained by combining 4.77 g HEPES, 21.04 g NaCl, 0.93 g KCl and 1.86 g EDTA in 995 mL MilliQ H_2O and by adjusting the pH to 8.0 with 6M NaOH. CMFS stock solution was stored in the fridge during the first 8 days of the experiment and was prepared fresh for the recovery time point (day 38). A 1st stock solution of neutral red dye was prepared fresh daily by adding 4 mg of neutral red powder to 1 mL DMSO (dimethyl sulfoxide). A 2nd stock solution was prepared right before each assay by adding 40 µL of the 1st stock solution to 1.96 mL of CMFS. The neutral red dye obtained was wrapped in foil to protect it from light and kept at room temperature.

Lysosomal membrane stability was assessed on fresh tissue samples. Approximately 3 mm^3 of choanosome were stored in filtered seawater for a maximum of 1 hour before it was minced to a paste-like consistency on a glass slide with a sterilized scalpel. The minced sponge tissue was placed into a well of a 24-well culture plate set on ice with 1 mL of freshly prepared CMFS. The 24-well culture plate set on ice was then agitated on a shaker at 120 rpm for 30 min. Subsequently, using a pasteur pipette with the tip broken off to make it larger, the tissue homogenate was gently sheared by taking up and releasing the solution to assist cell dissociation. It was then filtered through a 40 µm nylon screen into a 2 mL microcentrifuge tube. After a cool centrifugation (10ºC) at 300 g for 5 minutes, the supernatant was discarded and the pellet was resuspended in 1 mL CMFS prior to a second cool centrifugation (10ºC) at 300g for 5 minutes. The supernatant was discarded and the cells were resuspended in 50µL CMFS before 50 µL of the freshly prepared neutral red 2nd stock solution were mixed in using the plastic pipette tip. The samples were stored in a light protected humidified chamber at room temperature for a duration of 1 hour.

After one hour, the dyed cells were re-suspended in the solution using a pasteur pipette. One drop of the solution was placed on a microscope slide and covered with a coverslip and the cells were observed using a 40X lens. At least 50 cells were scored: they were scored as stable if the dye was contained discretely within the lysosomes or as unstable if the dye leaked in the cytoplasm (See **Figure 9**). For each sample, two rounds of scoring were performed and the ratios of unstable cells/stable cells were averaged.

Data from day 4 was discarded from the analysis due to a slight change in methodology which resulted in inconsistent results (full data available in **supplementary material E**).

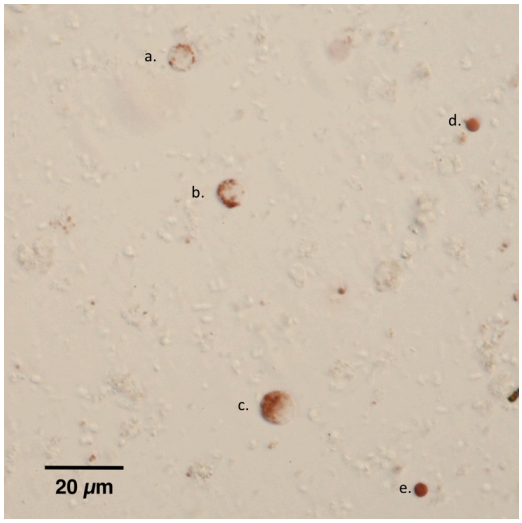

Figure 9 - Neutral red assay on choanosome cells. Microscopy image (sample: D4P3) taken during neutral red assay of lysosome membrane stability showing stable and destabilized cells. ***a. & b.*** **–** Stable cells: neutral red dye is contained in lysosomes which appear as discrete red circles. ***c.*** **–** Destabilised cell: neutral red dye has leaked into cytosol and lysosomes no longer appear as discrete red circles. ***d. & e.*** **–** Neutral red dye droplets outside of cells.

2.7. DNA extraction, sequencing and processing

In order to assess the community structure of the microbiome associated with *G. barretti*, DNA was extracted from the frozen tissue samples, amplified and sequenced using high-throughput sequencing (HTS) technology.

DNA extraction

DNA extractions on tissue samples and on Sterivex filters were performed using the PowerSoil® DNA Isolation Kit (MoBio Laboratories, Inc.). This kit uses a method based on Inhibitor Removal Technology® (IRT) for isolating genomic DNA from environmental samples. This method is usually intended for use on soil samples containing high humic acids levels which are efficiently removed through IRT but has also been previously used on frozen sponge tissues (Thomas et al. 2016) and on *G. barretti* tissue samples during a study carried out at the Institute of Marine Research of Bergen (Strand et al. 2017).

For each type of sample (tissues and filters), the protocol was optimised in order to retrieve DNA in sufficient concentrations for successful PCR amplifications. Test DNA extractions were performed on extra tissue samples that had been collected during the experiment (see **section 2.5**) and on Sterivex filters on which 1 L of seawater had been filtered. DNA concentrations were measured using the Nanodrop 1000 Spectrophotometer (Thermo Fisher Scientific) and a PCR (protocol described below) was performed in order to verify that the DNA isolated was in sufficient concentration and that PCR inhibitors were absent from the solution.

Prior to starting the MoBio protocol, approximately 0.2 g of frozen sponge tissue was macerated using a sterilized scalpel, placed in 2 mL microcentrifuge tubes with small ceramic beads immersed in 200 µL of the solution found in the PowerBead Tubes and shaken for 25 seconds using the FastPrep FP120 Cell Homogenizer (Thermo Savant). This aimed to break down the silica spicules and to dissociate the choanosome cells. After centrifugation at 10k rpm for 1 min, cells and supernatant were transferred to a PowerBead Tube to which 60µL of a lysis solution containing SDS and cell disruption agents were added. Prior to this, the lysis solution had been kept at 65ºC for 10 min to ensure that the SDS was completely dissolved. After a brief vortexing, the samples containing the lysis buffer were incubated at 65ºC for 10 min in order to aid chemical cell lysis. They were then placed horizontally on a shaker plate and agitated for 10 min at maximum speed for mechanical cell lysis. Subsequently, PCR inhibitors, non-DNA inorganic and organic material such as cell debris and proteins were precipitated by the use of 2 different IRT solutions. A high-concentration salt solution was added and the sample was filtered through a silica surface on which DNA binds tightly in high-salt concentrations while non-DNA material is eliminated. The silica surface was then washed with an ethanol-based solution which removes residual salt and other contaminants. Finally, 50 µL of DI H_2O was added as an eluting agent to the cleaned silica filter from which DNA was selectively released. DNA was preserved in the elution solution at 4ºC.

Extraction of DNA from the filters presented a different strategy for cell lysis. After thawing for 30 min, the filters were placed in 50 mL centrifuge tubes and were centrifuged at 1200 rpm for 1 min in order to remove any excess water trapped in the filter cavity. After incubation at 65ºC for 10 min, 300 µL of lysis buffer were added to the filter cavity and both openings of the filter were closed with Parafilm (Bemis Inc.). The filter was inverted and shook by hand to make sure that the lysis solution spread to all parts of the filter membrane before

it was placed on the shaker plate and was agitated at maximum speed for 10 min. The filter was then incubated at 65ºC for 10 min to help chemical cell lysis. Finally, Parafilm was removed from the filter, it was placed in a 50 mL tube and was centrifuged at 1200 rpm for 2 min. The lysis solution was recuperated from the bottom of the 50 mL centrifuge tube and transferred to a PowerBead Tube. From then on, the extraction method resumed to the normal protocol (shaking with beads, IRT solutions, high-salt solution and filtration on silica membrane, ethanol wash and elution in 50 µL DI H_2O).

Concentration and purity of the samples were assessed by a measure on the Nanodrop. DNA concentration is measured by absorbance (nucleic acids absorb at 260 nm) and purity of the sample is given by the absorbance ratios 260/280 and 260/230. DNA was preserved in the elution solution at 4ºC until further analysis.

1st PCR: amplification of the 16S V4 region

The analysis of 16S rDNA is commonly used in the comparison of microbial diversity in environmental samples as it provides valuable phylogenetic information and enables the simultaneous detection of a large panel of Bacteria and Archaea (Takahashi et al. 2014). The V4 region of the 16S rRNA was amplified from template DNA using a two-step nested PCR approach (**Figure 10**) (Wilson et al. 2017).

A first PCR aimed to amplify the 16S V4 region leaving an overhang that includes an Illumina adaptor and five Ns. The primers FAdapter-N5-519F (forward, 5'-CTACACTCTTTCCCT ACACGACGCTCTTCCGATCT-**NNNNN**-CAGC**M**GCCGCGGTAA-3') and RAdapter-806R (reverse, 5'-GTGACTGGAGTTCAGACGTGTGCTCTTCCGATCT-GGACTAC**NV**GGGT**W**TCTAAT-3') were used (with M=A/C, N=A/C/T/G, V=A/C/G, W=A/T). The reaction mixture was prepared as follow: 10 µL HotStarTaq Master Mix (Qiagen), 0.5 µL of primer 519F (10µM aliquot), 0.5 µL of primer 806R (10µM aliquot), 0.5 µL of 20 mg mL^{-1} BSA (bovine serum albumin) and 7.5 µL of nuclease-free water. 1 µL of template was added when working with DNA extracted from tissue samples and 5 µL of template were necessary when working with DNA extracted from the filters. The PCR included an initial denaturation at 95ºC for 15 min, followed by 25 cycles of denaturation at 95ºC for 20 sec, primer annealing at 55ºC for 30 sec and extension at 72ºC for 30 sec, followed by a final extension step of 72ºC for 7 min (Wilson et al. 2017). The quality of the amplified DNA was assessed by agarose gel electrophoresis: the samples migrated on a Gel Red (Biotium Inc.) agarose gel 1% for 45 min at 85 V in a TBE 0.5X buffer solution. The loading dye used is the 5X Green GoTaq Flexi Reaction Buffer (Promega) and the molecular ladder is the GeneRuler 100 bp DNA ladder 0.5 µg $µL^{-1}$ (Thermo Scientific) ranging from 100 to 1000 bp. The results were observed using the ChemiDoc™ XRS+ system (BioRAD). Some filter samples did not contain enough DNA to visualise clear PCR products. The 16S PCR protocol was adapted for those samples: 8.5 µL of template were added to 11.5 µL of Master Mix solution (no water was added to the mix as the volume could not exceed 20 µL) and the PCR included 30 cycles instead of 25.

2nd PCR: addition of unique barcodes through a nested PCR

The second step involved a nested PCR performed on the first PCR products. The primers are linked to the overhang adaptors of the amplicons through this second amplification and unique sample barcodes and Illumina flow cell P5/P7 adaptors are added to the extremities of the insert of interest. Eight different forward primers (F1 to F8) and twelve different reverse

primers (R1 to R12) were used in 96 combinations for tagging 96 samples. In this way, each template is specifically identifiable by its two barcodes. The primers are the FAdapter-barcode-Flinker (forward, 5'-AATGATACGGCGACCACCGAGATCTACAC-XXXXXXXX-ACACTCTTTCCCTACACGACG-3') and the RAdapter-barcode-RLinker (reverse, 5'-CAAGCAGAAGACGGCATACGAGAT-XXXXXXXX-GTGACTGGAGTTCAGACGTGTGCTCTTCCGATCT-3') and the 8 + 12 barcode sequences are displayed in supplementary material (**Section I**). The reaction mixture (50 µL) was prepared as follow: 25 µL HotStarTaq Master Mix (Qiagen), 18 µL of nuclease free water and a unique combination of 1 µL forward primer (diluted to 10µM) and 1 µL reverse primer (diluted to 10µM) for each sample with 5 µL template from the first PCR products. The PCR included and initial denaturation at 95ºC for 15 min followed by 10 cycles of denaturation at 95ºC for 20 sec, primer annealing at 62ºC for 30 sec and extension at 72ºC for 30 sec, ending with a final extension step at 72ºC for 7 min (Wilson et al. 2017). The quality of the amplified DNA was assessed by agarose gel electrophoresis according to the same protocol as the one described previously for the 16S PCR. Out of the 96 samples prepared, one (F D8 P4) did not give a PCR product. It was decided to discard this sample from the analysis and to work on the 95 samples that gave PCR products.

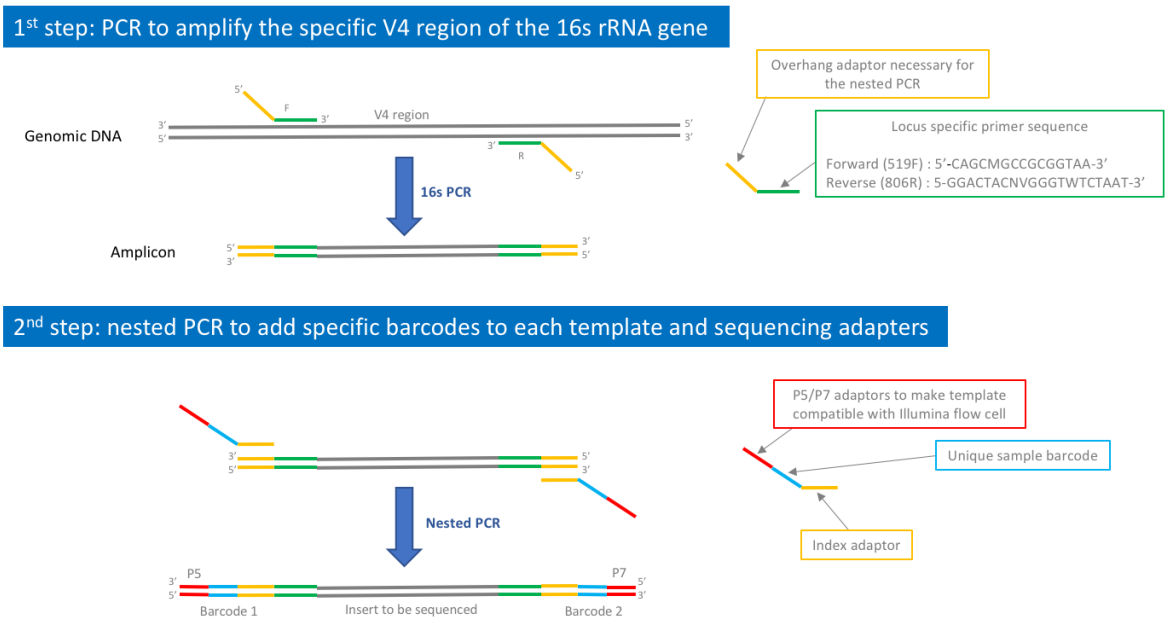

Figure 10 – 2 steps PCR for preparation of samples for Illumina sequencing. 1st step – Amplification of the V4 region of the 16s locus using primers with overhang adaptors. ***2nd step*** – Addition of unique sample barcodes to the amplicon through a nested PCR. The amplicons are equipped with P5/P7 adaptors for compatibility with Illumina flow cell and with unique barcodes allowing pooling of the different samples for Illumina sequencing.

Clean-up & pooling

Agencourt AMPure XP Beads (Beckman Coulter Inc., CA, USA) were used to purify the amplicons by eliminating PCR reagents and eluting the DNA in nuclease-free water. This purification system is based on solid-phase reversible immobilization (SPRI) paramagnetic bead technology and allows high-throughput purification of PCR amplicons. The AMPure solution consists of an optimized buffer and microscopic magnetic beads to which DNA fragments of 100 bp and larger bind specifically. The tubes containing the AMPure solution with the sample are placed against a magnet, this allows aggregation of the beads (to which the DNA is bound) on the side of the tube. Excess primers, nucleotides, salts and enzymes from the PCR are removed through two washes with freshly prepared 70% (v/v) ethanol.

Ethanol is then removed and 25 µL of nuclease-free water is added to elute the purified DNA fragments from the beads.

Each sample final concentration was measured using a Qubit Fluorometer (Thermo Fisher scientific). The library for sequencing was obtained by pooling the 95 samples together in equimolar concentration (75 ng of DNA per sample) in a single tube. Library's final concentration and purity were assessed by measures on the Qubit and on the NanoDrop.

High-throughput sequencing (HTS)

The library was sent to the Norwegian Sequencing Centre (NSC, Oslo, Norway) for paired-end HTS on the MiSeq platform (Illumina, CA, USA) using the MiSeq Reagent kit v3 to obtain reads of a length of 300 bp. NSC returned quality control files and the raw sequence data as FASTQ files which contained the read sequences for each sample.

Bioinformatics on raw data (performed by Dr. B. Wilson)

Bioinformatics on the raw 16S rRNA gene sequence data was performed by Dr. Bryan Wilson (University of Bergen) using the BBTools software package (https://jgi.doe.gov/data-and-tools/bbtools/). Briefly, PhiX control sequences were removed; paired-end reads were merged and linkers, forward and reverse primer sequences were removed. FASTQ files were quality end-trimmed at a phred quality score ≤ 27 and reads of a length < 200 bp were removed. The remaining reads were then checked for chimeras with the *identify chimeric seqs* and *filter fasta* scripts in QIIME (Quantitative Insights into Microbial Ecology, v1.9.0) (Caporaso et al. 2010b) using usearch61 (Edgar 2010) and the ChimeraSlayer (Haas et al. 2011) reference database (Gold.fa) found in the Broad Microbiome Utilities suite (http://microbiomeutil. sourceforge.net/). *De novo* OTU picking was performed using the *pick de novo otus* script in QIIME (with default parameters), using uclust (Edgar 2010) and a sequence similarity threshold of 97%. The *pick de novo* script on QIIME was further used for taxonomy assignment using PyNAST (Caporaso et al. 2010a) at 90% sequence similarity against the Greengenes core reference alignment database (Release 13_8) (DeSantis et al. 2006) and assembly of a table of OTU abundances with taxonomic identifiers.

Bioinformatics on OTU table

Using QIIME, the OTU table was outputted as a BIOM file. Additionally, the OTUs were grouped by classes and several BIOM files containing only parts of the data were created for the different types of samples (water and sponge tissues), for the different treatments (C, L, P and H) and for the different time points (D1, D2, D4, D8 and D38). The BIOM files were uploaded and processed on RStudio (v1.0.153, https://www.rstudio.com) using the phyloseq package (v1.22.3, https://joey711.github.io/phyloseq/index.html, McMurdie & Holmes, 2013). Different graphs were plotted in order to visualize trends in the microbial communities across the different samples. More specifically, global taxonomic diversity, beta- and alpha-diversity were analysed. All plots were created using phyloseq and vegan (v2.5-2, https://cran.r-project.org/web/packages/vegan/index.html) packages on RStudio.

- Taxonomic diversity

Taxonomic diversity and relative abundance at the class level was first represented as a stacked barplot over the whole data. For this, the OTU table with OTUs agglomerated by classes was used. The data was subset to the 20 most abundant classes and the abundances were sum-normalized. Additionally, data was subset to sponge tissue samples and replicates (n=3) were merged together. Using the 10 most abundant phyla, a taxonomic profile at the phylum level was created for each sample type (treatments across days).

In order to identify which OTUs were discriminating, a similarity percentage (SIMPER) analysis was performed using PRIMER 6+ (v6.1.16). Using the most discriminating OTUs explaining 80% of dissimilarity between each treatment group identified by SIMPER analysis, a network analysis was conducted on Cytoscape (v3.6.1, http://cytoscape.org). A network plot was drawn in order to visualise how the most discriminating OTUs were shared between the different treatments.

- Beta-diversity

Beta-diversity was visualized with ordination plots constructed from a constrained correspondence analysis (CCA) using Bray-Curtis dissimilarity. Additionally, differences in community structure were tested using permutational multivariate analysis of variance (PERMANOVA) based on Bray-Curtis distances of standardized abundance data on PRIMER 6+ (v6.1.16). Beta-diversity was assessed between the 2 types of samples, water and sponge tissue, using a one factor design, whereas beta-diversity was analysed within each type using a two crossed-factors design (day x treatment).

- Alpha-diversity

Alpha-diversity of each individual sample was calculated using Chao1. Rarefaction curves were plotted in order to visualize and compare observed diversity and Chao estimated diversity between sample types (water and sponge tissue) and between treatments for sponge tissue samples.

Search for oil degraders

A list of known oil degraders at the genera level was compiled from literature and presence and abundance of those genera in the data was investigated. Additionally, a literature research on the top most discriminating OTUs identified by SIMPER was carried out in order to decipher potential oil degrading functions within those OTUs.

2.8. Data analysis and statistics

The effect of oil exposure through time on respiration rates and on lysosomal membrane stability was tested using analyses of variance (ANOVAs) in RStudio (R v1.4.2 and RStudio v1.0.153). Respiration data (sponge and background respiration rates) was $\log_{10}$ transformed and LMS data (count of unstable lysosomes) was square-root transformed. All data conformed to the assumptions of ANOVA (homogeneity of variance and normality). Respiration rates of sponges were analysed with a 2-way (time x treatment) repeated-

measure ANOVA using the lme() function (linear mixed effect model) in the nlme package (v 3.1-137). Background respiration rates measured in the water of empty incubation chambers were analysed with a 2-way (time x treatment) ANOVA using the aov() function in R. Lysosomal membrane stability was analysed with a 2-way (time x treatment) ANOVA using the aov() function in R. If the treatments seemed to play a significant role in responses (respiration or LMS), a post-hoc Tukey test was performed to determine which treatments significantly differed. The models were checked for homogeneity of variance and normality using diagnostic residual plots (standardized residuals versus predicted value), histograms and Q-Q plots of residuals.

3. Results

A total of 80 individual sponge explants were used for the experiment and none of these explants during the experimental period showed clear visible signs of stress such as a change in colour, tissue loss, necrosis or death. Over the experimental period, water temperature in the mesocosms remained stable over time averaging 8.0 ºC ($\pm$ 0.03 ºC). Furthermore, the exposure of explants to the different experimental treatments of oil and associated PAHs remained stable during the 8 day exposure period (see supplementary material, **section B**).

3.1. Respiration rates

Exposure to the three different ecologically relevant oil concentrations did not significantly affect the respiration rates of *G. barretti* explants over the experimental period (2-way repeated measure ANOVA, P>0.05 for both main effects and main effects interactions, **Table 1**). Nonetheless, control sponges consistently had higher mean respiration rates (average rate of 0.680 $\pm$ 0.056 µmol O_2 h^{-1} g (tissue DW)$^{-1}$) than explants exposed to the three different oil concentrations during the experimental period (**Figure 11**). A decrease in respiration rates is observed after 24 hours in sponges exposed to oil. Exposure to high oil concentrations during the first 24 hours reduced sponge respiration rates (0.374 $\pm$ 0.125 µmol O_2 h^{-1} g (tissue DW)$^{-1}$)) by up to 52% compared to control sponges (0.714 $\pm$ 0.078 µmol O_2 h^{-1} g (tissue DW)$^{-1}$)). After 48 hours of exposure to oil, high variability precluded the possibility for statistically significant differences between treatments. Variability in sponge responses on day 2 was significantly greater than variability on day 1 (one-tailed F-test, P=0.017). Additionally, variability in the high oil treatment on day 2 was significantly greater than variability of control treatment on day 2 (one-tailed F-test, P=0.030). In this way, day 2 was characterized by an increased variability in respiration rates with increased oil concentrations. After 30 days of recovery in oil free mesocosms, sponges presented similar mean respiration rates across all experimental treatments with reduced variability.

Experimental oil treatments did not significantly impact background respiration rates of mesocosms' water (2-way ANOVA, P > 0.05, **Table 2**), although a trend of increased respiration rates was observed in the oil contaminated mesocosms (**Figure 11**). The elevated variability in background respiration rates did not allow for statistically significant differences. Of interest in the effect of treatment on background respiration rate is the fact that water containing oil (low, medium and high treatment) presented higher means and greater variability in background respiration rates than control water which was free of oil

contamination (**Figure 11).** Background respiration rates in the water presented similar patterns across all treatments after a 30 days recovery period.

Sponge respiration	dF	F	P
Within subject (factor: time)			
Day	60	1.172	0.2832
Day x Treatment	12	0.796	0.5192
Between subject (factor: treatment)			
Treatment	60	0.435	0.7287

Table 1 – Results of the repeated measures 2-way ANOVA model for respiration rates of *G. barretti* explants exposed to different crude oil concentrations (0 µg L^{-1}, 33 µg L^{-1}, 100 µg L^{-1} and 300 µg L^{-1}) over a 8 day period followed by a 30 day recovery. The values are the results of an ANOVA performed on a linear mixed effect model (Respiration ~ Day x Treatment).

Background respiration	dF	Mean Sq	F	P
Day	1	0.01389	0.232	0.6317
Treatment	3	0.14035	2.345	0.0812
Day x Treatment	3	0.02778	0.464	0.7083
Residuals	64	0.05986		

Table 2 – Results of the 2-way ANOVA model for background respiration rates measured in water containing 4 different crude oil concentrations (0 µg L^{-1}, 33 µg L^{-1}, 100 µg L^{-1} and 300 µg L^{-1}) over a 8 day period followed by a 30 days recovery.

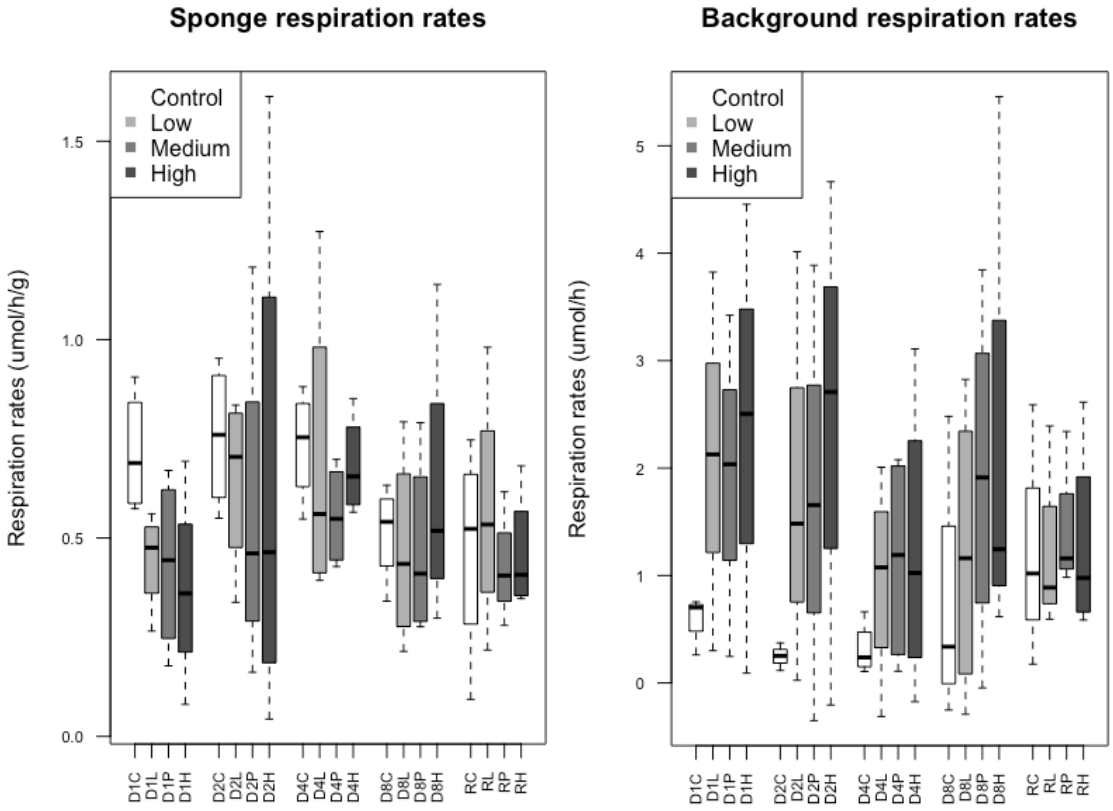

Figure 11 - Respiration rates across time and treatments. The horizontal black band in each boxplot represents the median, the ends of the box represent the 1st to the 3rd quartiles (25th to 75th percentiles) and the whiskers represent minimum and maximum range within 1.5 times the interquartile range of the lowest and upper quartile respectively. ***Left*** – Respiration rates (µmol O_2 h^{-1} g (tissue DW)$^{-1}$) ± SE (n=4) of cultivated *G. barreti* explants exposed to 4 different oil treatments (0 µg L^{-1}, 33 µg L^{-1}, 100 µg L^{-1} and 300 µg L^{-1}) over a 8 day exposure period followed by a 30 day recovery period. The data is separated according to the 5 time points: day 1 (D1), day 2 (D2), day 4 (D4), day 8 (D8) and recovery (R). ***Right*** – Background respiration rates (µmol O_2 h^{-1}) measured in empty incubation chambers. The data is separated according to the 5 time points and the boxes are coloured according to the 4 treatments (see legend on graph).

3.2. Bacterial count

The bacterial count was performed on water samples from day 1 and day 8. It was decided to not pursue with the analysis on the remaining samples for 2 reasons: calculation of rates of bacteria retention / release gave unsatisfactory results (see discussion) and a lack of time did not allow for improvement of method or novel experimentation.

Differences between bacterial counts in before and after incubation samples varied greatly and took positive values (indicating a retention or disappearance of bacteria) as well as negative values (indicating a release or appearance of bacteria). Additionally, the variability in the results did not allow for robust statistical analysis (**Figure 12**). It is unclear whether the variability seen in the data was an artefact of the methodology or if it reflected a biological reality. For this reason, the data was treated with great caution.

Interestingly, comparison of global bacterial abundances showed that cell densities were higher in water samples recovered from day 8 than in day 1 water samples (**Figure 12**).

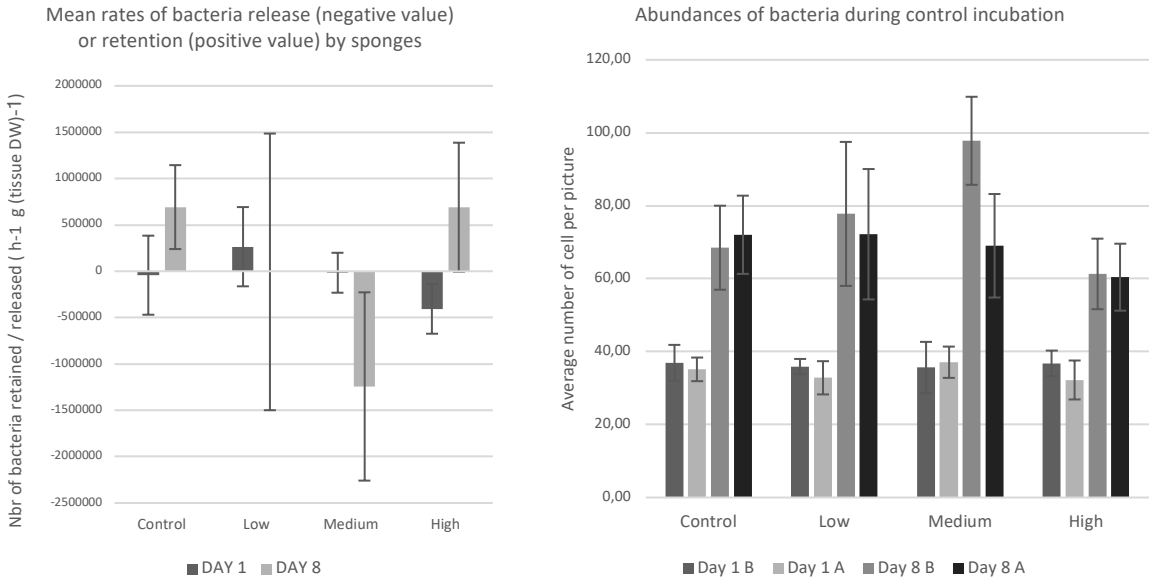

Figure 12 - Results from bacterial count. Left – Calculated mean rates of bacteria released or retained by sponges during incubations at time points day 1 and day 8. Negative values of bacteria count indicate that bacteria were released in the water during the incubation period (more bacteria in the water after than before incubation). Positive values of bacteria count indicate that bacteria were retained by the sponge (less bacteria in the water after than before incubation). ***Right*** – Abundances of bacteria measured in the water before and at the end of control incubations (no sponge in the water). The abundances are represented by the average number of cells counted on one microscope picture (surface area = 142876 μm^2). B = before incubation, A = after incubation.

3.3. Lysosomal membrane stability

Crude oil exposure induced a reduction in the stability of lysosome membranes within the sponge's mesophyl cells. Treatment and day of exposure independently showed significant main effects on lysosome membrane destabilization but their interaction did not significantly impact LMS (**Table 3**). Sponges exposed to oil consistently demonstrated higher mean abundances of destabilized lysosomes during the exposure period with increased number of destabilized cells in higher treatments (**Figure 13**). On day 1, the high treatment presented an average of 21.70% ($\pm$ 1.93%) of destabilized cells which is 3 times higher than the mean percentage observed in controls on day 1 (7.39 $\pm$ 0.43%). After 30 days of recovery,

destabilisation of lysosomal membranes was reduced in all treatments and did not differ significantly between treatments and controls. Tukey multiple comparisons of means showed that control sponges (C) and high treatment sponges (H) differed the most (Tukey score = 0.1166, p-value<0.001) regarding LMS whereas low treatment (L) and medium treatment (P) sponges were most similar (Tukey score=0.0146, p-value=0.9595) (**Figure 13**).

LMS	DF	Mean Sq	F value	p-value
Day	1	0.17363	20.054	**< 0.001**
Treatment	3	0.04699	5.427	**0.0020**
Day x Treatment	3	0.00992	1.146	0.3363
Residuals	72	0.00866		

Table 3 – Results of the 2-way ANOVA model for lysosomal membrane stability of *G. barretti* explants that were exposed to different crude oil concentrations (0 µg L^{-1}, 33 µg L^{-1}, 100 µg L^{-1} and 300 µg L^{-1}) over a 8 day period followed by a 30 day recovery. Significant p-values are marked in bold.

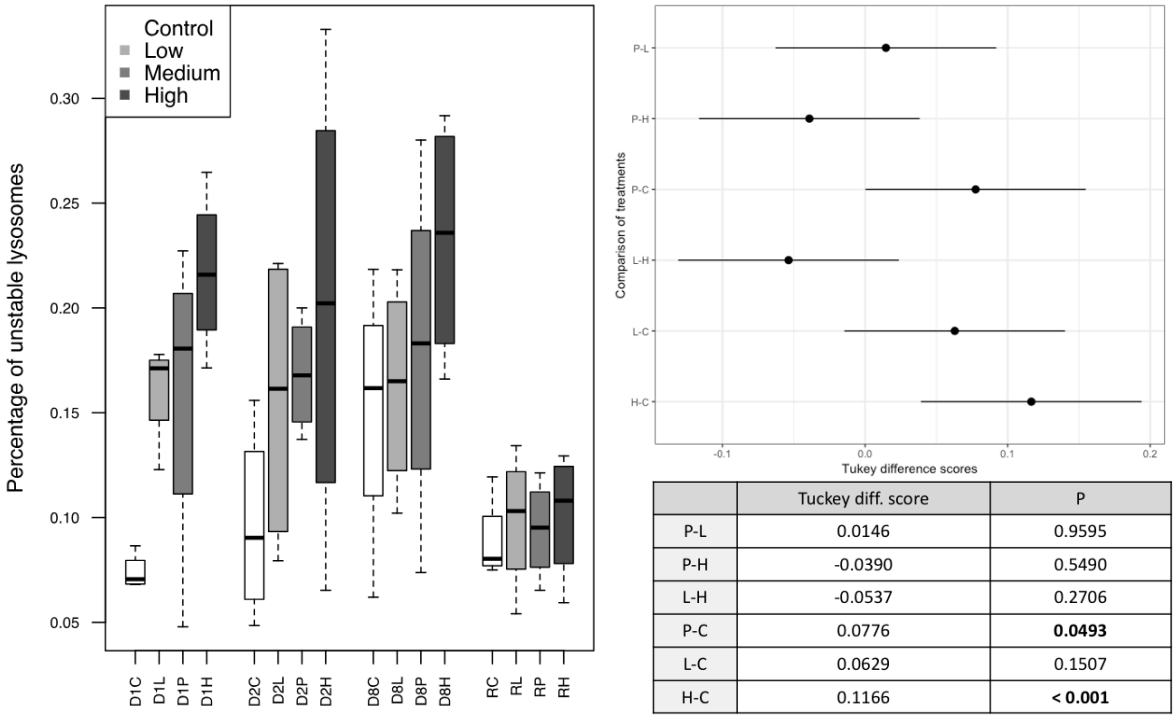

	Tuckey diff. score	P
P-L	0.0146	0.9595
P-H	-0.0390	0.5490
L-H	-0.0537	0.2706
P-C	0.0776	**0.0493**
L-C	0.0629	0.1507
H-C	0.1166	**< 0.001**

Figure 13 – Distribution of lysosomal membrane stability across time and treatment & Comparison of treatments using Tukey scores. Left – Percentages (%) of cells with destabilised lysosomal membranes ± SE (n=4) of *G. barretti* explants exposed to 4 different oil treatments (C=0 µg L^{-1}, L=33 µg L^{-1}, P=100 µg L^{-1} and H=300 µg L^{-1}) over a 8 day exposure period followed by a 30 day recovery period. The data is separated according to the 5 time points: day 1 (D1), day 2 (D2), day 4 (D4), day 8 (D8) and recovery (R). The horizontal black band in each boxplot represents the median, the ends of the box represent the 1st to the 3rd quartiles (25th to 75th percentiles) and the whiskers represent minimum and maximum range within 1,5 times the interquartile range of the lowest and upper quartile respectively. ***Right*** – Comparison between treatments using Tukey difference scores (mean ± SE). Difference between treatments increases with distance to zero. Significant p-values are marked in bold.

3.4. Microbiome

DNA was successfully extracted and amplified for 63 sponge tissue samples and 35 water samples (sample F D8 P4 was discarded because nested PCR was unsuccessful) with average DNA concentrations of 44.07 and 18.20 ng μL^{-1} respectively. Samples were pooled in a single library in equimolar volumes with a final concentration of 13.85 ng μL^{-1} (**Figure 14**). HTS of the 95 samples retrieved a total of 52280 OTUs (at a 97% sequence identity) spanning 45 bacterial phyla, 3 archaeal phyla and 157 classes.

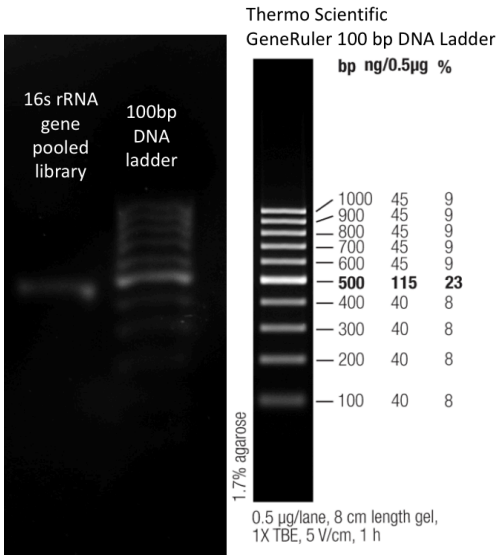

Figure 14 – Visualization of pooled library on agarose gel. Library of amplified PCR products (16S rRNA, V4 variable region). Insert size is 287 bp and total product size is approximately 500 bp (insert + primers + barcodes + adapters).

Comparison of sponge and seawater microbial communities

Microbial communities in water samples and in sponge tissues differed significantly (PERMANOVA, Pseudo-$F_{1,95}$=317.82, P=0.004). Seawater and sponge microbial communities segregated in two distinct groupings along the CA1 axis which explained 31.7% of the variation (**Figure 15**). Sponge microbial communities presented a tight cluster, whereas water microbial communities showed some variation along the CA2 axis (explained 16% of variation) for samples taken during the recovery time point.

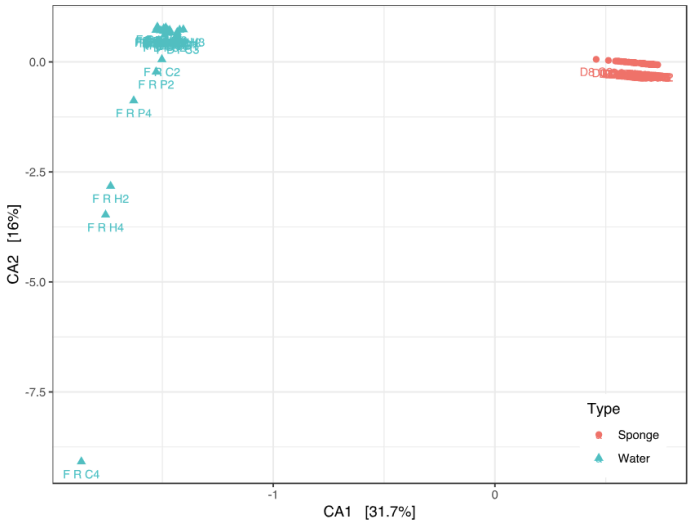

Figure 15 - CCA plot of microbial communities in water and sponge tissue samples. CCA plot was constructed using Bray-Curtis similarity obtained from 16S rRNA gene Illumina sequencing of *G. barretti* tissue (red) and of seawater (blue) samples subjected to different oil treatments.

The complexity of the microbial community is represented by the number of OTUs per sample (observed alpha diversity) which ranged between 853 and 5475 OTUs for sponge tissues and between 1392 and 6099 OTUs for seawater (alpha diversity table in supplementary material, **section K**). Overall, approximately 50% of the sponge tissue samples demonstrated similar microbial richness to water samples while the other 50% showed slightly less complex communities (**Figure 16**).

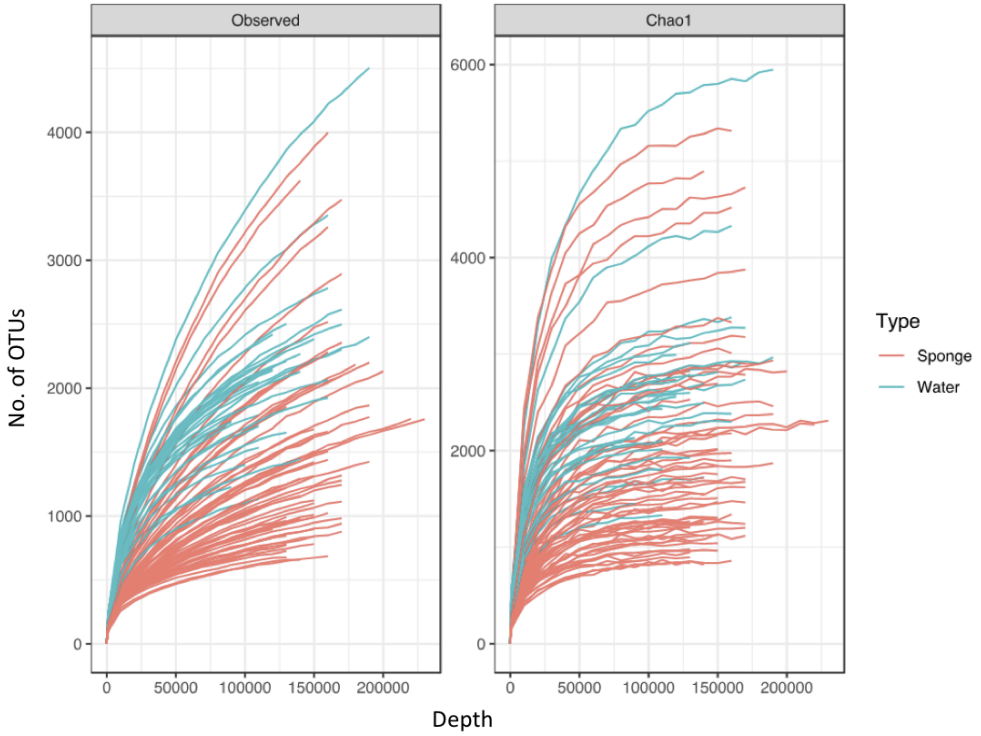

Figure 16 - Richness of individual samples from microbial communities in sponges and seawater. Rarefaction curves of 16S rRNA gene observed diversity (*left*) and Chao diversity (*right*) for sponge tissue samples (red) and seawater samples (blue).

Sponge microbial communities

At the phylum level, taxonomic diversity did not display visibly significant differences as relative abundances of the 10 most abundant phyla appeared stable across treatments and days (**Figure 17**). However, beta-diversity analysis using Bray-Curtis distances demonstrated that sponge microbial communities differed significantly across treatments (Pseudo-$F_{3,63}$=2.3232, P=0.001) and across days (Pseudo-$F_{5,63}$=6.8008, P=0.01) but the combined effect of day and treatment did not drive differences in communities (Pseudo-$F_{12,63}$=1.1987, P=0.214) (**Table 4**). Ordination of beta-diversity showed that clustering patterns changed over time and across treatments but treatments did not particularly cluster into tight groupings (**Figure 18**). Day 1 presented the most widespread pattern whereas recovery presented the most clustered pattern. Although tight clusters were not easily observed, there is a variability across treatments and between days. A clear separation between control and high treatments was observed on day 8 while low treatments slightly overlapped with controls and with medium treatments. All samples showed higher similarity during recovery and showed a tighter clustering. Overall, this data suggests that there is a slight variability in microbial sponge communities across treatments during oil exposure.

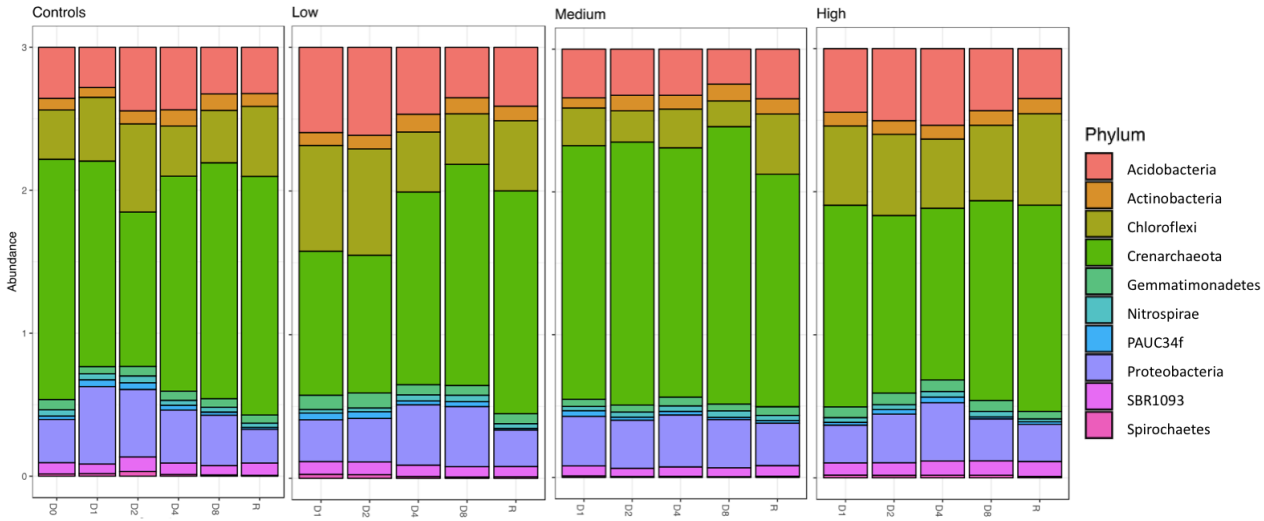

Figure 17 - Taxonomic profile at the phylum level (top 10 phyla) in sponge tissue samples. Replicate samples are merged into one bar and relative abundances of the 10 most abundant phyla are represented by the different colours.

PERMANOVA Sponge tissue	df	Pseudo-F	P-value	Unique perms.
Day	5	2.3232	**0.01**	997
Treatment	3	6.8008	**0.001**	999
Day * Treatment	12	1.1987	0.214	997
Residuals	42			

Table 4 – Results of the PERMANOVA on sponge tissue microbial community. PERMANOVA based on Bray-Curtis distances obtained from 16S rRNA gene HTS of G. barretti tissue samples subjected to different oil treatments. Significant p-values are marked in bold.

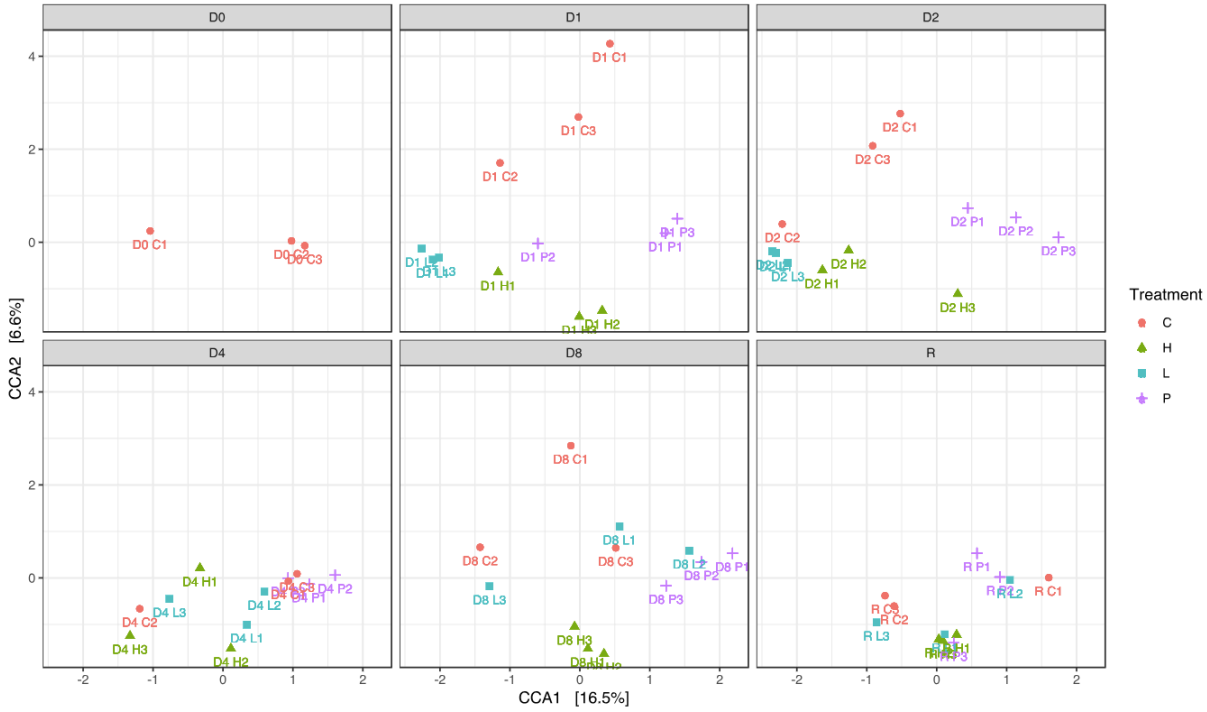

Figure 18 – CCA plot of microbial communities in sponge tissue samples. Plot constructed using Bray-Curtis similarity obtained from 16S rRNA gene Illumina sequencing of *G. barretti* tissue samples subjected to different oil treatments. CCA plot is divided by day (D0 = day 0, D1 = day 1, D2 = day 2, D4 = day 4, D8 = day 8 and R = recovery time point or day 38) and samples are coloured according to the oil treatment they were subjected to (C = 0 µg L^{-1}, L = 33 µg L^{-1}, P = 100 µg L^{-1}, H = 300 µg L^{-1}).

Alpha-diversity patterns did not indicate that certain treatments drove significant changes in community richness over time (**Figure 19**). Indeed, rarefaction curves of the different treatments overlapped (especially for day 2, 4 and 8) and none of the treatments showed consistent patterns of lower or higher diversity. Of interested is the stratification in day 1: high treatments presented the lowest diversity, followed by the medium treatments followed by an overlap of the low treatments and controls. Comparison of observed diversity and Chao estimated diversity demonstrated that only five out of ninety-five samples approached complete saturation (no rarefaction curve of observed diversity levelled out). This suggests that sequencing depth was not sufficient to uncover full diversity in the samples.

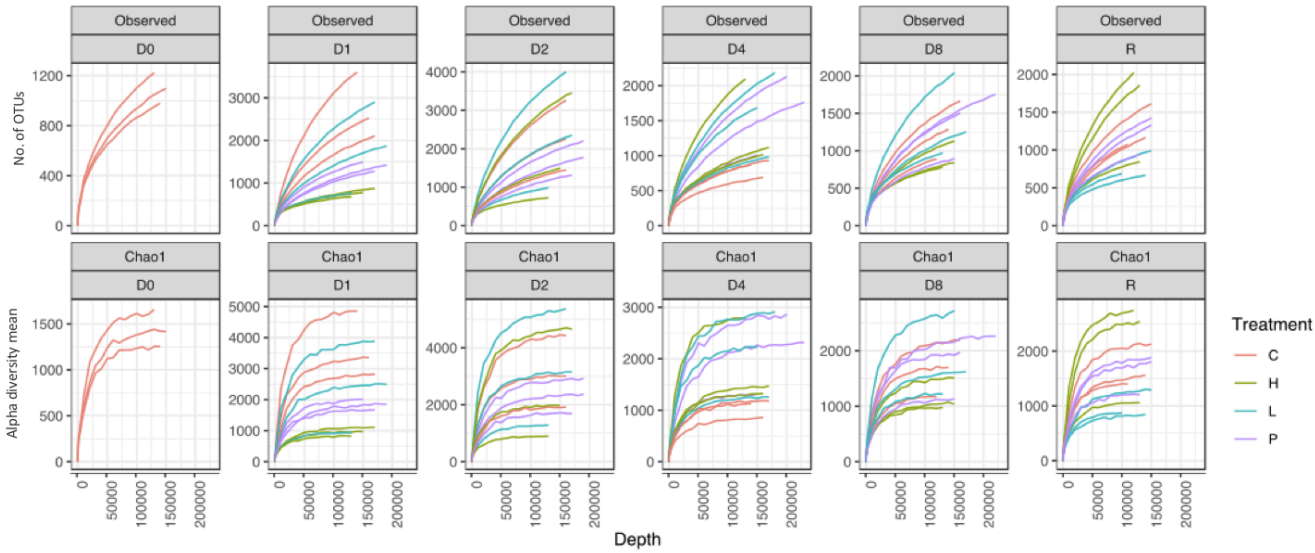

Figure 19 - Richness of individual samples from microbial communities in sponges. Rarefaction curves of 16S rRNA gene observed diversity and Chao1 diversity for sponge tissue samples across days. Control (red), low treatment (blue), medium treatment (purple) and high treatment (green).

Cytoscape network analysis using the most discriminating OTUs (explaining 80% of the dissimilarity) demonstrated that the most discriminating OTUs were present in all treatment groups. Additionally, the different treatments showed similar trends in OTU abundance patterns (**Figure 20**). No discriminating OTU was exclusively detected in one treatment meaning that the discriminatory character of those OTUs was based on their relative abundance in each treatment group.

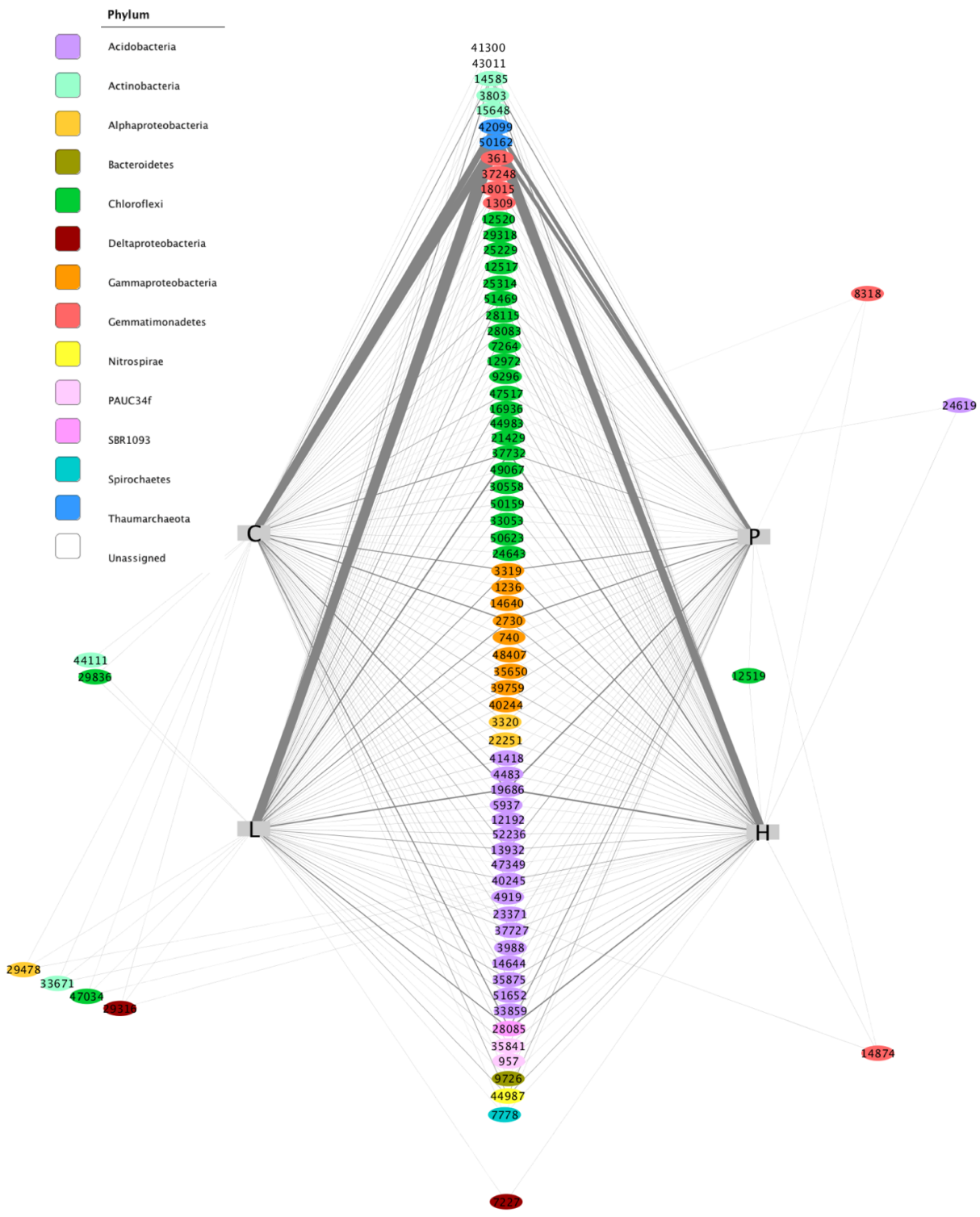

Figure 20 - Cytoscape network of the G. barretti microbiome under the different oil treatments. Network was created from the most discriminating OTUs (97% similarity) identified in SIMPER analysis as driving the differences between oil treatments (80% of the dissimilarity explained). The different OTUs are represented by coloured ellipses. The numbers are the OTUs identification numbers and the ellipse colour represent the OTU phylum or class (in the case of *Thaumarchaeota* and *Proteobacteria*). The width of the lines represents the average relative abundance of the OTU in each treatment.

Discriminating OTUs contained some of the most abundant OTUs across all samples. The 2 most discriminating OTUs (50162 and 42099) were from the dominating class, *Thaumarchaeota* (of the *Crenarchaeoata* phylum), and accounted for 48.4% of the global microbial diversity in sponge tissues. The most discriminating phyla (**Figure 20**) corresponded to the most abundant phyla (**Figure 21**). They encompassed *Thaumarchaeaota* (48.65%), *Chloroflexi* (14.80%), *Acidobacteria* (13.20%), *Gammaproteobacteria* (8.79%), *Actinobacteria* (3.25%), candidate phylum *SBR1093* (2.65%), *Gemmatimonadetes* (2.22%), *Alpha-proteobacteria* (1.36%), *Nitrospirae* (1.18%), *Deltaproteobacteria* (1.12%), candidate phylum *PAUC34f* (0.93%) and *Spirochaetes* (0.47%) and accounted for 99% of the global microbial diversity in sponge tissues.

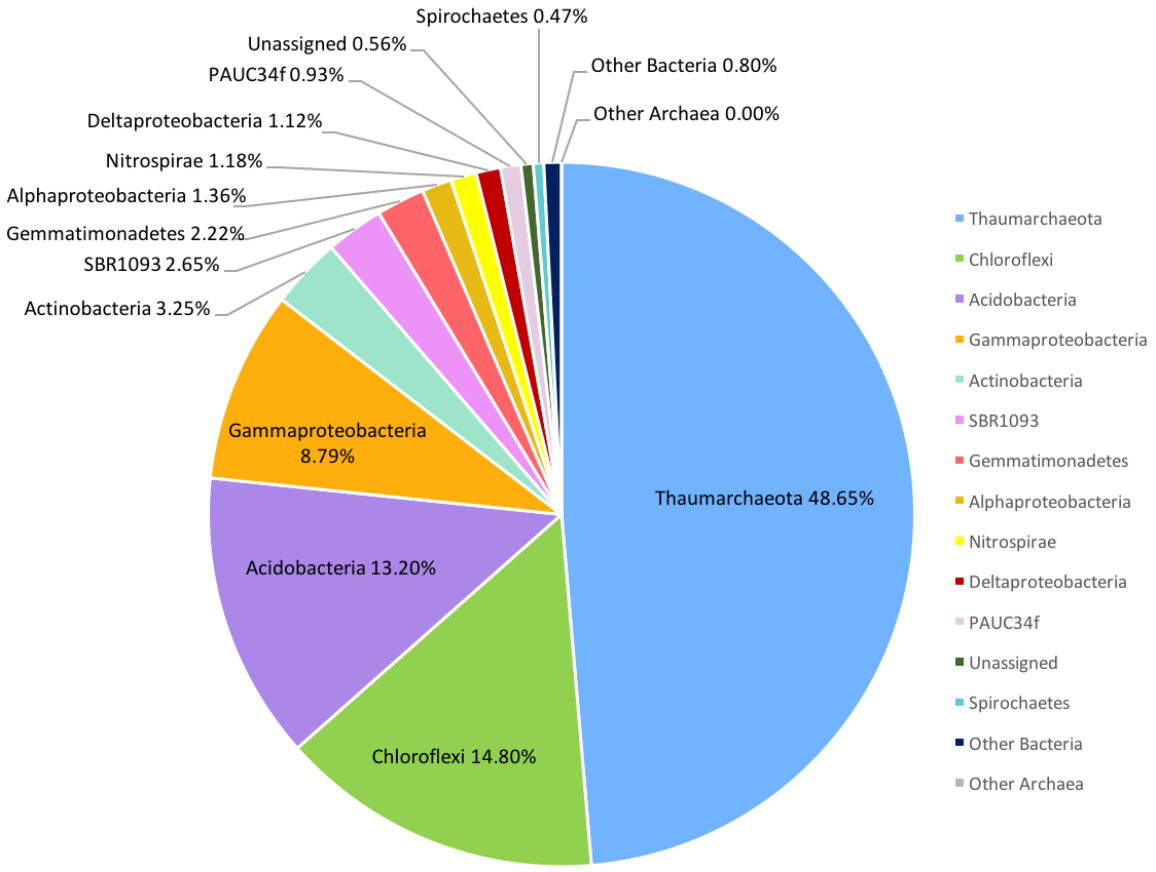

Figure 21 – Relative importance of the most abundant taxa in G. barretti. Most abundant phyla (*Proteobacteria* divided into classes and *Thaumarchaeta* is a class of the phylum *Crenarchaeota*) of prokaryotes present in *G. barretti*'s tissue identified from Illumina sequencing data of 16S rRNA gene.

Oil degraders in sponges

A short literature review on known genera of oil degraders resulted in the identification of around 40 genera of oil degraders, 22 of which were present in sponge tissues (**Table 5**). Although present, the identified oil degraders only accounted for 0.0023% of the global microbial community of sponge tissues. Oil degraders were found in each type of samples and across all time points (**Figure 22**) but the low occurrence of those genera in the sequencing data did not allow for statistical analyses or accurate representations of the abundances.

Class	Family	Genus	Abundance in sponge tissue	Reference
Gammaproteobacteria	Pseudomonadaceaea	*Pseudomonas*	0,000490%	1, 2, 3
Gammaproteobacteria	Pseudoalteromonadaceae	*Pseudoalteromonas*	0,000417%	1
Bacilli	Staphylococcaceae	*Staphylococcus*	0,000254%	4
Gammaproteobacteria	Alcanivoracaceae	*Alcanivorax*	0,000221%	1, 2
Alphaproteobacteria	Rhodobacteraceae	*Paracoccus*	0,000150%	4
Gammaproteobacteria	Oceanospirillaceae	*Marinomonas*	0,000119%	1
Bacilli	Bacillaceae	*Geobacillus*	0,000115%	2
Actinobacteria	Mycobacteriaceae	*Mycobacterium*	0,000084%	2
Actinobacteria	Micrococcaceae	*Micrococcus*	0,000083%	3
Gammaproteobacteria	Moraxellaceae	*Psychrobacter*	0,000076%	1
Gammaproteobacteria	Alteromonadaceae	*Marinobacter*	0,000075%	1, 2
Gammaproteobacteria	Moraxellaceae	*Acinetobacter*	0,000069%	3
Flavobacteriia	Flavobacteriaceae	*Flavobacterium*	0,000048%	3
Flavobacteriia	Flavobacteriaceae	*Polaribacter*	0,000037%	1
Gammaproteobacteria	Shewanellaceae	*Shewanella*	0,000028%	1
Flavobacteriia	Weeksellaceae	*Chryseobacterium*	0,000017%	4
Gammaproteobacteria	Oceanospirillaceae	*Oleispira*	0,000011%	1, 2
Bacilli	Bacillaceae	*Bacillus*	0,000011%	3
Alphaproteobacteria	Sphingomonadaceae	*Sphingomonas*	0,000010%	1, 2
Gammaproteobacteria	Colwelliaceae	*Colwelia*	0,000010%	1
Gammaproteobacteria	Moritellaceae	*Moritella*	0,000009%	1
Flavobacteriia	Flavobacteriaceae	*Ulvibacter*	0,000009%	1

Table 5 - Taxonomy and abundance of oil degrading bacteria identified in sponge tissues. References: 1. (Brakstad et al. 2017), 2. (Brooijmans et al. 2009), 3. (Xue et al. 2015), 4 (MetaMicrobe.com 2014)

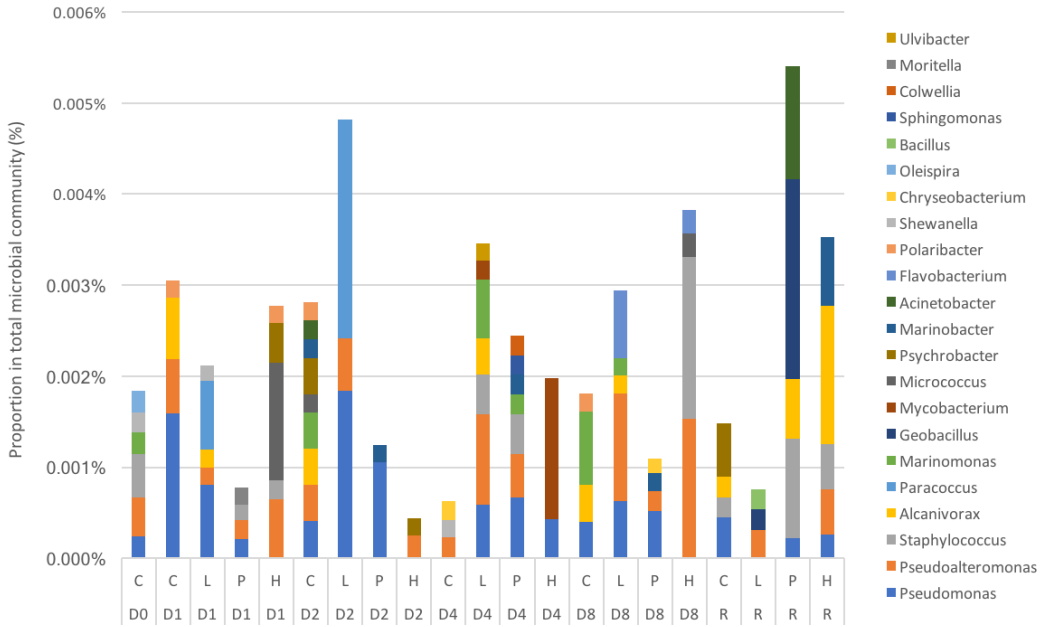

Figure 22 - Occurrence of oil degrading bacteria in sponge tissues. Stacked barplot representing the absolute abundance of identified oil degrading genera in each sample type.

4. Discussion

Using the model sponge *Geodia barretti*, this study demonstrated for the first time under laboratory conditions, the potential resilience of a keystone species in deep-sea ecosystems to acute crude oil contamination. With oil and gas exploration activities expanding in deep offshore areas, concerns about potential impacts on benthic ecosystems are increasing. It is necessary to improve our knowledge on the vulnerability of key components of these ecosystems in order to strengthen science-based management advice on the expansion of oil drilling activities in vulnerable and sensitive areas of the Northern Atlantic. The experimental exposure of *G. barretti* to 3 ecologically relevant crude oil concentrations for a duration of 8 days did not induce visible signs of compromised sponge health or clear shifts in the structure of the associated microbial community, despite increased variation in metabolic performance and evidence of cellular stress associated with reduced lysosomal membrane stability.

4.1. Physiological effects on the sponge host

G. barretti has previously been studied in the context of anthropogenic stressors, with field observations on the Norwegian continental shelf demonstrating mass mortality events in association with increased temperatures (Guihen et al. 2012) and stressed sponges being afflicted by a disease-like syndrome, leading to discoloration, tissue disintegration, fouling and change in the composition of the microbial community (Luter et al. 2017). Previous *ex situ* experiments assessing the response of *G. barretti* to various stresses such as increased temperatures (Strand et al. 2017), drilling muds (Edge et al. 2016) or oil-drilling waste (Fang et al. 2018) have induced sub-lethal physiological and cellular stress such as increased or reduced respiration rates, lysosome membrane destabilization and reduced nitrite / nitrate release. However, the sponges in these earlier studies have proven to be quite resilient in the face of *ex situ* stress exposure with no visible signs of disease or mortality.

Respiration

Oil treatments did not significantly impact sponge respiration rates. Although treated sponges displayed a reduction in O_2 consumption after 24h of exposure, the high variability in individual sponge responses over the exposure period hindered the possibility for significant statistical results. Average control respiration rates were lower than previously reported but still stood within the lower boundaries of observed ranges (Kutti et al. 2013b; Leys et al. 2017; Strand et al. 2017). *G. barretti*'s responses in the face of environmental disturbances vary depending on the nature of the stress: thermally stressed sponges increased their respiration rates (Strand et al. 2017), whereas exposure to particulate contaminants such as suspended sediments and oil drilling waste led to reductions in oxygen consumption (Kutti et al. 2015; Fang et al. 2018). Sponge explants exposed to crude oil displayed great variability in individual responses while control sponges presented more constant respiration rates. Individual sponges showed a sudden increase in respiration rates (e.g. P2 and H2 on day 2 which presented respiration rates twice as high as the previous day) while others had declines in respiration rates (e.g. P4 and H3 on day 2, with H3 reaching almost null oxygen consumption) (**Figure 23**). This contrast in responses makes it difficult to

interpret what metabolic processes are occurring as a result of crude oil exposure. An elevation in respiration likely indicates an increase in metabolic activity and filtering (Leys et al. 2017) whereas a decrease leads to a decline in tissue oxygenation which favours anaerobic processes such as denitrification and sulphate reduction (Hoffmann et al. 2009; Fang et al. 2018). Oil biodegradation is carried out by a large consortium of microorganisms which use aerobic as well as anaerobic pathways of degradation. The anaerobic pathways is widespread and is notably performed under nitrate- or sulphate-reducing conditions (Varjani and Upasani 2017) which can be met in anaerobic portions of sponge tissues. *G. barretti* has been qualified as a "microbial farmer" because it has the potential to control the nature and the functions of its associated microbial communities by regulating the balance between aerobic and anaerobic states in its tissue and by regulating its filter feeding activity (Leys et al. 2017). Moreover, fluctuation of the pumping behaviour by sponges leads to a change in oxygen concentrations in sponge tissues and this has been observed in the field and during cultivation (Hoffmann et al. 2009). Hypothetically, sponges could present varying or cyclic patterns of metabolic / pumping activity which could be enhanced when they are exposed to new toxic compounds. Aerobic and anaerobic processes linked to hydrocarbon degradation or detoxification could be alternatively favoured. This remains highly speculative but it may help to explain why different explants from the same treatment present such variability in metabolic responses.

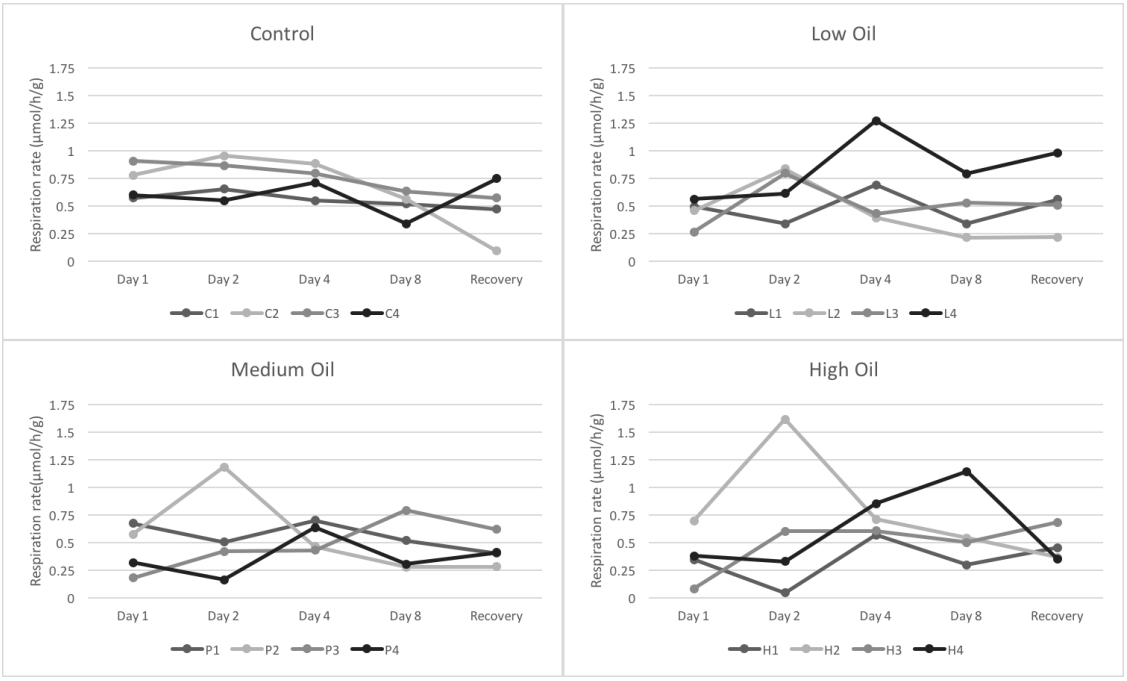

Figure 23 - Individual tracking of sponges' respiration rates during a crude oil exposure experiment. Four cultivated *G. barretti* explants kept in separate mesocosms were exposed to the same oil treatment (Control=0 µg L^{-1}, Low=33 µg L^{-1}, Medium=100 µg L^{-1} and High=300 µg L^{-1}). Individual plotting of the four explants for each treatment across time illustrates the variability in respiration rates between explants of the same oil treatment.

Both unusually high and low respiration rates can negatively impact the sponge's health. If the sponge favours respiration and metabolic activity, other physiological processes such as growth, defence against pathogens or reproduction might be reduced (Strand et al. 2017). Trade-offs in resources allocation could impact the sponge ability to cope with environmental stress in terms of life history traits or physiological function. Although such trade-offs have not yet been highlighted in deep-sea sponges, evidence show that, for example, allocation of

resources for cell regeneration in sponges and corals impairs growth, sexual reproduction and defences against predators (Henry and Hart 2005). On the contrary, if sponges decrease their respiration extensively, anaerobic processes might be overly favoured and lead to harmful microbial processes such as high sulphate reduction rates. Excessive sulphate reduction can lead to sulphide toxicity (precipitation of iron sulphide and discharge of free sulphide) which can evolve into a disease characterized by sulfidic odour and blackened tissues (Hoffmann et al. 2006).

Background respiration rates within the mesocosms demonstrated a higher trend and greater variability in oil contaminated water than in control water indicating an increase in microbial heterotrophic activity and / or an increase in microbial abundance. Such observations have been made in benthic sediments following an oil spill where bacterial respiration increased and a shift from an autotrophic system to a heterotrophic system occurred (Lee and Lin 2013). It was also shown that the release of oil and gas from the DWH blowout stimulated an increase in microbial respiration rates which in turn lowered dissolved oxygen concentrations in the deep sea (Du and Kessler 2012). Blooms of bacteria biomass were observed following the release of hydrocarbons in the Gulf of Mexico after the DWH blowout (Du and Kessler 2012).

Cellular stress

Exposure to crude oil contributed to destabilisation of lysosomal membranes in the sponge choanosome cells with an increasingly marked effect in high oil concentration treatments. The interaction of time and treatment was not significant in influencing LMS meaning that lysosomes did not present an evolution over time that was dependent on the treatment. Destabilisation of lysosomes without any signs of disease or mortality indicates that a crude oil exposure represents a chemical sub-lethal stress. LMS is a general stress biomarker that has been recommended in cases of chemical pollution as lysosomes accumulate contaminants and quickly show destabilisation in pollutant-exposed organisms (Martínez-Gómez et al. 2015). Several studies demonstrated a significant reduction in LMS following an exposure to oil and oil related contaminants in mussels (Turja et al. 2013; Ruiz et al. 2014) and in fish (Bilbao et al. 2010; Ruiz et al. 2012). *G. barretti* displayed higher counts of destabilized lysosomes when they were exposed to increased temperatures (Strand et al. 2017), or to barite and TSS (Edge et al. 2016).

Control sponges showed a proportion of destabilized lysosomal membranes (10.25 $\pm$ 1.68%) within the range of what has previously been observed in healthy sponges (Edge et al. 2016; Strand et al. 2017). The high treatments presented the highest count of destabilized lysosomes which did not change significantly between day 1 and day 8 (21.70 $\pm$ 1.93% on day 1 and 23.24 $\pm$ 4.19% on day 8). Similar patterns were observed for sponges that were exposed to a slightly elevated temperature (4ºC above normal seawater temperature) (Strand et al. 2017) or to medium doses of barite (Edge et al. 2016). Yet, although sponges exposed to high doses of crude oil presented up to 23.24 $\pm$ 4.19% of destabilised lysosomes, *G. barretti* have displayed much higher proportions (~45%) for higher temperature (5ºC above normal seawater temperature) and barite treatments (Edge et al. 2016; Strand et al. 2017). A 30 day recovery period allowed LMS to return to control levels indicating that cellular stress did not persist once the oil exposure ceased. This contrasts with the results from Strand et al. (2017)

that showed that thermally stressed sponges still presented a greater number of destabilized lysosomes after 65 days of recovery (Strand et al. 2017).

Lysosomal membranes are destabilized when hydrolytic enzymes are activated and, in some cases, liberated into the cytosol (Martínez-Gómez et al. 2015). Oxidative stress and the production of ROS (reactive oxygen species) which often result from toxicity in the cell, are one of the reasons for the destabilization of lysosomes via the peroxidation of the lysosomal membranes (Kurz et al. 2008). The knowledge on cellular responses of sponges after oil exposure is reduced but it was shown that diesel oil in seawater activated the Mitogen-Activated Protein Kinase (MAPK) in a temperate sponge and that the cytochrome P450-dependant monooxygenase pathway of 2 sponges was involved in PAH detoxification (Solé and Livingstone 2005). Both MAPK and the cytochrome P450 pathway are known to play important roles in cellular response to oxidative stress (Vad et al. 2018). This provides a link between hydrocarbon toxicity in the cell and destabilisation of lysosomal membranes due to oxidative stress.

Cellular stress could impede cellular processes and lead to cellular damage and compromised sponge health. Rapid cell turnover has been observed in tropical sponges (De Goeij et al. 2009) and sponges are known for efficient regeneration of damaged tissue (Wulff 2010). However, *G. barretti* are slow growing sponges compared to warm-water species (Hoffmann et al. 2003) which could make them more vulnerable to cellular damage. Even so, a short-term exposure to crude oil only caused moderate cell destabilisation and did not hamper a full recovery.

Sponge pumping rates and bacterial densities

Although no information concerning pumping rates could be retrieved from the bacterial counts, a significant difference in abundances of microbial cells in the water between day 1 and day 8 was detected. This could indicate a proliferation of microorganisms in the mesocosms which occurred in all treatments. Nothing, however, can be concluded from this analysis as we are unsure whether the method was adapted to our samples. It is possible that staining of the cells was not homogenous and that cell densities were misevaluated. Nevertheless, this type of analysis has the potential to reveal interesting processes. On one hand, evaluating the sponges pumping rate across treatments would give an insight into the sponge metabolic activity which could be related to respiration rates and, eventually, to nutrient fluxes. On the other hand, this could detect variation in bacterial cell densities in the water which could be related to background respiration rates in order to evaluate whether global microorganisms' biomass and / or metabolic activity increase during oil exposure.

It is necessary that the bacterial count method be revised and some suggestions as to how we might improve the analysis are listed below. SYBR Green was added to sample before filtration with a final dilution in the sample water of 5×10^{-5}. While this insures that there is no noise in the fluorescence signal because of an overload of SYBR Green, this might be too diluted to correctly stain all bacterial DNA present in the sample. Indeed, the fluorescence signal was faint and camera settings had to be set to long exposure with high gain in order to visualise the cells on microscopy images. Additionally, as soon as the stained filter was taken off the ice for microscope observation, the fluorescence signal seemed to decrease in intensity with time meaning that pictures had to be taken quickly. Finally, fluorescent cells often came in and out of focus as the objective moved above the filter plane. Consequently, SYBR Green final concentration should be increased and the staining procedure should be

revised. A study assessing the effectiveness of SYBR Green I for epifluorescent counts of marine bacteria and viruses suggested to use a final SYBR Green dilution of 2.5 x 10^{-3} and to first filter the sample onto the polycarbonate membrane before incubating it on a SYBR green drop in the dark for 15 min (Noble and Fuhrman 1998). In order to avoid fading of the fluorescence, the use of an anti-fade reagent such as *p*-phenylenediamine in combination with PBS is necessary (Noble and Fuhrman 1998; Patel et al. 2007). Finally, the filter should be dried before visualization on the microscope to make sure all cells appear in focus (Patel et al. 2007).

4.2. Effects on the associated microbiome

Microbial communities in the water and in the sponge differed significantly and sponge tissue presented a slightly less complex community than that of water. This reinforces the knowledge that sponges host unique microbial communities which differ from those found in surrounding seawater or sea sediment with most sponge species showing slightly less complex communities than the two other habitats (Thomas et al. 2016).

The main taxa identified in the microbiome of *G. barretti* using 16S rRNA gene sequencing corresponded to some of the main taxa known to be most abundant across all sponges such as *Alpha-* and *Gammaproteobacteria*, *Actinobacteria*, *Acidobacteria* and *Chloroflexi* (Webster and Taylor 2012). The dominance of *Thaumarchaeota* and *Chloroflexi* in sponge tissue is typical of HMA sponges (Bayer et al. 2018) and *G. barretti* presented a bacterial community similar to what had previously been identified in another deep-sea HMA sponge, *Stelleta normani* (Kennedy et al. 2014).

G. barretti's associated microbiome demonstrated taxonomic stability at the phyla and class level across all treatments. Additionally, although bacterial communities showed slight fluctuations in beta-diversity patterns over time, they did not cluster into clear separate groups associated with treatment groups. Finally, community richness was not correlated to treatment and Cytoscape analysis showed that all OTUs that were found to be "most discriminating" between the different treatments were shared among all samples in similar proportions. These results indicate that crude oil exposure did not drive clear changes in the structure of *G. barretti*'s microbiome with no variation of taxonomic diversity and no reduction or increase in community richness. However, a PERMANOVA analysis based on Bray-Curtis distances revealed that treatments drove significant differences in microbial communities. Although those differences could not be clearly identified and visualized using taxonomic profiling, ordination, rarefaction curves or network analysis, it is possible that they occurred at lower taxonomic levels or between less abundant OTUs. It is important to note that the large dominance of two OTUs (representing 48.4% of the sequences) from the *Thaumarchaeota* class overwhelm the importance of the other taxa. An additional consideration is that sequencing depth was not sufficient to drive rarefaction curves of observed diversity to saturation indicating that some of the diversity was not represented in our data. Estimating and comparing microbial diversity are challenging due to low frequency counts and possible sequencing errors. Deeper sequencing might be beneficial to detect differences in *G. barretti*'s microbial communities because the samples being compared are closely related (Lemos et al. 2011).

The lack of clear variation patterns in the sponge microbial communities exposed to different crude oil concentrations can be explained by the stability of *G. barretti*'s microbiome in the face of environmental perturbations. It was previously demonstrated that *G. barretti*

hosts a specific homogenous microbial community in its mesophyl that survives and stays stable over long cultivation periods (Hoffmann et al. 2006). Moreover, *G. barretti*'s microbiome remained stable during an acute thermal stress in spite of clear disruption of the sponge's respiration and of LMS (Strand et al. 2017). Several hypotheses might explain this stability: (i) the duration of exposure might not have been long enough to induce visible changes in taxonomy or taxa relative abundance; (ii) *G. barretti* could naturally host microbial communities that are adapted to oil degradation.

Microbial communities do not necessarily change rapidly following oil exposure. A microcosm experiment on oil contaminated sediments qualified some bacterial taxa as "early responders" because they increased their relative abundance within 2 weeks of oil exposure whereas other taxa were qualified as "late responders" because they only started to change their abundance after 3 weeks of exposure (Koo et al. 2015). Another study analysing hydrocarbon biodegradation in mudflats found that, although significant hydrocarbon degradation was perceived after 3 days, significant differences in bacterial community structure between oil-contaminated and control mesocosms were only significant between day 12 and day 28 of exposure (Sanni et al. 2015). It is possible that 8 days of exposure to crude oil was insufficient to induce clear observable changes in *G. barretti*'s microbiome. It seems that the sponge is able to control its microbial partners by regulating pumping rates and DOC uptake (Leys et al. 2017), therefore, the sponge host could potentially slow down any changes in the bacterial composition of its tissue.

Natural seeps are the first source of hydrocarbon in marine ecosystems, they are widespread in oceans and marine microorganisms are constantly exposed to hydrocarbons (Brakstad et al. 2017). Consequently, a question arises: could *G. barretti* and its microbial partners be naturally exposed to hydrocarbons in the marine environment? Sponge grounds in the Northern Atlantic are most abundant at the base of the continental slope and close to deep seafloors (Howell et al. 2016). It is not evident to determine whether sponge grounds are situated in the vicinity of natural oil seeps, however, numerous oil and gas fields have been identified in the Northern Atlantic and mapping of clustered oil-slick data indicates the possibility of natural oil seeps in the Mid-Norway shelf and in the Tromsø and Harstad basin (Vis 2017). A comparison of the distribution of observed sponge grounds and of possible natural oil sources along the Norwegian Continental Shelf suggests a possible close proximity of sponge habitats and oil seeps (**Figure 24**). Natural hydrocarbon discharges near benthic communities have potential adverse outcomes as well as positive effects. Organic enrichment and increased microbial activity can lead to greater food supplies which benefit the benthic community; alternatively, certain organic compounds or chemical by-products of their degradation such as sulphide and ammonia can be toxic and have adverse effects on benthic organisms (Steichen Jr. et al. 1996). It would be worth investigating whether deep-sea sponges are naturally exposed to hydrocarbons originating from the seafloor. The species might have evolved a metabolism and a microbiome adapted to oil exposure.

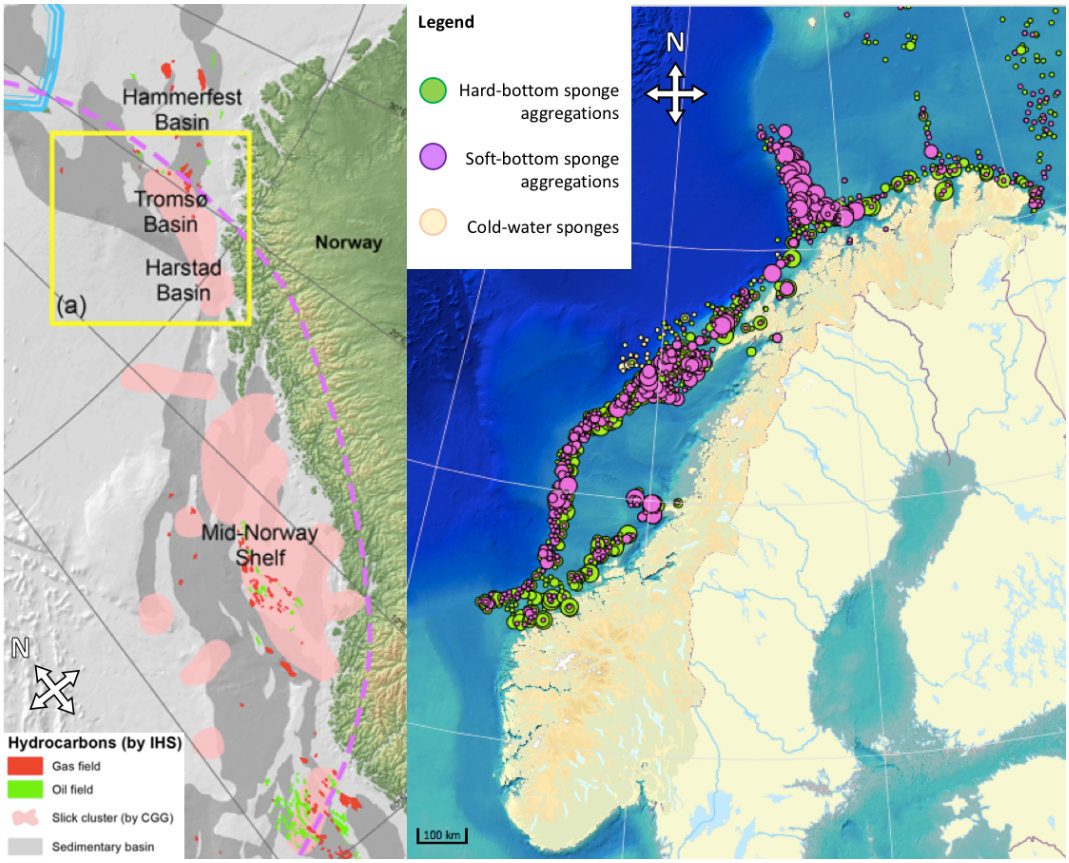

Figure 24 - Distribution of oil sources and of sponge aggregations along the Norwegian Continental Shelf. Left – Distribution of oil and gas fields and mapping of clustered oil-slick data which indicate possible active natural oil seeps. The map is tilted so the north-east is on the top (see compass for orientation). Map retrieved and modified from (Vis 2017). ***Right*** – Distribution of observed sponge grounds along the Mid- and North-Norwegian Continental Shelf. Data is retrieved from MAREANO research cruises and the map was created using the MAREANO map tool (http://www.mareano.no/en/maps/mareano_en.html). Map projection WGS84, UTM 33N. (Mareano 2018).

A short literature review to identify the most well-known and well characterized genera of oil degraders resulted in the identification of 22 of those genera which accounted for 0.0023% of the microbial community in our sponge tissue samples. The abundance of oil degraders associated with *G. barretti* is likely to be underestimated for different reasons: (i) the literature research, although extensive, was not exhaustive; (ii) not all OTUs identified using sequence similarity against the Greengenes database were characterised to the genus levels (many were unassigned at the phylum, class, order, family or genus level) meaning that many OTUs were excluded from the search based on genera; (iii) it is likely that many species capable of oil degradation have not yet been formerly identified and characterized; (iv) alpha-diversity rarefaction curves showed that the sequencing depth did not allow the sampling of the potential total microbial diversity of the sponge tissue, meaning that some taxa were potentially not well represented in our data.

Oil degraders are not restricted to the few genera listed above and could potentially be found in some of the more abundant taxa. For example, OTU 3319, the 7th most abundant OTU in sponge tissues, is a member of the *Chromatiales* (purple sulphur oxidizing bacteria) which have been associated with the initial stages of crude oil degradation (Acosta-González et al. 2015) and harbour an enzyme (methane monooxygenase / ammonia monooxygenase) involved in aliphatic hydrocarbon degradation (Abbasian et al. 2016). Both OTU 39759 and OTU 740, *G. barretti*'s 13th and 19th most abundant OTUs, are part of the family *Piscirickettsiaceae* which encompasses oil degraders such as the well-known *Cycloclasticus*

(Brakstad et al. 2017; Lofthus et al. 2018). Some of the major phyla identified in *G. barretti* have been associated with hydrocarbon degradation and / or responses to oil exposure. Some 175 prokaryotic genera from archaeal phylum *Halobacteria* and from bacterial phyla *Proteobacteria* (alpha-, beta-, gamma- and delta-), *Actinobacteria*, *Firmicutes*, *Bacteroidetes*, *Deinococcus-Thermus* and *Cyanobacteria* use hydrocarbons as their sole or major carbon source (Hazen et al. 2016). Those bacterial phyla were among the most abundant phyla in the sponge tissues (*Proteobacteria*: 11.3%, *Actinobacteria*: 3.25%, *Bacteroidetes*: 0.15%, *Firmicutes*: 0.0014%, *Cyanobacteria*: 0.001%) and might encompass oil degraders that we did not identified based on the genera search. *Gammaproteobacteria* is the class most often associated with hydrocarbon degradation in marine ecosystems (Brakstad et al. 2017). *Chloroflexi*, the most abundant bacterial phylum in *G. barretti*, have demonstrated increased abundances in oil-rich sediments in many studies while *Anaerolineae*, the most abundant class of *Chloroflexi* in our samples, has been associated with degradation of hydrocarbons under anaerobic and sulphate-reducing conditions (Sanni et al. 2015). A previous study using Fluorescence In Situ Hybridization (FISH) to monitor *G. barretti*'s microbial community showed that the sponge hosts numerous genera of sulphate-reducers (Hoffmann et al. 2006). Yet, sulphate-reducing bacteria are able to use sulphate in oil as an alternative to O_2 in anaerobic conditions and they produce H_2S which stimulates the growth of other bacteria (Radax et al. 2012).

Some of the main bacterial taxa identified in *G. barretti* have been associated with responses to oil contamination in the past and several pieces of evidence in the literature indicate that *G. barretti* might host oil-degrading bacteria within the sulphate reducing bacteria or the very abundant *Gammaproteobacteria*, *Chloroflexi* or *Actinobacteria*.

4.3. Implications and future prospects

Sponge explants were exposed to three different crude oil concentrations (33 µg L^{-1}, 100 µg L^{-1} and 300 µg L^{-1}) that were chosen to match realistic hydrocarbon doses found in seawater following an oil spill. For example, total hydrocarbon doses that were measured in the water column in the months following the DWH oil spill ranged from 7.5 µg L^{-1} to 100 µg L^{-1}, representing a 160-fold increase compared to concentrations measured in years prior to the oil spill (Murawski et al. 2016). The experimental setup used in this study had previously been employed with similar oil doses for several oil exposure experiments on fish eggs and embryos which showed visible signs of impacts from oil contamination (Sørhus et al. 2015, 2016; Sørensen et al. 2017). Although the concentrations used in this experiment are relevant based on previous research, they are still subjected to debate. Indeed, depending on depth and distance from the oil discharge and depending on the type of oil spill, total hydrocarbon and PAH concentrations might vary greatly. Peak PAH concentrations were measured three weeks after the DWH and reached up to 189 µg L^{-1} at 1320 m depth near the wellhead (Diercks et al. 2010) which is 50 times higher than the PAH concentrations measured in our high treatment (3.856 µg L^{-1}). Such extreme concentrations, however, remained localised in the deep-sea plume a few hundred meters above the seafloor.

Sponge explants were subjected to an acute crude oil exposure of a duration of 8 days and did not show strong sub-lethal effects. Respiration rates displayed varying patterns of decreased and increased oxygen uptake while moderate lysosomal destabilisation was observed. Those effects had disappeared after a 30 day recovery period. This suggests that the duration of the exposure or the oil doses in the water might not have been sufficient to

induce strong physiological effects on the sponge. Bacterial communities did not show clear signs of change in their structure or richness. This is not surprising as several studies on bacterial communities of oil contaminated sediments showed that several weeks were sometimes necessary to induce significant changes. Future mesocosm experiments aiming to characterize the sponge responses to oil contamination should look into long term exposure to crude oil that could extend to several months. It would also be interesting to monitor the sponges regularly during the recovery period in order to characterize how fast the sponges return to "normal" physiological rates. In order to best assess the sponge physiological response to an exposure to oil, different types of analyses should be considered. The time frame of this study did not allow for supplementary analyses, but water samples were collected in the aim of measuring nutrient levels (ammonium, nitrite / nitrate, silicate and phosphate) before and after incubations. Such data would allow to perceive changes in nutrient utilisation by the sponge and its associated microbial community which could indicate a compromised health or an adaptation to oil exposure. However, it is necessary to revisit the standard methods for nutrient analysis as most are based on fluorometric assays which might be impacted by the oil auto-fluorescence.

Sponges, if they are able to survive crude oil exposure, might actually help in the clean-up and detoxification following an oil spill. This remains to be investigated, but it is possible that by the combined action of their filtering and microbial activity, they could be efficient in removing hydrocarbons from the surrounding water. Alternatively, *G. barretti*, if they effectively accumulate hydrocarbons (currently under investigation by master student Elise Otnes) and survive an oil exposure, could act as biomonitors in cases of oil contamination of benthic ecosystems. A shallow water tropical coastal sponge, *Hymeniacidon heliophila*, was shown to effectively accumulate PAHs, correctly reflecting the levels found in its natural environment and was therefore suggested as a bioindicator for contamination surveillance of estuarine waters (Batista et al. 2013). Sponges are usually good candidate species for biomonitoring as they have ubiquitous distribution in the oceans, are sedentary in nature, have a long life span, tolerate fluctuations of physical and chemical parameters and have an ability to remain stable over long periods (Srikanth and Rao 2016).

An area of interest for future research are the functions performed by *G. barretti*'s microbiome and how it is involved in the sponge's metabolism and survival. It would be interesting to use shotgun metagenomics and examine functional genes involved in hydrocarbon degradation during an exposure to oil. HTS of the 16S rRNA gene of Prokaryotes did not allow investigation of the non-prokaryotic communities. Yet, deep-sea sponges also host diverse algae and fungi (Li et al. 2016) and many genera of marine algae and fungi are capable of oil degradation (Xue et al. 2015). A metatranscriptomic approach was performed once on *G. barretti*, allowing the characterization of the sponge holobiont taxonomic profile for Eukaryotes and Prokaryotes as well as the quantification of the relative abundance of functional transcripts (Radax et al. 2012). New technologies of next generation sequencing (NGS) are increasingly used to investigate microbial responses to oil pollution (Mukherjee and Chattopadhyay 2017). It would be interesting to monitor the expression of certain genes related to both aerobic and anaerobic degradation of aliphatic and aromatic hydrocarbons such as the *alkB* (n-alkane degradation) or the *PAH-RHDa* (PAH ring-hydroxylating dioxygenase) (Marques et al. 2018) during a long term exposure of *G. barretti* to high doses of crude oil in order to identify whether the sponge hosts microbial organisms with a potential for oil bioremediation. Interestingly, deep-sea microorganisms have already shown great potential for bioremediation or natural attenuation of hydrocarbons following the DWH spill.

It was found that microbial functional genes involved in aerobic and anaerobic hydrocarbon degradation as well as genes involved in carbon, nitrogen, sulphur, phosphorus and iron cycling were enriched in the deep-sea oil plume (Lu et al. 2012). Additionally, oil contaminated sediments presented an enrichment in an uncultured *Gammaproteobacterium* and a *Colwellia* species accompanied with expression of genes involved in key hydrocarbon degradation pathways (Mason et al. 2014).

G. barretti is an HMA sponge, meaning that it harbours dense microbial communities. It is not yet clear how HMA and LMA sponges differ from a functional perspective. HMA sponges are known to present lower pumping rates than LMA sponges, allowing them to increase the contact time with seawater containing POM, DOM and inorganic compounds on which the sponge and its dense microbial community feed (Weisz et al. 2008). It was shown that the transcriptional activity of LMA and HMA sponges associated microbiome was correlated with their abundance (Moitinho-Silva et al. 2014), meaning that HMA sponges host more microbial activity than LMA sponges. Moreover, HMA sponges were found to host a more diverse, even and similar symbiont community than LMA sponges which presented more transient communities (Erwin et al. 2015). HMA and LMA sponges have not yet been compared in physiological responses to environmental stress but it would be interesting to investigate whether a denser, more stable microbial community is an asset when dealing with oil toxicity. The lower pumping rates of HMA sponges (Weisz et al. 2008) could also be an advantage when faced with contaminants in the seawater.

Finally, the fact that *G. barretti* could cope with a crude oil exposure in a mesocosm does not necessarily imply that sponges in their natural habitat would cope with oil contamination. Indeed, a mesocosm experiment could not simulate the exact environmental conditions the sponges could be subjected to. For example, it is possible that crude oil associated to marine snow, also called MOSSFA (marine oil snow sedimentation and flocculent accumulation), following an oil spill, has much more adverse impacts on the sponge because of the larger particles (particle size > 0.5 mm and up to tens of centimetres) (Murawski et al. 2016) which could clog the sponge canals. In addition, it has been suggested that deep-sea sponges derive part of their food from resuspended sediment (Vad et al. 2018); the close relationship of the sponge with post-spill oil contaminated sediments could also impact the sponge health.

5. Conclusion

This study constitutes the first attempt at deciphering the responses of a boreal deep-sea sponge holobiont, *Geodia barretti*, to an oil exposure. Sponges in benthic deep-sea ecosystems are key organisms that support vital processes such as benthic-pelagic coupling and provide habitat for a suite of organisms. Understanding how their functioning might be impacted by hydrocarbon contamination will give insightful information for monitoring, management and decision making surrounding oil and gas exploration in the Northern Atlantic. Using mesocosms, we proceeded to the experimental acute exposure of *G. barretti* explants to three ecologically relevant crude oil doses. The results provided us with the first evidence that this high microbial abundance sponge is resilient to a simulated short-term oil exposure. The sponge did not show strong sub-lethal stress responses and presented a stable microbial community across all treatments. However, the variability in respiration rates and lysosomal membrane destabilisation of sponges during the exposure period suggest that sponges experience slight changes in their metabolic functioning. It would be interesting to unravel whether those effects evolve and persist during a chronic exposure to oil.

Further research should aim at characterizing the impacts of a long-term crude oil contamination on the sponge's physiology, cellular integrity, metabolism and associated microbial community. Of particular interest are the functions carried out by the sponge symbionts when dealing with high hydrocarbons concentrations. We hypothesized that sponges might naturally host oil degraders which allow them to cope with hydrocarbon toxicity. Future questions to address are whether a long-term exposure to crude oil induce stronger physiological / cellular / microbial responses and whether the sponge holobiont as a whole could play a role in assimilation and detoxification of oil in contaminated benthic ecosystems.

References

Abbasian F, Palanisami T, Megharaj M, et al (2016) Microbial diversity and hydrocarbon degrading gene capacity of a crude oil field soil as determined by metagenomics analysis. Biotechnol Prog 32:638–648. doi: 10.1002/btpr.2249

Acosta-González A, Martirani-von Abercron S-M, Rosselló-Móra R, et al (2015) The effect of oil spills on the bacterial diversity and catabolic function in coastal sediments: a case study on the Prestige oil spill. Environ Sci Pollut Res 22:15200–15214. doi: 10.1007/s11356-015-4458-y

APPEA (2017) APPEA - the voice of australia's oil and gas industry. https://www.appea.com.au. Accessed 4 Nov 2017

Baguley JG, Montagna PA, Cooksey C, et al (2015) Community response of deep-sea soft-sediment metazoan meiofauna to the Deepwater Horizon blowout and oil spill. 528:127–140. doi: 10.3354/meps11290

Batista D, Tellini K, Nudi AH, et al (2013) Marine sponges as bioindicators of oil and combustion derived PAH in coastal waters. Mar Environ Res 92:234–243. doi: 10.1016/j.marenvres.2013.09.022

Bayer K, Kamke J, Hentschel U (2018) Quantification of bacterial and archaeal symbionts in high and low microbial abundance sponges using real-time PCR. FEMS Microbiol Ecol 89:679–690. doi: 10.1111/1574-6941.12369

Bell JJ (2008) The functional roles of marine sponges. Estuar Coast Shelf Sci 79:341–353. doi: 10.1016/j.ecss.2008.05.002

Bell JJ, Carballo JL (2008) Patterns of sponge biodiversity and abundance across different biogeographic regions. Mar Biol 155:563–570. doi: 10.1007/s00227-008-1036-6

Bell JJ, Mcgrath E, Biggerstaff A, et al (2015) Global conservation status of sponges. Conserv Biol 29:42–53. doi: 10.1111/cobi.12447

Bennear LS (2018) Offshore Oil and Gas Drilling : A Review of Regulatory Regimes in the United States , United Kingdom , and Norway. 9:2–22. doi: 10.1093/reep/reu013

Beyer J, Trannum HC, Bakke T, et al (2016) Environmental effects of the Deepwater Horizon oil spill: A review. Mar Pollut Bull 110:28–51. doi: 10.1016/j.marpolbul.2016.06.027

Bilbao E, Raingeard D, de Cerio OD, et al (2010) Effects of exposure to Prestige-like heavy fuel oil and to perfluorooctane sulfonate on conventional biomarkers and target gene transcription in the thicklip grey mullet Chelon labrosus. Aquat Toxicol 98:282–296. doi: 10.1016/j.aquatox.2010.02.018

Blanchard A, Hiis K, Andersen G, et al (2014) Harmful routines ? Uncertainty in science and con fl icting views on routine petroleum operations in Norway. 43:313–320. doi: 10.1016/j.marpol.2013.07.001

Boehm PD (1964) 15 - Polycyclic Aromatic Hydrocarbons (PAHs) A2 - Morrison, Robert D. In: Murphy BLBT-EF (ed). Academic Press, Burlington, pp 313–337

Bond C (1992) Continuous cell movements rearrange anatomical structures in intact sponges. J Exp Zool 263:284–302. doi: 10.1002/jez.1402630308

Bowerbank JS (1858) On the Anatomy and Physiology of the Spongiadae. Part I. On the Spicula.

BP (2017) BP Statistical Review of World Energy 2017.

Brakstad OG, Lofthus S, Ribicic D, Netzer R (2017) Biodegradation of Petroleum Oil in Cold Marine Environments BT - Psychrophiles: From Biodiversity to Biotechnology. In: Margesin R (ed). Springer International Publishing, Cham, pp 613–644

Brooijmans RJW, Pastink MI, Siezen RJ (2009) Hydrocarbon-degrading bacteria: the oil-spill clean-up crew. Microb Biotechnol 2:587–594. doi: 10.1111/j.1751-7915.2009.00151.x

Brümmer F, Pfannkuchen M, Baltz A, et al (2008) Light inside sponges. J Exp Mar Bio Ecol 367:61–64. doi: 10.1016/j.jembe.2008.06.036

Canganella F, Kato C (2014) Deep-Ocean Ecosystems. In: eLS. American Cancer Society,

Caporaso JG, Bittinger K, Bushman FD, et al (2010a) PyNAST: A flexible tool for aligning sequences to a template alignment. Bioinformatics 26:266–267. doi: 10.1093/bioinformatics/btp636

Caporaso JG, Kuczynski J, Stombaugh J, et al (2010b) QIIME allows analysis of high-throughput community sequencing data. Nat Methods 7:335–336. doi: 10.1038/nmeth.f.303

Carballo JL, Bell JJ (2017) Climate change, ocean acidification and sponges: Impacts across multiple levels of organization.

Cárdenas P, Rapp HT, Klitgaard AB, et al (2013) Taxonomy, biogeography and DNA barcodes of Geodia species

(Porifera, Demospongiae, Tetractinellida) in the atlantic boreo-arctic region. 169:351–311. doi: 10.1111/zoj.12060
Cathalot C, Van Oevelen D, Cox TJS, et al (2015) Cold-water coral reefs and adjacent sponge grounds: Hotspots of benthic respiration and organic carbon cycling in the deep sea. Front Mar Sci. doi: 10.3389/fmars.2015.00037
Danovaro R, Molari M, Corinaldesi C, Dell'Anno A (2016) Macroecological drivers of archaea and bacteria in benthic deep-sea ecosystems. Sci Adv 2:e1500961. doi: 10.1126/sciadv.1500961
De Goeij JM, De Kluijver A, Van Duyl FC, et al (2009) Cell kinetics of the marine sponge Halisarca caerulea reveal rapid cell turnover and shedding. J Exp Biol 212:3892 LP-3900.
DeSantis TZ, Hugenholtz P, Larsen N, et al (2006) Greengenes, a chimera-checked 16S rRNA gene database and workbench compatible with ARB. Appl Environ Microbiol 72:5069–5072. doi: 10.1128/AEM.03006-05
Diercks A-R, Highsmith RC, Asper VL, et al (2010) Characterization of subsurface polycyclic aromatic hydrocarbons at the Deepwater Horizon site. Geophys Res Lett. doi: 10.1029/2010GL045046
Du M, Kessler JD (2012) Assessment of the Spatial and Temporal Variability of Bulk Hydrocarbon Respiration Following the Deepwater Horizon Oil Spill. Environ Sci Technol 46:10499–10507. doi: 10.1021/es301363k
Edgar RC (2010) Search and clustering orders of magnitude faster than BLAST. Bioinformatics 26:2460–2461. doi: 10.1093/bioinformatics/btq461
Edge KJ, Dafforn KA, Simpson SL, et al (2015) Resuspended contaminated sediments cause sublethal stress to oysters: A biomarker differentiates total suspended solids and contaminant effects. Environ Toxicol Chem 34:1345–1353. doi: 10.1002/etc.2929
Edge KJ, Johnston EL, Dafforn KA, et al (2016) Sub-lethal effects of water-based drilling muds on the deep-water sponge Geodia barretti. Environ Pollut 212:525–534. doi: 10.1016/j.envpol.2016.02.047
Edge KJ, Johnston EL, Roach AC, Ringwood AH (2012) Indicators of environmental stress: Cellular biomarkers and reproductive responses in the Sydney rock oyster (Saccostrea glomerata). Ecotoxicology 21:1415–1425. doi: 10.1007/s10646-012-0895-2
Egres AG, Martins CC, Oliveira VM de, Lana P da C (2012) Effects of an experimental in situ diesel oil spill on the benthic community of unvegetated tidal flats in a subtropical estuary (Paranaguá Bay, Brazil). 64:2681–2691. doi: 10.1016/j.marpolbul.2012.10.007
EIA (2017a) International Energy Outlook 2017 Overview. Energy Inf Adm US Dep Energy. doi: DOE/EIA-0484(2017)
EIA (2017b) International - U.S. Energy Information Administration (EIA). In: eia Beta. https://www.eia.gov/beta/international/. Accessed 4 Nov 2017
Erwin PM, Coma R, López-Sendino P, et al (2015) Stable symbionts across the HMA-LMA dichotomy: Low seasonal and interannual variation in sponge-associated bacteria from taxonomically diverse hosts. FEMS Microbiol Ecol. doi: 10.1093/femsec/fiv115
Fang JKH, Rooks CA, Krogness CM, et al (2018) Impact of particulate sediment , bentonite and barite (oil-drilling waste) on net fl uxes of oxygen and nitrogen in Arctic-boreal sponges *. Environ Pollut 238:948–958. doi: 10.1016/j.envpol.2017.11.092
Fisher CR, Montagna PA, Sutton TT (2016) How did the Deepwater Horizon oil spill impact deep-sea ecosystems? 29:182–195. doi: 10.5670/oceanog.2016.82
Forsgren E, Christensen-Dalsgaard S, Fauchald P, et al (2009) Norwegian marine ecosystems – are northern ones more vulnerable to pollution from oil than southern ones? NINA Rep 514 32 pp.
Freiwald A, Fosså JH, Grehan A, et al (2004) Cold-water Coral Reefs.
Gautier DL, Bird KJ, Charpentier RR, et al (2009) Assessment of Undiscovered Oil and Gas in the Arctic. Science (80-) 324:1175 LP-1179.
Glover AG, Smith CR (2003) The deep-sea floor ecosystem: Current status and prospects of anthropogenic change by the year 2025. Environ. Conserv. 30:219–241.
Guihen D, White M, Lundälv T (2012) Temperature shocks and ecological implications at a cold-water coral reef. doi: 10.1017/S1755267212000413
Haas BJ, Gevers D, Earl AM, et al (2011) Chimeric 16S rRNA sequence formation and detection in Sanger and 454-pyrosequenced PCR amplicons. Genome Res 21:494–504. doi: 10.1101/gr.112730.110
Hazen TC, Prince RC, Mahmoudi N (2016) Marine Oil Biodegradation. Environ Sci Technol 50:2121–2129. doi: 10.1021/acs.est.5b03333
Henry L-A, Hart M (2005) Regeneration from injury and resource allocation in sponges and corals - A review. Int Rev Hydrobiol 90:125–158. doi: 10.1002/iroh.200410759
Hoffmann F, Radax R, Woebken D, et al (2009) Complex nitrogen cycling in the sponge Geodia barretti. 11:2228–2243. doi: 10.1111/j.1462-2920.2009.01944.x

Hoffmann F, Rapp HT, Reitner J (2006) Monitoring microbial community composition by fluorescence in situ hybridization during cultivation of the marine cold-water sponge Geodia barretti. Mar Biotechnol 8:373–379. doi: 10.1007/s10126-006-5152-3

Hoffmann F, Rapp HT, Zöller T, Reitner J (2003) Growth and regeneration in cultivated fragments of the boreal deep water sponge Geodia barretti bowerbank, 1858 (Geodiidae, Tetractinellida, Demospongiae). 100:109–118. doi: 10.1016/S0168-1656(02)00258-4

Hogg MM, Tendal OS, Conway KW, et al (2010) Deep-sea Sponge Grounds: Reservoirs of Biodiversity.

Howell K-L, Piechaud N, Downie A-L, Kenny A (2016) The distribution of deep-sea sponge aggregations in the North Atlantic and implications for their effective spatial management. Deep Res Part I Oceanogr Res Pap 115:203–220. doi: 10.1016/j.dsr.2016.07.005

ITOPF (2014) The International Tanker Owners Pollution Federation Limited. http://www.itopf.com. Accessed 4 Nov 2017

Kennedy J, Flemer B, Jackson SA, et al (2014) Evidence of a putative deep sea specific microbiome in marine sponges. PLoS One. doi: 10.1371/journal.pone.0091092

Konoki K, Okada K, Kohama M, et al (2015) Identification of okadaic acid binding protein 2 in reconstituted sponge cell clusters from Halichondria okadai and its contribution to the detoxification of okadaic acid. Toxicon 108:38–45. doi: 10.1016/j.toxicon.2015.09.026

Koo H, Mojib N, Huang JP, et al (2015) Bacterial community shift in the coastal Gulf of Mexico salt-marsh sediment microcosm in vitro following exposure to the Mississippi Canyon Block 252 oil (MC252). 3 Biotech 5:379–392. doi: 10.1007/s13205-014-0233-x

Kurz T, Terman A, Gustafsson B, Brunk UT (2008) Lysosomes and oxidative stress in aging and apoptosis. Biochim Biophys Acta - Gen Subj 1780:1291–1303. doi: https://doi.org/10.1016/j.bbagen.2008.01.009

Kutti T, Bannister RJ, Fosså JH, et al (2015) Metabolic responses of the deep-water sponge Geodia barretti to suspended bottom sediment, simulated mine tailings and drill cuttings. J Exp Mar Bio Ecol 473:64–72. doi: 10.1016/j.jembe.2015.07.017

Kutti T, Bannister RJ, Fosså JH (2013a) Community structure and ecological function of deep-water sponge grounds in the Traenadypet MPA-Northern Norwegian continental shelf. 69:21–30. doi: 10.1016/j.csr.2013.09.011

Kutti T, Bannister RJ, Fosså JH (2013b) Community structure and ecological function of deep-water sponge grounds in the Traenadypet MPA—Northern Norwegian continental shelf. Cont Shelf Res 69:21–30. doi: 10.1016/j.csr.2013.09.011

Lee LH, Lin HJ (2013) Effects of an oil spill on benthic community production and respiration on subtropical intertidal sandflats. 73:291–299. doi: 10.1016/j.marpolbul.2013.05.006

Lemos LN, Fulthorpe RR, Triplett EW, Roesch LFW (2011) Rethinking microbial diversity analysis in the high throughput sequencing era. J Microbiol Methods 86:42–51. doi: 10.1016/j.mimet.2011.03.014

Leys SP, Kahn AS, Fang JKH, et al (2017) Phagocytosis of microbial symbionts balances the carbon and nitrogen budget for the deep-water boreal sponge Geodia barretti. Limnol Oceanogr 63:187–202. doi: 10.1002/lno.10623

Li Z, Wang Y, Li J, et al (2016) Metagenomic Analysis of Genes Encoding Nutrient Cycling Pathways in the Microbiota of Deep-Sea and Shallow-Water Sponges. Mar Biotechnol 18:659–671. doi: 10.1007/s10126-016-9725-5

Lidgren G, Bohlin L, Bergman J (1986) Studies of swedish marine organisms VII. A novel biologically active indole alkaloid from the sponge geodia baretti. Tetrahedron Lett 27:3283–3284. doi: https://doi.org/10.1016/S0040-4039(00)84776-0

Lind KF, Hansen E, Østerud B, et al (2013) Antioxidant and anti-inflammatory activities of barettin. Mar Drugs 11:2655–2666. doi: 10.3390/md11072655

Lofthus S, Netzer R, Lewin AS, et al (2018) Biodegradation of n-alkanes on oil–seawater interfaces at different temperatures and microbial communities associated with the degradation. Biodegradation 29:141–157. doi: 10.1007/s10532-018-9819-z

Lu Z, Deng Y, Van Nostrand JD, et al (2012) Microbial gene functions enriched in the Deepwater Horizon deep-sea oil plume. ISME J 6:451–460. doi: 10.1038/ismej.2011.91

Ludeman DA, Reidenbach MA, Leys SP (2017) The energetic cost of filtration by demosponges and their behavioural response to ambient currents. J Exp Biol 220:995–1007. doi: 10.1242/jeb.146076

Luter HM, Bannister RJ, Whalan S, et al (2017) Microbiome analysis of a disease affecting the deep-sea sponge Geodia barretti. FEMS Microbiol Ecol 93:1–6. doi: 10.1093/femsec/fix074

Mareano (2018) Mareano - collecting marine knowledge. In: Havforskningsinstituttet.

Marques JM, Paixão CTM, Palma Pantoja GVM, et al (2018) Petroleum microbiology and genetics. In: Advances

in Genetics Research. pp 1–51
Martínez-Gómez C, Bignell J, Lowe D (2015) Lysosomal membrane stability in mussels. ICES Tech Mar Environ Sci 41 pp.
Mason OU, Scott NM, Gonzalez A, et al (2014) Metagenomics reveals sediment microbial community response to Deepwater Horizon oil spill. ISME J 8:1464–1475. doi: 10.1038/ismej.2013.254
McMurdie PJ, Holmes S (2013) phyloseq: An R Package for Reproducible Interactive Analysis and Graphics of Microbiome Census Data. PLoS One 8:e61217.
MetaMicrobe.com (2014) List of bacterial genera important in oil bioremediation. http://www.metamicrobe.com/petroleum-microbiology/oil-bioremediation-bacteria.html. Accessed 9 Jul 2018
Moitinho-Silva L, Bayer K, Cannistraci C V, et al (2014) Specificity and transcriptional activity of microbiota associated with low and high microbial abundance sponges from the Red Sea. Mol Ecol 23:1348–1363. doi: 10.1111/mec.12365
Mori T, Iwamoto K, Wakaoji S, et al (2016) Characterization of a novel gene involved in cadmium accumulation screened from sponge-associated bacterial metagenome. Gene 576:618–625. doi: 10.1016/j.gene.2015.10.018
Muehlenbachs L, Cohen MA, Gerarden T (2013) The impact of water depth on safety and environmental performance in offshore oil and gas production. 55:699–705. doi: 10.1016/j.enpol.2012.12.074
Mukherjee A, Chattopadhyay D (2017) Exploring environmental systems and processes through next-generation sequencing technologies: insights into microbial response to petroleum contamination in key environments. Nucl 60:175–186. doi: 10.1007/s13237-016-0190-3
Murawski SA, Fleeger JW, Patterson WF, et al (2016) How did the Deepwater Horizon oil spill affect coastal and continental shelf ecosystems of the Gulf of Mexico? 29:160–173. doi: 10.5670/oceanog.2016.80
NAS (2002) Oil in the Sea III: Inputs, Fates, and Effects. National Academies Press, Washington, D.C.
Negri AP, Brinkman DL, Flores F, et al (2016) Acute ecotoxicology of natural oil and gas condensate to coral reef larvae. doi: 10.1038/srep21153
NOAA (2017a) How toxic is oil? In: Natl. Ocean. Atmos. Adm. - Off. Response Restor. https://response.restoration.noaa.gov/oil-and-chemical-spills/significant-incidents/exxon-valdez-oil-spill/how-toxic-oil.html. Accessed 16 Nov 2017
NOAA (2017b) Oil types. In: Natl. Ocean. Atmos. Adm. - Off. Response Restor. https://response.restoration.noaa.gov/oil-and-chemical-spills/oil-spills/oil-types.html. Accessed 16 Nov 2017
NOAA (2017c) What is weathering? In: Natl. Ocean. Atmos. Adm. - Off. Response Restor. https://response.restoration.noaa.gov/oil-and-chemical-spills/significant-incidents/exxon-valdez-oil-spill/what-weathering.html. Accessed 16 Nov 2017
NOAA (2018) How far does light travel in the ocean? In: Natl. Ocean Serv. website. https://oceanservice.noaa.gov/facts/light_travel.html. Accessed 30 May 2018
NOAA, Coral Reef Conservation Program (2010) NOAA Strategic Plan for Deep-Sea Coral and Sponge Ecosystems: Research, Management and International Cooperation. 67 pp.
Noble RT, Fuhrman JA (1998) Use of SYBR Green I for rapid epifluorescence counts of marine viruses and bacteria. Aquat Microb Ecol 14:113–118. doi: 10.3354/ame014113
Nordtug T, Olsen AJ, Altin D, et al (2011) Method for generating parameterized ecotoxicity data of dispersed oil for use in environmental modelling. Mar Pollut Bull 62:2106–2113. doi: 10.1016/j.marpolbul.2011.07.015
Norwegian Petroleum Directorate (2018) Licensing position for the Norwegian continental shelf. In: norskpetroleum.no. https://www.norskpetroleum.no/en/exploration/licensing-position-for-the-norwegian-continental-shelf/. Accessed 28 May 2018
Norwegian Petroleum Directorate (2017) How is petroleum formed? In: norskpetroleum.no. https://www.norskpetroleum.no/en/petroleum-resources/petroleum-formation/. Accessed 4 Nov 2017
Norwegian Petroleum Directorate, Norwegian Ministry of Petroleum and Energy (2018) Norwegian Petroleum Facts. https://www.norskpetroleum.no/. Accessed 28 May 2018
OSPAR commission (2010) Background document for Deep-sea sponge aggregations. London
Pallela R, Ehrlich H (2016) Marine sponges: Chemicobiological and biomedical applications. Springer India
Patel A, Noble RT, Steele JA, et al (2007) Virus and prokaryote enumeration from planktonic aquatic environments by epifluorescence microscopy with SYBR Green I. Nat Protoc 2:269.
Petrick S, Riemann-campe K, Hoog S, et al (2017) Climate change , future Arctic Sea ice , and the competitiveness of European Arctic offshore oil and gas production on world markets. 46:410–422. doi: 10.1007/s13280-017-0957-z

Radax R, Rattei T, Lanzen A, et al (2012) Metatranscriptomics of the marine sponge Geodia barretti: Tackling phylogeny and function of its microbial community. 14:1308–1324. doi: 10.1111/j.1462-2920.2012.02714.x

Ramirez-llodra E, Tyler PA, Baker MC, et al (2011) Man and the Last Great Wilderness : Human Impact on the Deep Sea. PLoS One. doi: 10.1371/journal.pone.0022588

Ringwood AH, Conners DE, Hoguet J (1998) Effects of natural and anthropogenic stressors on lysosomal destabilization in oysters Crassostrea virginica. Mar Ecol Prog Ser 166:163–171. doi: 10.3354/meps166163

Ringwood AH, Conners DE, Hoguet J, Ringwood LA (2005) Lysosomal destabilization assays for estuarine organisms. In: Ostrander GK (ed) Techniques in Aquatic Toxicology, Volume 2. CRC press, Taylor and Francis, pp 287–300

Roberts DA, Johnston EL, Poore AGB (2008) Contamination of marine biogenic habitats and effects upon associated epifauna. Mar Pollut Bull 56:1057–1065. doi: 10.1016/j.marpolbul.2008.03.003

Ruiz P, Ortiz-Zarragoitia M, Orbea A, et al (2012) Responses of conventional and molecular biomarkers in turbot Scophthalmus maximus exposed to heavy fuel oil no. 6 and styrene. Aquat Toxicol 116–117:116–128. doi: 10.1016/j.aquatox.2012.02.004

Ruiz P, Ortiz-Zarragoitia M, Orbea A, et al (2014) Short- and long-term responses and recovery of mussels Mytilus edulis exposed to heavy fuel oil no. 6 and styrene. Ecotoxicology 23:861–879. doi: 10.1007/s10646-014-1226-6

Sanni GO, Coulon F, McGenity TJ (2015) Dynamics and distribution of bacterial and archaeal communities in oil-contaminated temperate coastal mudflat mesocosms. Environ Sci Pollut Res 22:15230–15247. doi: 10.1007/s11356-015-4313-1

Santos-Gandelman JF, Giambiagi-Demarval M, Muricy G, et al (2014) Mercury and methylmercury detoxification potential by sponge-associated bacteria. Antonie van Leeuwenhoek, Int J Gen Mol Microbiol 106:585–590. doi: 10.1007/s10482-014-0224-2

Schöttner S, Hoffmann F, Cárdenas P, et al (2013) Relationships between Host Phylogeny, Host Type and Bacterial Community Diversity in Cold-Water Coral Reef Sponges. PLoS One 8:1–11. doi: 10.1371/journal.pone.0055505

SHELL (2018) Unlocking Energy from Deep Water. In: Energy Innov. https://www.shell.com/energy-and-innovation/deep-water/unlocking-energy-from-deep-water.html. Accessed 1 Jun 2018

Sjögren M, Dahlström M, Göransson U, et al (2004) Recruitment in the field of Balanus improvisus and Mytilus edulis in response to the antifouling cyclopeptides barettin and 8,9-dihydrobarettin from the marine sponge Geodia barretti. 20:291–297. doi: 10.1080/08927010400027027

Smith LC, Stephenson SR (2013) New Trans-Arctic shipping routes navigable by midcentury. 2013:6–10. doi: 10.1073/pnas.1214212110

Soetaert K, van Oevelen D (2009) Modeling food web interactions in benthic deep-sea ecosystems: A practical guide. Oceanography 22:128–143.

Solé M, Livingstone DR (2005) Components of the cytochrome P450-dependent monooxygenase system and “NADPH-independent benzo[a]pyrene hydroxylase” activity in a wide range of marine invertebrate species. Comp Biochem Physiol - C Toxicol Pharmacol 141:20–31. doi: 10.1016/j.cca.2005.04.008

Sørensen L, Sørhus E, Nordtug T, et al (2017) Oil droplet fouling and differential toxicokinetics of polycyclic aromatic hydrocarbons in embryos of Atlantic haddock and cod. PLoS One 12:1–26. doi: 10.1371/journal.pone.0180048

Sørhus E, Edvardsen RB, Karlsen Ø, et al (2015) Unexpected interaction with dispersed crude oil droplets drives severe toxicity in atlantic haddock embryos. PLoS One 10:1–21. doi: 10.1371/journal.pone.0124376

Sørhus E, Incardona JP, Furmanek T, et al (2017) Novel adverse outcome pathways revealed by chemical genetics in a developing marine fish. Elife 6:1–30. doi: 10.7554/eLife.20707

Sørhus E, Incardona JP, Karlsen Ø, et al (2016) Crude oil exposures reveal roles for intracellular calcium cycling in haddock craniofacial and cardiac development. Sci Rep 6:1–21. doi: 10.1038/srep31058

Spetland F, Rapp HT, Hoffmann F, Tendal OS (2007) Sexual reproduction of Geodia barretti Bowerbank, 1858 (Porifera, Astrophorida) in two Scandinavian fjords. Mus Nac Ser Livros 1858:613–620.

Srikanth K, Rao J V (2016) Sponges as biomonitors of metal toxicity in the aquatic systems. In: Marine Sponges: Chemicobiological and Biomedical Applications. pp 105–114

Steichen Jr. DJ, Holbrook SJ, Osenberg CW (1996) Distribution and abundance of benthic and demersal macrofauna within a natural hydrocarbon seep. Mar Ecol Prog Ser 138:71–82. doi: 10.3354/meps138071

Strand R, Whalan S, Webster NS, et al (2017) The response of a boreal deep-sea sponge holobiont to acute thermal stress. doi: 10.1038/s41598-017-01091-x

Sunil Kumar P (2016) Remarks on the chemo biological applications of marine sponges. In: Marine Sponges:

Chemicobiological and Biomedical Applications. pp 97–103
Takahashi S, Tomita J, Nishioka K, et al (2014) Development of a prokaryotic universal primer for simultaneous analysis of Bacteria and Archaea using next-generation sequencing. PLoS One. doi: 10.1371/journal.pone.0105592
Thakur NL, Singh A (2016) Chemical ecology of marine sponges. Springer India, pp 37–52
Thistle D (2003) The Deep-Sea Floor: an Overview. In: Ecosystems of the World, P. A. Tyle. Elsevier, Amsterdam, pp 5–37
Thomas T, Moitinho-Silva L, Lurgi M, et al (2016) Diversity, structure and convergent evolution of the global sponge microbiome. Nat Commun 7:11870.
Thurber AR, Sweetman AK, Narayanaswamy BE, et al (2014) Ecosystem function and services provided by the deep sea. Biogeosciences 3941–3963. doi: 10.5194/bg-11-3941-2014
Tjensvoll I, Kutti T, Fosså J, Bannister R (2013) Rapid respiratory responses of the deep-water sponge Geodia barretti exposed to suspended sediments. Aquat Biol 19:65–73. doi: 10.3354/ab00522
Turja R, Soirinsuo A, Budzinski H, et al (2013) Biomarker responses and accumulation of hazardous substances in mussels (Mytilus trossulus) transplanted along a pollution gradient close to an oil terminal in the Gulf of Finland (Baltic Sea). Comp Biochem Physiol - C Toxicol Pharmacol 157:80–92. doi: 10.1016/j.cbpc.2012.09.006
Vad J, Kazanidis G, Henry L, et al (2018) Potential Impacts of Offshore Oil and Gas Activities on Deep-Sea Sponges and the Habitats They Form, 1st edn. Elsevier Ltd.
van Soest RWM, Boury-Esnault N, Vacelet J, et al (2012) Global diversity of sponges (Porifera). PLoS One. doi: 10.1371/journal.pone.0035105
Varjani SJ, Upasani VN (2017) A new look on factors affecting microbial degradation of petroleum hydrocarbon pollutants. Int Biodeterior Biodegradation 120:71–83. doi: https://doi.org/10.1016/j.ibiod.2017.02.006
Vis G-J (2017) Geology and seepage in the NE Atlantic region. Geol. Soc. Spec. Publ. 447:443–455.
Webster NS, Blackall LL (2009) What do we really know about sponge-microbial symbioses. 3:1–3. doi: 10.1038/ismej.2008.102
Webster NS, Taylor MW (2012) Marine sponges and their microbial symbionts: Love and other relationships. Environ Microbiol 14:335–346. doi: 10.1111/j.1462-2920.2011.02460.x
Weisz JB, Lindquist N, Martens CS (2008) Do associated microbial abundances impact marine demosponge pumping rates and tissue densities? Oecologia 155:367–376. doi: 10.1007/s00442-007-0910-0
Wilkinson CR (1984) Immunological evidence for the Precambrian origin of bacterial symbioses in marine sponges. Proc R Soc London - Biol Sci 220:509–517.
Wilson B, Müller O, Nordmann E-L, et al (2017) Changes in Marine Prokaryote Composition with Season and Depth Over an Arctic Polar Year. Front Mar Sci 4:1–17. doi: 10.3389/fmars.2017.00095
Word JQ (2014) Environmental Impacts of Arctic Oil Spills and Arctic Spill Response Technologies.
Wulff J (2010) Regeneration of sponges in ecological context: Is regeneration an integral part of life history and morphological strategies? Integr Comp Biol 50:494–505. doi: 10.1093/icb/icq100
Xue J, Yu Y, Bai Y, et al (2015) Marine Oil-Degrading Microorganisms and Biodegradation Process of Petroleum Hydrocarbon in Marine Environments: A Review. Curr Microbiol 71:220–228. doi: 10.1007/s00284-015-0825-7

Supplementary Material

A. Summary of experimental and recovery periods

Date	C1 to H1	C2 to H2	C3 to H3	C4 to H4
04/02/2018	Day 0	-	Day 0	-
05/02/2018	**Day 1**	Day 0	**Day 1**	Day 0
06/02/2018	**Day 2**	**Day 1**	**Day 2**	**Day 1**
07/02/2018	-	**Day 2**	-	**Day 2**
08/02/2018	**Day 4**	-	**Day 4**	-
09/02/2018	-	**Day 4**	-	**Day 4**
10/02/2018	-	-	-	-
11/02/2018	-	-	-	-
12/02/2018	**Day 8**	-	**Day 8**	-
13/02/2018	-	**Day 8**	-	**Day 8**
14/02/2018	1st day of recovery	1st day of recovery	1st day of recovery	1st day of recovery
…	-	-	-	-
14/03/2018	**Last day of recovery**	-	**Last day of recovery**	-
15/03/2018	-	**Last day of recovery**	-	**Last day of recovery**

Date	Day of experiment	Run	Mesocosms concerned	Tº of water before incubation (ºC)
05/02/2018	Day 1	Run 1	C1-H1	7.9
05/02/2018	Day 1	Run 2	C1-H1 controls	7.9
05/02/2018	Day 1	Run 3	C3-H3	7.9
05/02/2018	Day 1	Run 4	C3-H3 controls	7.9
06/02/2018	Day 2	Run 1	C1-H1	7.9
06/02/2018	Day 2	Run 2	C3-H3	7.9
06/02/2018	Day1	Run3	C2-H2	8.0
06/02/2018	Day 1	Run 4	C2-H2 controls	8.0
06/02/2018	Day 1	Run 5	C4-H4	7.9
06/02/2018	Day 2	Run 6	C3-H3 controls	7.9
07/02/2018	Day 2	Run 1	C2-H2	7.9
07/02/2018	Day 2	Run 2	C2-H2 controls	8.0
07/02/2018	Day 2	Run3	C4-H4	8.1
07/02/2018	Day 2	Run 4	C4-H4 controls	8.1
08/02/2018	Day 4	Run 1	C1-H1	8.0
08/02/2018	Day 4	Run 2	C1-H1 controls	8.1
08/02/2018	Day 4	Run3	C3-H3	8.1
08/02/2018	Day 4	Run 4	C3-H3 controls	8.1-8.2
09/02/2018	Day 4	Run 1	C2-H2	8.1
09/02/2018	Day 4	Run 2	C2-H2 controls	8.1
09/02/2018	Day 4	Run3	C4-H4	8.1
09/02/2018	Day 4	Run 4	C4-H4 controls	8.1
12/02/2018	Day 8	Run 1	C1-H1	7.9
12/02/2018	Day 8	Run 2	C1-H1 controls	8.0
12/02/2018	Day 8	Run3	C3-H3	8.0
12/02/2018	Day 8	Run 4	C3-H3 controls	8.0
13/02/2018	Day 8	Run 1	C2-H2	7.9-8.0
13/02/2018	Day 8	Run 2	C2-H2 controls	8.0-8.1
13/02/2018	Day 8	Run3	C4-H4	NA
13/02/2018	Day 8	Run 4	C4-H4 controls	8.1
14/03/2018	Recovery	Run 1	C1-H1	8.0
14/03/2018	Recovery	Run 2	C3-H3	8.0
14/03/2018	Recovery	Run3	C3-H3 controls	NA
14/03/2018	Recovery	Run 4	C1-H1 controls	8.0
15/03/2018	Recovery	Run 5	C2-H2	7.8
15/03/2018	Recovery	Run 6	C4-H4	8.2
15/03/2018	Recovery	Run 7	C4-H4 controls	8.7
15/03/2018	Recovery	Run 8	C2-H2 controls	8.5

B. Chemistry of the water during exposure period

Master student Elise Otnes and postdoctor Carey Donald analysed the chemistry of the mesocosms' water. Their analysis showed that PAH doses were stable throughout the 8 days exposure and corresponded to the expected concentrations of the different treatments.

PAH levels relative to nominal oil doses (PAH % of oil)

Treatment	Oil exposure time (sec min^{-1})	Nominal doses (µg oil L^{-1})	PAH doses (µg PAH L^{-1})	SD	RSD	Average PAH % of oil	Estimated real oil doses (µg L^{-1})*
Control	0	0	70 x 10^{-3}	11	16	–	–
Low	1.1	33	284 x 10^{-3}	78	27	0.86	22
Medium	3.4	100	1342 x 10^{-3}	156	12	1.34	103
High	10.1	300	3856 x 10^{-3}	624	16	1.28	297

*The percentage of PAHs is the Trold oil is 1.3 %. The real oil doses in the mesocosms are estimated from the measured PAHs doses.

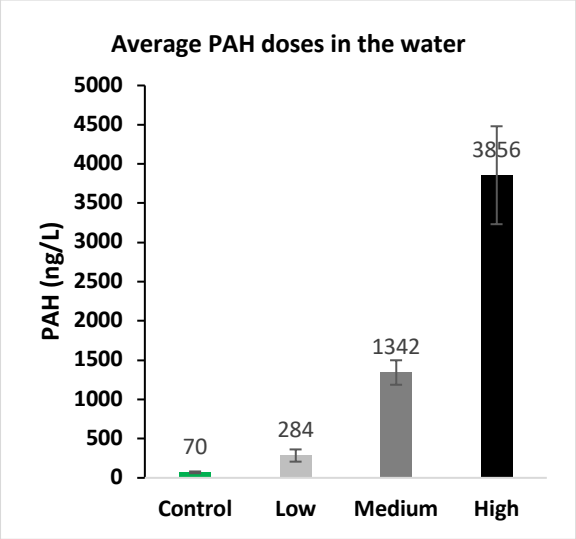

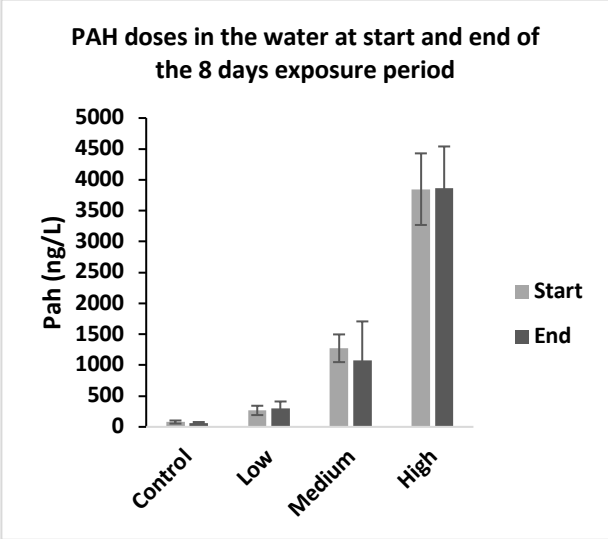

C. Weight of sponge explants & volume of water in incubation chamber

Sponge explant	Wet weight (g)	Dry weight (g)	Volume of water in empty incubation chamber (L)	Volume of water in incubation chamber with sponge (L)
C1	29,154	5,831	0,7313	0,7021
L1	35,446	7,089	0,7313	0,6958
P1	31,025	6,205	0,7313	0,7003
H1	29,692	5,938	0,7313	0,7016
C2	28,479	5,696	0,7313	0,728
L2	32,396	6,479	0,7313	0,6989
P2	27,009	5,402	0,7313	0,7043
H2	31,767	6,353	0,7313	0,6995
C3	33,649	6,730	0,7313	0,6976
L3	31,195	6,239	0,7313	0,7001
P3	35,860	7,172	0,7313	0,6954
H3	34,193	6,839	0,7313	0,6971
C4	30,721	6,144	0,7313	0,7006
L4	27,262	5,452	0,7313	0,7040
P4	36,865	7,373	0,7313	0,6944
H4	25,560	5,112	0,7313	0,7057

D. Respiration data & summary

Date	Day	Treatment	Replicate	Sponges (µmol O_2 h^{-1} g^{-1})	Background (µmol O_2 h^{-1})
05/02/2018	D1	C	C1	0,5740	0,2610
06/02/2018	D1	C	C2	0,7776	0,7546
05/02/2018	D1	C	C3	0,9056	0,7022
06/02/2018	D1	C	C4	0,6004	NA
05/02/2018	D1	L	L1	0,4950	0,3002
06/02/2018	D1	L	L2	0,4565	2,1276
05/02/2018	D1	L	L3	0,2653	3,8242
06/02/2018	D1	L	L4	0,5610	NA
05/02/2018	D1	P	P1	0,6704	0,2466
06/02/2018	D1	P	P2	0,5728	2,0363
05/02/2018	D1	P	P3	0,1778	3,4223
06/02/2018	D1	P	P4	0,3158	NA
05/02/2018	D1	H	H1	0,3445	0,0908
06/02/2018	D1	H	H2	0,6933	2,5034
05/02/2018	D1	H	H3	0,0807	4,4558
06/02/2018	D1	H	H4	0,3765	NA
06/02/2018	D2	C	C1	0,6545	NA
07/02/2018	D2	C	C2	0,9530	0,1162
06/02/2018	D2	C	C3	0,8660	0,2526
07/02/2018	D2	C	C4	0,5499	0,3728
06/02/2018	D2	L	L1	0,3379	NA
07/02/2018	D2	L	L2	0,8349	0,0246
06/02/2018	D2	L	L3	0,7943	1,4821
07/02/2018	D2	L	L4	0,6146	4,0146
06/02/2018	D2	P	P1	0,5028	NA
07/02/2018	D2	P	P2	1,1827	-0,3510
06/02/2018	D2	P	P3	0,4196	1,6564
07/02/2018	D2	P	P4	0,1617	3,8876
06/02/2018	D2	H	H1	0,0437	NA
07/02/2018	D2	H	H2	1,6129	-0,2051
06/02/2018	D2	H	H3	0,6010	2,7084
07/02/2018	D2	H	H4	0,3273	4,6660
08/02/2018	D4	C	C1	0,5476	0,2816
09/02/2018	D4	C	C2	0,8816	0,1072
08/02/2018	D4	C	C3	0,7961	0,6630
09/02/2018	D4	C	C4	0,7114	0,1941
08/02/2018	D4	L	L1	0,6895	-0,3119
09/02/2018	D4	L	L2	0,3933	2,0082
08/02/2018	D4	L	L3	0,4313	1,1809
09/02/2018	D4	L	L4	1,2724	0,9694
08/02/2018	D4	P	P1	0,6981	0,1091
09/02/2018	D4	P	P2	0,4611	2,0782
08/02/2018	D4	P	P3	0,4281	1,9602
09/02/2018	D4	P	P4	0,6356	0,4210
08/02/2018	D4	H	H1	0,5651	-0,1750
09/02/2018	D4	H	H2	0,7073	1,3978
08/02/2018	D4	H	H3	0,6027	3,1099
09/02/2018	D4	H	H4	0,8516	0,6493
12/02/2018	D8	C	C1	0,5183	-0,2524
13/02/2018	D8	C	C2	0,5634	0,2380
12/02/2018	D8	C	C3	0,6328	0,4372
13/02/2018	D8	C	C4	0,3410	2,4820
12/02/2018	D8	L	L1	0,3395	-0,2917
13/02/2018	D8	L	L2	0,2144	2,8252
12/02/2018	D8	L	L3	0,5302	0,4612

13/02/2018	D8	L	L4	0,7929	1,8606
12/02/2018	D8	P	P1	0,5175	-0,0458
13/02/2018	D8	P	P2	0,2765	2,2895
12/02/2018	D8	P	P3	0,7905	3,8456
13/02/2018	D8	P	P4	0,3030	1,5354
12/02/2018	D8	H	H1	0,2980	0,6162
13/02/2018	D8	H	H2	0,5385	1,2929
12/02/2018	D8	H	H3	0,4980	5,4575
13/02/2018	D8	H	H4	1,1393	1,1952
14/03/2018	R	C	C1	0,4726	0,9990
15/03/2018	R	C	C2	0,0935	2,5899
14/03/2018	R	C	C3	0,5737	0,1754
15/03/2018	R	C	C4	0,7472	1,0391
14/03/2018	R	L	L1	0,5591	0,5933
15/03/2018	R	L	L2	0,2177	2,3933
14/03/2018	R	L	L3	0,5090	0,8942
15/03/2018	R	L	L4	0,9809	0,8816
14/03/2018	R	P	P1	0,4014	0,9834
15/03/2018	R	P	P2	0,2798	2,3411
14/03/2018	R	P	P3	0,6165	1,1379
15/03/2018	R	P	P4	0,4094	1,1808
14/03/2018	R	H	H1	0,4519	0,5863
15/03/2018	R	H	H2	0,3625	2,6143
14/03/2018	R	H	H3	0,6822	0,7345
15/03/2018	R	H	H4	0,3473	1,2213

Mean sponge respiration rates (µmol/h/g)

	Day 1	Day 2	Day 4	Day 8	Recovery
Control	0,714	0,756	0,734	0,514	0,472
Low	0,444	0,645	0,697	0,469	0,567
Medium	0,434	0,567	0,556	0,472	0,427
High	0,374	0,646	0,682	0,618	0,461

Background rate of O2 consumption (µmol/h)

	Day 1	Day 2	Day 4	Day 8	Recovery
Control	0,573	0,247	0,311	0,726	1,543
Low	2,084	1,840	0,962	1,214	1,289
Medium	1,902	1,731	1,142	1,906	1,502
High	2,350	2,390	1,246	2,140	1,474

E. Lysosome data & summary

Date	Day	Treatment	Replicate	Blindtest	Method	Unstable
05/02/2018	1	C	C1	No	A	0,0727
06/02/2018	1	C	C2	Yes	A	0,0681
05/02/2018	1	C	C3	No	A	0,0865
06/02/2018	1	C	C4	Yes	A	0,0685
05/02/2018	1	L	L1	No	A	0,1724
06/02/2018	1	L	L2	Yes	A	0,1778
05/02/2018	1	L	L3	No	A	0,1700
06/02/2018	1	L	L4	Yes	A	0,1229
05/02/2018	1	P	P1	No	A	0,2272
06/02/2018	1	P	P2	Yes	A	0,0479
05/02/2018	1	P	P3	No	A	0,1746
06/02/2018	1	P	P4	Yes	A	0,1866
05/02/2018	1	H	H1	No	A	0,2647
06/02/2018	1	H	H2	Yes	A	0,1714
05/02/2018	1	H	H3	No	A	0,2241
06/02/2018	1	H	H4	Yes	A	0,2076
06/02/2018	2	C	C1	No	A	0,0735
07/02/2018	2	C	C2	Yes	A	0,1072
06/02/2018	2	C	C3	No	A	0,0485
07/02/2018	2	C	C4	Yes	A	0,1559
06/02/2018	2	L	L1	No	A	0,1072
07/02/2018	2	L	L2	Yes	A	0,2212
06/02/2018	2	L	L3	No	A	0,0794
07/02/2018	2	L	L4	Yes	A	0,2157
06/02/2018	2	P	P1	No	A	0,1373
07/02/2018	2	P	P2	Yes	A	0,2000
06/02/2018	2	P	P3	No	A	0,1539
07/02/2018	2	P	P4	Yes	A	0,1818
06/02/2018	2	H	H1	No	A	0,2362
07/02/2018	2	H	H2	Yes	A	0,0653
06/02/2018	2	H	H3	No	A	0,1682
07/02/2018	2	H	H4	Yes	A	0,3329
08/02/2018	4	C	C1	Yes	B	0,1653
09/02/2018	4	C	C2	Yes	B	0,2597
08/02/2018	4	C	C3	Yes	B	0,1927
09/02/2018	4	C	C4	Yes	B	0,2441
08/02/2018	4	L	L1	Yes	B	0,2675
09/02/2018	4	L	L2	Yes	B	0,2421
08/02/2018	4	L	L3	Yes	B	0,3173
09/02/2018	4	L	L4	Yes	B	0,3142
08/02/2018	4	P	P1	Yes	B	0,2709
09/02/2018	4	P	P2	Yes	B	0,3659
08/02/2018	4	P	P3	Yes	B	0,3883
09/02/2018	4	P	P4	Yes	B	0,3606
08/02/2018	4	H	H1	Yes	B	0,3456
09/02/2018	4	H	H2	Yes	B	0,3840
08/02/2018	4	H	H3	Yes	B	0,4113
09/02/2018	4	H	H4	Yes	B	0,3333
12/02/2018	8	C	C1	Yes	A	0,1648
13/02/2018	8	C	C2	Yes	A	0,2184
12/02/2018	8	C	C3	Yes	A	0,0620
13/02/2018	8	C	C4	Yes	A	0,1587
12/02/2018	8	L	L1	Yes	A	0,1021
13/02/2018	8	L	L2	Yes	A	0,1426
12/02/2018	8	L	L3	Yes	A	0,1875
13/02/2018	8	L	L4	Yes	A	0,2182
12/02/2018	8	P	P1	Yes	A	0,0738
13/02/2018	8	P	P2	Yes	A	0,1937

12/02/2018	8	P	P3	Yes	A	0,1725
13/02/2018	8	P	P4	Yes	A	0,2801
12/02/2018	8	H	H1	Yes	A	0,1661
13/02/2018	8	H	H2	Yes	A	0,2917
12/02/2018	8	H	H3	Yes	A	0,1999
13/02/2018	8	H	H4	Yes	A	0,2718
14/03/2018	R	C	C1	Yes	A	0,0817
15/03/2018	R	C	C2	Yes	A	0,1194
14/03/2018	R	C	C3	No	A	0,0750
15/03/2018	R	C	C4	No	A	0,0790
14/03/2018	R	L	L1	Yes	A	0,0967
15/03/2018	R	L	L2	Yes	A	0,1095
14/03/2018	R	L	L3	No	A	0,1343
15/03/2018	R	L	L4	No	A	0,0541
14/03/2018	R	P	P1	Yes	A	0,1213
15/03/2018	R	P	P2	Yes	A	0,0653
14/03/2018	R	P	P3	No	A	0,0873
15/03/2018	R	P	P4	No	A	0,1031
14/03/2018	R	H	H1	Yes	A	0,0967
15/03/2018	R	H	H2	Yes	A	0,0594
14/03/2018	R	H	H3	No	A	0,1194
15/03/2018	R	H	H4	No	A	0,1294

Summary	Average %				
	Day 1	Day 2	Day 4	Day 8	Recovery
Control	7,39%	9,62%	21,55%	15,10%	8,88%
Low	16,08%	15,59%	28,53%	16,26%	9,87%
Medium	15,91%	16,82%	34,64%	18,00%	9,43%
High	21,70%	20,07%	36,85%	23,24%	10,12%

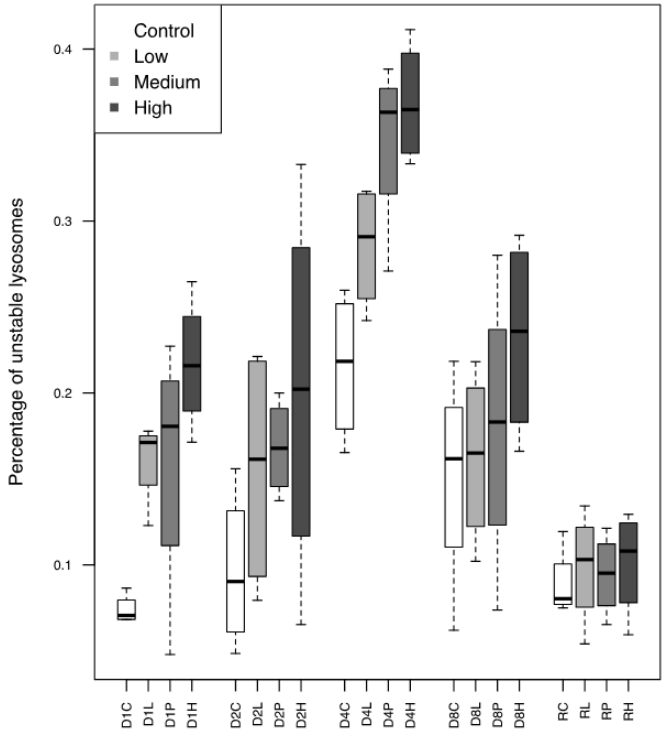

Here, the full data is represented. However, day 4 was discarded from the analysis and from the main body of the thesis because a slight change in methodology (method B) introduced dubious results (global increase in % of destabilized cells). On day 4, the staining solution was prepared fresh before staining each individual sample, resulting in stronger coloration of the cells.

F. Sponge respiration – LME model checking plots

Model description in R:

```
respi.lme <- lme(log10(Sponges+1) ~ day * Treatment, random=~+1|Replicate,
cor=corAR1())
```

The assumptions to be verified when applying an anova to a lme model is that the model's residuals present homogeneity of variance and a normal distribution.

- Homogeneity of variance

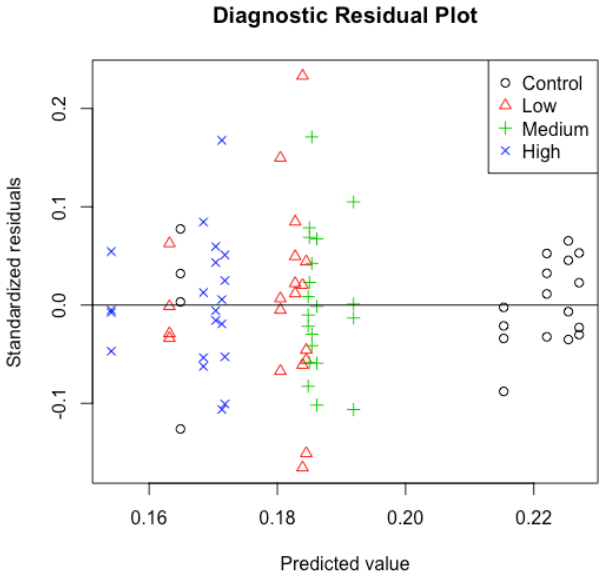


```
Levene's Test for Homogeneity of
Variance (center = median)

      Df F value Pr(>F)
group 19   0.914 0.5688
      60
```

➔ Homogeneity of variance is verified

- Normality

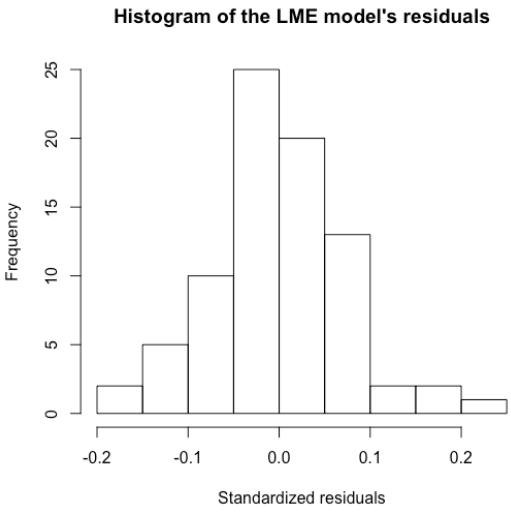

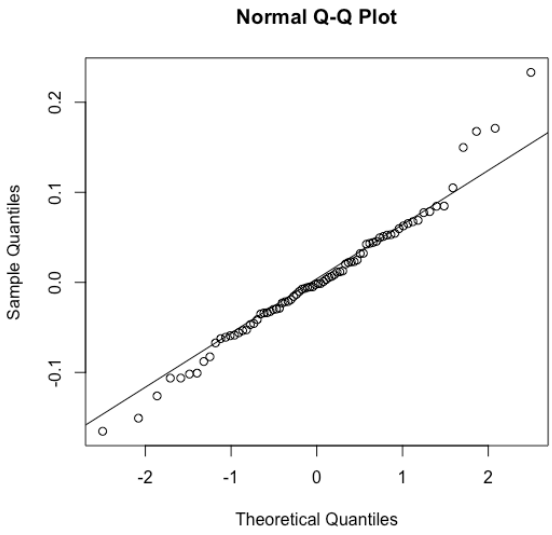


```
Shapiro-Wilk normality test
data:  respi.resid
W = 0.97602, p-value = 0.1374
```

➔ The model's residuals follow a normal distribution

G. Background respiration – ANOVA model checking plots

Model description in R:

```
model <- aov(log10(Background+1) ~ day * Treatment)
```

The assumptions to be verified when applying an anova to a data set is that the data (background respiration rates) presents homogeneity of variance and a normal distribution.

- Homogeneity of variance

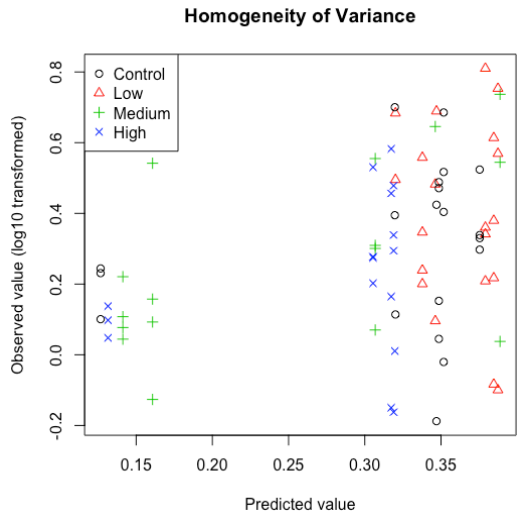


```
Levene's Test for Homogeneity of
Variance (center = median)

      Df F value Pr(>F)
group 19  0.6968 0.8048
      52
```

➔ Homogeneity of variance of the log10 transformed background respiration values is not rejected

- Normality

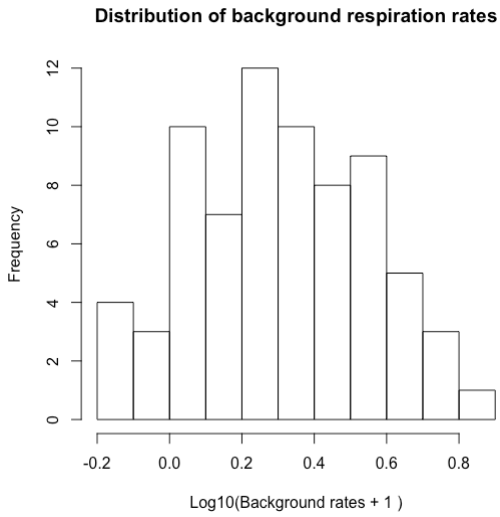

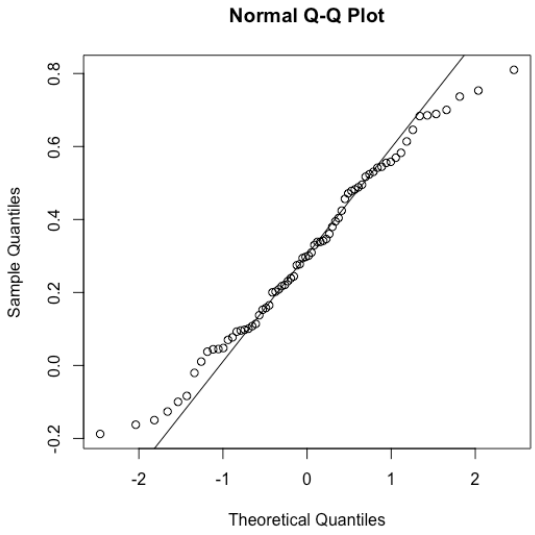


```
Shapiro-Wilk normality test

data:  log10(Background + 1)
W = 0.98154, p-value = 0.3712
```

➔ Normality of the log10 transformed background respiration values is not rejected

H. LMS – ANOVA model checking plots

Model description in R:

```
model <- aov(sqrt(Unstable) ~ day * Treatment, data=lyso)
```

- Homogeneity of variance

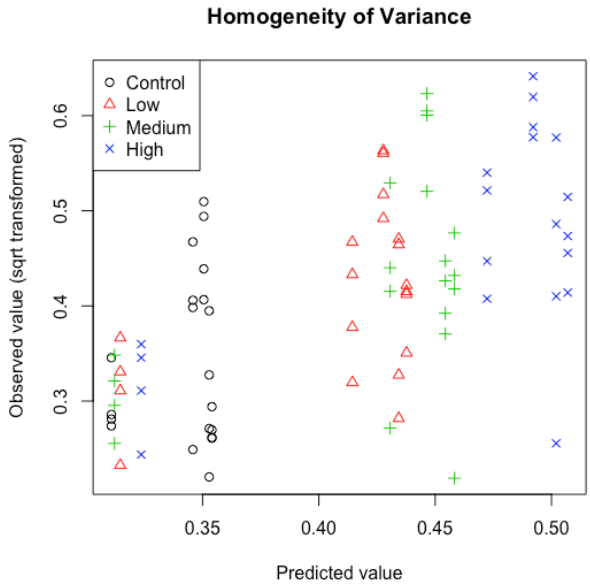


```
Levene's Test for Homogeneity of
Variance (center = median)

      Df F value Pr(>F)
group 19   1.245 0.2547
      60
```

➔ Homogeneity of variance of the square-root transformed counts of unstable lysosomes is not rejected

- Normality

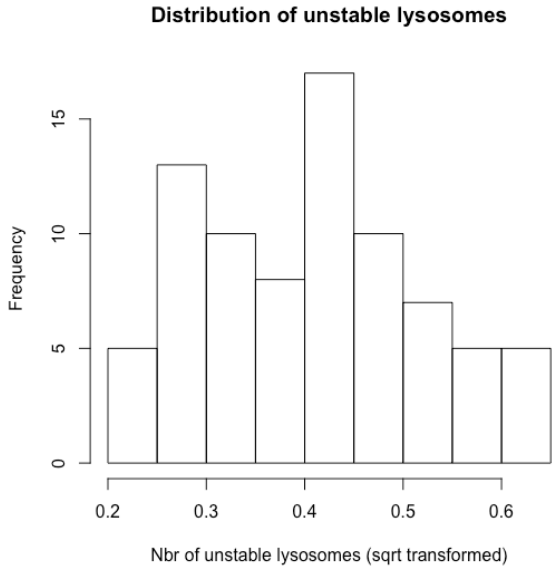

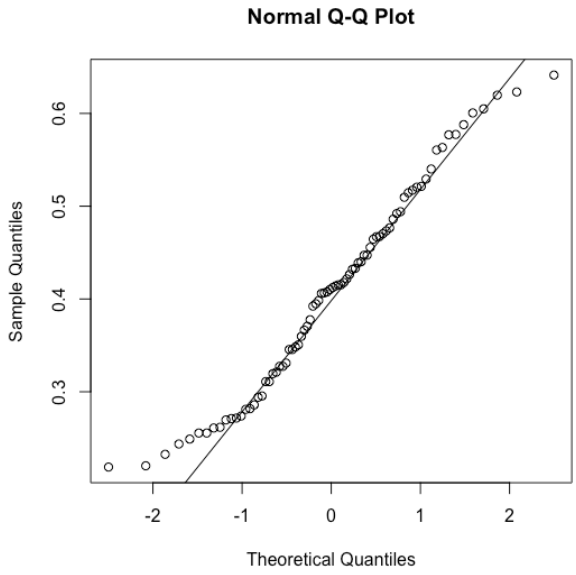


```
Shapiro-Wilk normality test

data:  sqrt(Unstable)
W = 0.97023, p-value = 0.05872
```

➔ Normality of the square-root transformed counts of unstable lysosomes is not rejected

I. Table of barcoded F- and R-primers for 2nd PCR (nested)

Fwd. ID	Sequence
F1 ('N501')	A**A**TGATACGGCGACCACCGAGATCTACAC**TAGATCGC**ACACTCTTTCCCTACACGACG
F2	A**A**TGATACGGCGACCACCGAGATCTACAC**CTCTCTAT**ACACTCTTTCCCTACACGACG
F3	AATGATACGGCGACCACCGAGATCTACAC**TATCCTCT**ACACTCTTTCCCTACACGACG
F4	AATGATACGGCGACCACCGAGATCTACAC**AGAGTAGA**ACACTCTTTCCCTACACGACG
F5	AATGATACGGCGACCACCGAGATCTACAC**GTAAGGAG**ACACTCTTTCCCTACACGACG
F6	AATGATACGGCGACCACCGAGATCTACAC**ACTGCATA**ACACTCTTTCCCTACACGACG
F7	AATGATACGGCGACCACCGAGATCTACAC**AAGGAGTA**ACACTCTTTCCCTACACGACG
F8	AATGATACGGCGACCACCGAGATCTACAC**CTAAGCCT**ACACTCTTTCCCTACACGACG

Rev. ID	Sequence
R1 ('N701')	CAAGCAGAAGACGGCATACGAGAT**TCGCCTTA**GTGACTGGAGTTCAGACGTGTGCTCTTCCGATCT
R2	CAAGCAGAAGACGGCATACGAGAT**CTAGTACG**GTGACTGGAGTTCAGACGTGTGCTCTTCCGATCT
R3	CAAGCAGAAGACGGCATACGAGAT**TTCTGCCT**GTGACTGGAGTTCAGACGTGTGCTCTTCCGATCT
R4	CAAGCAGAAGACGGCATACGAGAT**GCTCAGGA**GTGACTGGAGTTCAGACGTGTGCTCTTCCGATCT
R5	CAAGCAGAAGACGGCATACGAGAT**AGGAGTCC**GTGACTGGAGTTCAGACGTGTGCTCTTCCGATCT
R6	CAAGCAGAAGACGGCATACGAGAT**CATGCCTA**GTGACTGGAGTTCAGACGTGTGCTCTTCCGATCT
R7	CAAGCAGAAGACGGCATACGAGAT**GTAGAGAG**GTGACTGGAGTTCAGACGTGTGCTCTTCCGATCT
R8	CAAGCAGAAGACGGCATACGAGAT**CCTCTCTG**GTGACTGGAGTTCAGACGTGTGCTCTTCCGATCT
R9	CAAGCAGAAGACGGCATACGAGAT**AGCGTAGC**GTGACTGGAGTTCAGACGTGTGCTCTTCCGATCT
R10	CAAGCAGAAGACGGCATACGAGAT**CAGCCTCG**GTGACTGGAGTTCAGACGTGTGCTCTTCCGATCT
R11	CAAGCAGAAGACGGCATACGAGAT**TGCCTCTT**GTGACTGGAGTTCAGACGTGTGCTCTTCCGATCT
R12	CAAGCAGAAGACGGCATACGAGAT**TCCTCTAC**GTGACTGGAGTTCAGACGTGTGCTCTTCCGATCT

J. Taxonomic profile of sponge and seawater samples at the class level

Taxonomic profile established from the 20 most abundant classes identified from the sequencing data. A stacked barplot of the 20 most abundant classes in each sample revealed the marked difference between microbial communities at the class level in sponge tissues and communities found in the water.

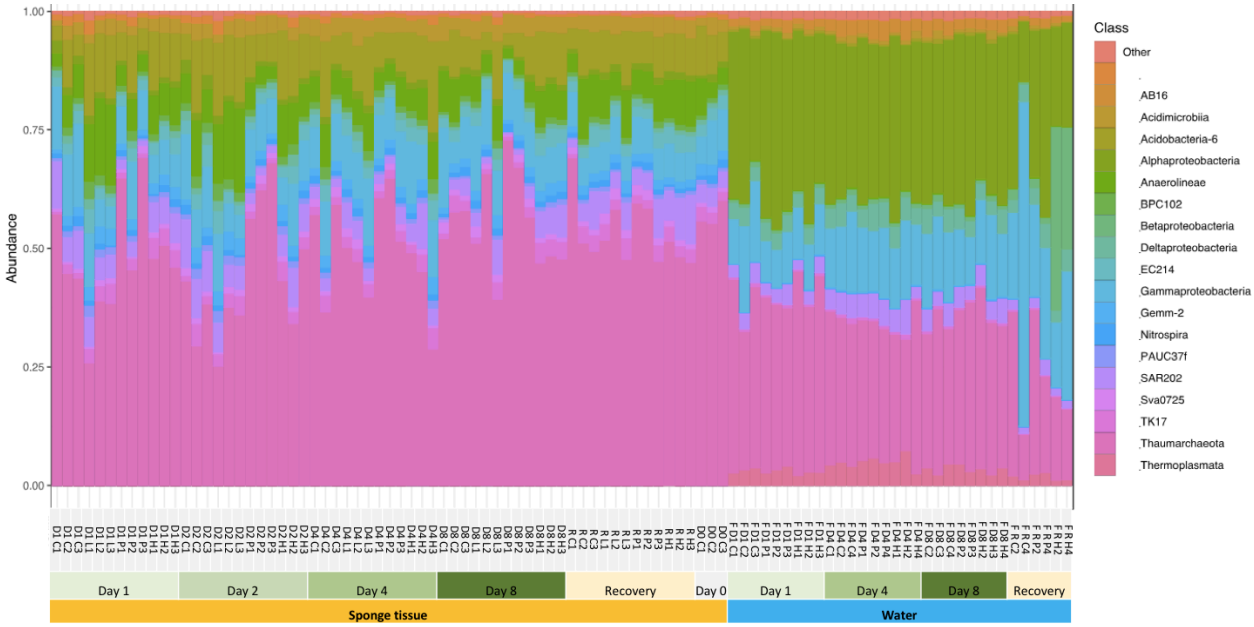

K. Alpha diversity of sponge and water microbial communities

SAMPLE ID	TYPE	DAY	TREATMENT	SAMPLE NAME	OBSERVED	CHAO1	SE.CHAO1
IMR01	Sponge	D1	C	D1 C1	5017	14223,52866	493,6373795
IMR02	Sponge	D1	C	D1 C2	3435	10179,51531	449,0382322
IMR03	Sponge	D1	C	D1 C3	2881	8874,315625	437,3472545
IMR04	Sponge	D1	L	D1 L1	3970	11358,10766	449,3418583
IMR05	Sponge	D1	L	D1 L2	2567	7532,278571	389,6902349
IMR06	Sponge	D1	L	D1 L3	962	2388,25	204,9242038
IMR07	Sponge	D1	P	D1 P1	1728	5201,289941	344,9502303
IMR08	Sponge	D1	P	D1 P2	2059	5896,428571	334,0130645
IMR09	Sponge	D1	P	D1 P3	1906	5053,556561	285,2808099
IMR10	Sponge	D1	H	D1 H1	853	2223,15873	220,8860911
IMR11	Sponge	D1	H	D1 H2	996	2897,554054	278,198585
IMR12	Sponge	D1	H	D1 H3	1125	3626,463415	342,0344747
IMR13	Sponge	D2	C	D2 C1	3096	9351,156695	438,3102574
IMR14	Sponge	D2	C	D2 C2	4566	14201,2659	552,8222373
IMR15	Sponge	D2	C	D2 C3	1960	5713,047619	339,7062763
IMR16	Sponge	D2	L	D2 L1	5475	16113,97523	554,7207836
IMR17	Sponge	D2	L	D2 L2	3237	9900,828729	458,1282399
IMR18	Sponge	D2	L	D2 L3	1307	3972	317,6271106
IMR19	Sponge	D2	P	D2 P1	2992	9183,467085	450,7271367
IMR20	Sponge	D2	P	D2 P2	1757	4775,673171	282,8972046
IMR21	Sponge	D2	P	D2 P3	2431	6944,090909	360,6069298
IMR22	Sponge	D2	H	D2 H1	910	2159,879518	183,243746
IMR23	Sponge	D2	H	D2 H2	4827	13720,72896	489,064146
IMR24	Sponge	D2	H	D2 H3	2041	6738,238095	432,5261021
IMR25	Sponge	D4	C	D4 C1	1215	3458,209091	276,1246519
IMR26	Sponge	D4	C	D4 C2	1144	3061,81982	239,4143524

IMR27	Sponge	D4	C	D4 C3	870	2357,776119	232,1276277
IMR28	Sponge	D4	L	D4 L1	2968	8800,053097	417,4987663
IMR29	Sponge	D4	L	D4 L2	1287	3492,080645	259,6539794
IMR30	Sponge	D4	L	D4 L3	2284	6527,861111	353,1371
IMR31	Sponge	D4	P	D4 P1	2913	8991,957237	451,8231299
IMR32	Sponge	D4	P	D4 P2	1342	3781,202899	272,513316
IMR33	Sponge	D4	P	D4 P3	2361	6697,938931	354,6513262
IMR34	Sponge	D4	H	D4 H1	2900	7790,69863	347,6943111
IMR35	Sponge	D4	H	D4 H2	1341	4042,123967	314,0380709
IMR36	Sponge	D4	H	D4 H3	1484	4653,529412	346,1136347
IMR37	Sponge	D8	C	D8 C1	2237	5883,128788	303,5654216
IMR38	Sponge	D8	C	D8 C2	1202	3626,526316	291,8608995
IMR39	Sponge	D8	C	D8 C3	1750	5233,481481	331,1585813
IMR40	Sponge	D8	L	D8 L1	2750	7381,167164	342,3158592
IMR41	Sponge	D8	L	D8 L2	1666	4292,520619	255,6390505
IMR42	Sponge	D8	L	D8 L3	1245	3896,641304	344,2966653
IMR43	Sponge	D8	P	D8 P1	2320	5813,302083	283,0932829
IMR44	Sponge	D8	P	D8 P2	2020	5616,882096	316,5143924
IMR45	Sponge	D8	P	D8 P3	1165	2851,496063	203,229014
IMR46	Sponge	D8	H	D8 H1	994	3022,75	298,1381436
IMR47	Sponge	D8	H	D8 H2	1538	5502,04878	440,864268
IMR48	Sponge	D8	H	D8 H3	1071	3435,133333	336,8468721
IMR49	Sponge	R	C	R C1	1576	4639,727273	311,392343
IMR50	Sponge	R	C	R C2	1428	4071,103448	287,0992767
IMR51	Sponge	R	C	R C3	2187	6626,531915	377,5570708
IMR52	Sponge	R	L	R L1	855	2433,515625	249,200237
IMR53	Sponge	R	L	R L2	1304	3876,439024	298,7148384
IMR54	Sponge	R	L	R L3	888	2697,571429	283,5853859
IMR55	Sponge	R	P	R P1	1822	5845,366667	383,7678926
IMR56	Sponge	R	P	R P2	1908	5767,119171	359,7955569
IMR57	Sponge	R	P	R P3	1231	3494,313043	273,5679102
IMR58	Sponge	R	H	R H1	1087	3201,117647	289,696244
IMR59	Sponge	R	H	R H2	2821	9200,055172	480,4758354
IMR60	Sponge	R	H	R H3	2583	8073,646429	426,1039525
IMR61	Sponge	D0	C	D0 C1	1673	4740,04918	299,5332274
IMR62	Sponge	D0	C	D0 C2	1283	4009,894737	324,2347745
IMR63	Sponge	D0	C	D0 C3	1464	4426,431655	323,0297351
IMR64	Water	D1	C	F D1 C1	2556	4082,280864	134,4186723
IMR65	Water	D1	C	F D1 C2	3010	4739,326923	137,396511
IMR66	Water	D1	C	F D1 C3	2524	3794,294461	113,4865286
IMR67	Water	D1	P	F D1 P1	2904	4726,12987	147,1062769
IMR68	Water	D1	P	F D1 P2	2779	4441,277045	137,0567872
IMR69	Water	D1	P	F D1 P3	2458	3833,131868	130,4254561
IMR70	Water	D1	H	F D1 H1	2681	4278,502825	135,6070882
IMR71	Water	D1	H	F D1 H2	3471	6673,669903	230,8719802
IMR72	Water	D1	H	F D1 H3	2791	4772,009317	167,4356561
IMR73	Water	D4	C	F D4 C1	3080	5463,908482	174,9290072
IMR74	Water	D4	C	F D4 C2	2464	3957,58	128,7636047
IMR75	Water	D4	C	F D4 C4	2201	3538,960432	126,7321578
IMR76	Water	D4	P	F D4 P1	4461	10025,75085	326,05
IMR77	Water	D4	P	F D4 P2	2627	4188,655367	133,0904392
IMR78	Water	D4	P	F D4 P4	2115	3277,657343	111,8349884
IMR79	Water	D4	H	F D4 H1	2854	5016,007519	167,5935765
IMR80	Water	D4	H	F D4 H2	3190	6243,695962	220,0451648
IMR81	Water	D4	H	F D4 H4	1847	3257,183673	149,0311785
IMR82	Water	D8	C	F D8 C2	2500	4165,673077	146,3578611
IMR83	Water	D8	C	F D8 C3	2371	4650,662447	210,0522847
IMR84	Water	D8	C	F D8 C4	2147	3334,195122	113,6424298
IMR85	Water	D8	P	F D8 P2	2660	4529,123626	153,0542348
IMR86	Water	D8	P	F D8 P3	1713	3212,4375	163,0605076
IMR88	Water	D8	H	F D8 H2	6099	15069	440,2872393
IMR89	Water	D8	H	F D8 H3	1483	2431,594937	114,8381426
IMR90	Water	D8	H	F D8 H4	2124	3283,577508	106,7476329
IMR91	Water	R	C	F R C2	3002	6253,192308	250,9208569
IMR92	Water	R	C	F R C4	1362	2172,056497	96,96648996
IMR93	Water	R	P	F R P2	1991	3271,733051	129,0184204
IMR94	Water	R	P	F R P4	2090	3368,100358	121,8769405
IMR95	Water	R	H	F R H2	1783	3250,247573	151,4917874
IMR96	Water	R	H	F R H4	3370	7328,605634	273,492667

SPONGES	Treatment	Average observed	SE observed	Average Chao	SE Chao
	Control	2619	340	7706	1017
	Low	1712	157	4869	384
	Medium	1607	149	4874	497
	High	2089	275	6046	830

WATER	Treatment	Average observed	SE observed	Average Chao	SE Chao
	Control	2793	94	4615	255
	Low	–	–	–	–
	Medium	2502	447	4964	1237
	High	2634	215	4748	593